*Kinetic Waves and Instabilities in a Uniform Plasma**

Ronald C. Davidson

Plasma Fusion Center, Massachusetts Institute of Technology
Cambridge, Massachusetts 02139, USA

Contents

*Work supported by the Office of Naval Research and in part by the Department of Energy.

Handbook of Plasma Physics, Eds. M.N. Rosenbluth and R.Z. Sagdeev
Volume 1 Basic Plasma Physics I, edited by A.A. Galeev and R.N. Sudan
© North-Holland Publishing Company 1983

3.3.1. General dispersion relation

Introduction

This chapter presents a theoretical survey of the *basic* kinetic waves and instabilities characteristic of a spatially uniform plasma immersed in a uniform, applied magnetic field $\boldsymbol{B}_0 = B_0\hat{\boldsymbol{e}}_z$. Isotropic equilibria $F_j(v^2)$ that are monotonic decreasing functions of v^2 are stable to electromagnetic perturbations with arbitrary polarization. In this chapter are examined a wide variety of kinetic instabilities in which the free energy source for the instability is associated with nonthermal features of the equilibrium distribution function $F_j(v)$, ranging from the relative directed motion of plasma components to anisotropy in plasma kinetic energy. The present stability analysis, based on the *linearization approximation*, is instrinsically *classical* in that it does not include the influence of turbulence effects on wave–particle resonances, nor does it include the influence of stochastic particle motion on stability behavior. Finally, it should be emphasized that the kinetic waves and instabilities selected for analysis here have a broad range of applications to laboratory plasmas, space plasmas, beam–plasma interactions, and magnetic and inertial confinement fusion.

The physical model utilized in the present analysis is based on the collisionless Vlasov–Maxwell equations in which the one-particle distribution function $f_j(\boldsymbol{x}, \boldsymbol{v}, t)$ evolves according to the Vlasov equation,

$$\left[\frac{\partial}{\partial t} + \boldsymbol{v}\cdot\frac{\partial}{\partial \boldsymbol{x}} + \frac{e_j}{m_j}\left(\boldsymbol{E}(\boldsymbol{x},t) + \frac{\boldsymbol{v}\times\boldsymbol{B}(\boldsymbol{x},t)}{c}\right)\cdot\frac{\partial}{\partial \boldsymbol{v}}\right] f_j(\boldsymbol{x},\boldsymbol{v},t) = 0, \tag{1}$$

where $\boldsymbol{E}(\boldsymbol{x}, t)$ and $\boldsymbol{B}(\boldsymbol{x}, t)$ are the electric and magnetic fields, and e_j and m_j are the charge and mass, respectively, of a particle of species j. Here, $f_j(\boldsymbol{x}, \boldsymbol{v}, t)$ is the density of particles of species j in the six-dimensional phase space $(\boldsymbol{x}, \boldsymbol{v})$. Moreover, the electric and magnetic fields are determined self-consistently from Maxwell's equations in terms of the plasma current density,

$$\boldsymbol{J}(\boldsymbol{x}, t) = \sum_j e_j \int \mathrm{d}^3\boldsymbol{v}\, \boldsymbol{v} f_j(\boldsymbol{x}, \boldsymbol{v}, t),$$

and charge density,

$$\rho(\boldsymbol{x}, t) = \sum_j e_j \int \mathrm{d}^3\boldsymbol{v} f_j(\boldsymbol{x}, \boldsymbol{v}, t),$$

as well as external charge and current sources. Throughout the present analysis, it is assumed that the plasma is immersed in a uniform, externally applied magnetic field $\boldsymbol{B}_0 = B_0\hat{\boldsymbol{e}}_z$, and that the plasma equilibrium state $(\partial/\partial t = 0)$ is characterized by charge neutrality, $\sum_j \hat{n}_j e_j = 0$, and zero electric field $\boldsymbol{E}_0$. It is also assumed that the equilibrium plasma current (if any) is sufficiently weak that the corresponding equilibrium self-magnetic field has a negligibly small effect on stability behavior in comparison with the applied magnetic field $B_0\hat{\boldsymbol{e}}_z$.

The organization of this chapter is the following. In the remainder of Section 3.3.1, use is made of the linearized Vlasov–Maxwell equations to determine the general dispersion relation for electromagnetic wave propagation in a spatially uniform, magnetized plasma. The analysis is carried out for arbitrary propagation direction with respect to $B_0\hat{e}_z$, and arbitrary gyrotropic equilibrium $F_j(v_\perp^2, v_z)$. The general dispersion relation is also simplified in Section 3.3.1 for several limiting cases, including wave propagation parallel to $B_0\hat{e}_z$, perpendicular to $B_0\hat{e}_z$, and in the absence of applied magnetic field ($B_0 = 0$). In Section 3.3.2, a proof of Newcomb's theorem is presented, which shows that monotonic decreasing equilibria with $\partial F_j(v^2)/\partial v^2 \leq 0$ (where $v^2 = v_\perp^2 + v_z^2$) are stable to small-amplitude electromagnetic perturbations with arbitrary polarization. Specific examples of kinetic waves and instabilities are examined in Sections 3.3.3–3.3.7, where the nonthermal equilibrium features that drive the instabilities range from anisotropy in plasma kinetic energy to the relative directed motion of the plasma components. The waves and instabilities discussed in Sections 3.3.3–3.3.7 include: electrostatic waves and instabilities in an unmagnetized plasma in Section 3.3.3 (e.g. bump-in-tail instability, ion acoustic instability, strong two-stream instability, etc.); transverse electromagnetic Weibel instabilities driven by kinetic energy anisotropy in an unmagnetized plasma in Section 3.3.4 (e.g. electromagnetic instabilities driven by thermal anisotropy or directed counterstreaming motion); transverse electromagnetic instabilities for wave propagation parallel to $B_0\hat{e}_z$ in Section 3.3.5 (e.g. firehose instability, electromagnetic ion cyclotron instability, and electron whistler instability); and electromagnetic and electrostatic waves and instabilities for wave propagation perpendicular (or nearly perpendicular) to $B_0\hat{e}_z$ in Sections 3.3.6 and 3.3.7 (e.g. ordinary-mode electromagnetic instability, cyclotron harmonic loss-cone instability, convective loss-cone instability, ion–ion two-stream instability, and modified two-stream instability).

Finally, a brief list of references follows Section 3.3.7. This reference list, while forming an incomplete bibliography, identifies several classical papers and early treatises on the kinetic waves and instabilities discussed in Sections 3.3.1–3.3.7.

Kinetic dispersion relation for a magnetized plasma

Perturbations are considered about an equilibrium ($\partial/\partial t = 0$) characterized by zero electric field and a uniform, externally applied magnetic field $\boldsymbol{B}_0 = B_0\hat{e}_z$, where $B_0 =$ constant. It is also assumed that the equilibrium distribution function $f_j^0(\boldsymbol{x}, \boldsymbol{v})$ for species j is spatially uniform with

$$f_j^0(\boldsymbol{x}, \boldsymbol{v}) = \hat{n}_j F_j(v_\perp^2, v_z), \tag{2}$$

where $v_\perp = (v_x^2 + v_y^2)^{1/2}$ is the perpendicular speed, and v_z is the axial velocity. In (2), $\hat{n}_j =$ constant is the ambient density of species j, and $F_j(v_\perp^2, v_z)$ is normalized according to

$$2\pi \int_0^\infty dv_\perp\, v_\perp \int_{-\infty}^{\infty} dv_z\, F_j = 1.$$

In the present analysis, the electromagnetic wave perturbations, $\delta\boldsymbol{E}(\boldsymbol{x}, t)$ and

$\delta \boldsymbol{B}(\boldsymbol{x}, t)$, are represented as Fourier–Laplace transforms

$$\delta \boldsymbol{E}(\boldsymbol{x}, t) = \int \mathrm{d}^3\boldsymbol{k} \exp(\mathrm{i}\boldsymbol{k}\cdot\boldsymbol{x}) \int_C \frac{\mathrm{d}\omega}{2\pi \mathrm{i}} \exp(-\mathrm{i}\omega t)\, \widehat{\delta \boldsymbol{E}}(\boldsymbol{k}, \omega),$$

$$\delta \boldsymbol{B}(\boldsymbol{x}, t) = \int \mathrm{d}^3\boldsymbol{k} \exp(\mathrm{i}\boldsymbol{k}\cdot\boldsymbol{x}) \int_C \frac{\mathrm{d}\omega}{2\pi \mathrm{i}} \exp(-\mathrm{i}\omega t)\, \widehat{\delta \boldsymbol{B}}(\boldsymbol{k}, \omega), \tag{3}$$

where $\mathrm{Im}\,\omega > 0$ is chosen sufficiently large and positive that the Laplace transform integrals $\widehat{\delta \boldsymbol{E}}(\boldsymbol{k}, \omega) = \int_0^\infty \mathrm{d}t \exp(\mathrm{i}\omega t)\, \widehat{\delta \boldsymbol{E}}(\boldsymbol{k}, t)$ etc. converge. In (3), the contour C is parallel to the Re-ω axis with $\int_C \mathrm{d}\omega = \int_{-\infty + \mathrm{i}\sigma}^{\infty + \mathrm{i}\sigma} \mathrm{d}\omega$ and $\mathrm{Im}\,\omega > \sigma$. Neglecting initial ($t = 0$) perturbations, Maxwell's equations can be expressed as

$$\boldsymbol{k} \times \widehat{\delta \boldsymbol{E}} = (\omega/c)\, \widehat{\delta \boldsymbol{B}}, \tag{4}$$

$$\mathrm{i}\boldsymbol{k} \times \widehat{\delta \boldsymbol{B}} = (4\pi/c)\, \widehat{\delta \boldsymbol{J}} - \mathrm{i}(\omega/c)\, \widehat{\delta \boldsymbol{E}}, \tag{5}$$

together with

$$\boldsymbol{k} \cdot \widehat{\delta \boldsymbol{B}} = 0, \tag{6}$$

$$\mathrm{i}\boldsymbol{k} \cdot \widehat{\delta \boldsymbol{E}} = 4\pi \widehat{\delta \rho}. \tag{7}$$

In (5) and (7), the perturbed current and charge densities, $\delta \boldsymbol{J}(\boldsymbol{x}, t)$ and $\delta \rho(\boldsymbol{x}, t)$, are related self-consistently to the perturbed distribution function $\delta f_j(\boldsymbol{x}, \boldsymbol{v}, t)$ by

$$\delta \boldsymbol{J}(\boldsymbol{x}, t) = \sum_j e_j \int \mathrm{d}^3\boldsymbol{v}\, \boldsymbol{v}\, \delta f_j(\boldsymbol{x}, \boldsymbol{v}, t), \tag{8}$$

$$\delta \rho(\boldsymbol{x}, t) = \sum_j e_j \int \mathrm{d}^3\boldsymbol{v}\, \delta f_j(\boldsymbol{x}, \boldsymbol{v}, t). \tag{9}$$

Moreover, for small-amplitude perturbations, $\delta f_j(\boldsymbol{x}, \boldsymbol{v}, t)$ evolves according to the linearized Vlasov equation

$$\left(\frac{\partial}{\partial t} + \boldsymbol{v} \cdot \frac{\partial}{\partial \boldsymbol{x}} + \frac{e_j}{m_j} \frac{\boldsymbol{v} \times B_0 \hat{\boldsymbol{e}}_z}{c} \right) \cdot \frac{\partial}{\partial \boldsymbol{v}} \delta f_j(\boldsymbol{x}, \boldsymbol{v}, t)$$

$$= -\frac{\hat{n}_j e_j}{m_j} \left(\delta \boldsymbol{E}(\boldsymbol{x}, t) + \frac{\boldsymbol{v} \times \delta \boldsymbol{B}(\boldsymbol{x}, t)}{c} \right) \cdot \frac{\partial}{\partial \boldsymbol{v}} F_j(v_\perp^2, v_z), \tag{10}$$

where e_j and m_j are the charge and mass, respectively, of a particle of species j, and c is the speed of light in vacuo. Substituting (4) and (8) into (5), the $\nabla \times \delta \boldsymbol{B}$ Maxwell equation becomes

$$\boldsymbol{k} \times (\boldsymbol{k} \times \widehat{\delta \boldsymbol{E}}) + \frac{\omega^2}{c^2} \widehat{\delta \boldsymbol{E}} + \frac{4\pi \mathrm{i}\omega}{c^2} \sum_j e_j \int \mathrm{d}^3\boldsymbol{v}\, \boldsymbol{v}\, \widehat{\delta f_j}(\boldsymbol{k}, \boldsymbol{v}, \omega) = 0. \tag{11}$$

Making use of the method of characteristics, the linearized Vlasov equation for

$$\delta f_j(\boldsymbol{x}, \boldsymbol{v}, t) = \int \mathrm{d}^3\boldsymbol{k} \exp(\mathrm{i}\boldsymbol{k}\cdot\boldsymbol{x}) \int_C \frac{\mathrm{d}\omega}{2\pi \mathrm{i}} \exp(-\mathrm{i}\omega t)\, \widehat{\delta f_j}(\boldsymbol{k}, \boldsymbol{v}, \omega)$$

can be solved for $\widehat{\delta f_j}(\boldsymbol{k}, v, \omega)$ to give

$$\widehat{\delta f_j}(\boldsymbol{k}, v, \omega) = -\frac{\hat{n}_j e_j}{m_j}\int_{-\infty}^{t} \mathrm{d}t' \exp[\mathrm{i}\boldsymbol{k}\cdot(\boldsymbol{x}'-\boldsymbol{x})-\mathrm{i}\omega(t'-t)]$$
$$\times\left(\widehat{\delta \boldsymbol{E}}+\frac{\boldsymbol{v}'\times(\boldsymbol{k}\times\widehat{\delta \boldsymbol{E}})}{\omega}\right)\cdot\frac{\partial}{\partial \boldsymbol{v}'}F_j(v_\perp'^2, v_z'), \tag{12}$$

where $\mathrm{Im}\,\omega > 0$ is assumed, and initial perturbations have been neglected. In (12), the particle trajectories $\boldsymbol{x}'(t')$ and $\boldsymbol{v}'(t')$ satisfy the orbit equations $\mathrm{d}\boldsymbol{x}'/\mathrm{d}t' = \boldsymbol{v}'$ and $\mathrm{d}\boldsymbol{v}'/\mathrm{d}t' = (e_j/c)\boldsymbol{v}'\times B_0\hat{\boldsymbol{e}}_z$ with initial conditions $\boldsymbol{x}'(t'=t)=\boldsymbol{x}$ and $\boldsymbol{v}'(t'=t)=\boldsymbol{v}$.

Making use of the fact that $v_\perp'$ and v_z' are constant (independent of t') along a particle trajectory in the equilibrium field configuration, it is straightforward to show that the integrand in (12) can be expressed as

$$\left(\widehat{\delta \boldsymbol{E}}+\frac{\boldsymbol{v}'\times(\boldsymbol{k}\times\widehat{\delta \boldsymbol{E}})}{\omega}\right)\cdot\frac{\partial}{\partial \boldsymbol{v}'}F_j(v_\perp'^2, v_z')$$
$$=\frac{\boldsymbol{v}_\perp'\cdot\widehat{\delta \boldsymbol{E}}}{v_\perp}\left[\frac{\partial}{\partial v_\perp}F_j(v_\perp^2, v_z)-\frac{k_z v_z}{\omega}\left(\frac{\partial}{\partial v_\perp}F_j(v_\perp^2, v_z)-\frac{v_\perp}{v_z}\frac{\partial}{\partial v_z}F_j(v_\perp^2, v_z)\right)\right]$$
$$+\widehat{\delta E}_z\left[\frac{\partial}{\partial v_z}F_j(v_\perp^2, v_z)-\frac{\boldsymbol{k}\cdot\boldsymbol{v}_\perp'}{\omega}\left(\frac{\partial}{\partial v_z}F_j(v_\perp^2, v_z)-\frac{v_z}{v_\perp}\frac{\partial}{\partial v_\perp}F_j(v_\perp^2, v_z)\right)\right], \tag{13}$$

where the only explicit t' dependence in (13) occurs in the $\boldsymbol{v}_\perp'$ factors in $\boldsymbol{v}_\perp'\cdot\widehat{\delta \boldsymbol{E}}$ and $\boldsymbol{k}\cdot\boldsymbol{v}_\perp'$. Introducing the cyclotron frequency

$$\omega_{cj} = e_j B_0/m_j c, \tag{14}$$

and defining the perpendicular velocity phase ϕ at $t'=t$ by $(v_x, v_y) = (v_\perp\cos\phi, v_\perp\sin\phi)$, the solutions to the orbit equations can be expressed as

$$v_x' = v_\perp\cos(\phi-\omega_{cj}\tau), \qquad v_y' = v_\perp\sin(\phi-\omega_{cj}\tau), \qquad v_z' = v_z, \tag{15}$$

and

$$x' = x-(v_\perp/\omega_{cj})[\sin(\phi-\omega_{cj}\tau)-\sin\phi],$$
$$y' = y+(v_\perp/\omega_{cj})[\cos(\phi-\omega_{cj}\tau)-\cos\phi], \qquad z' = z+v_z\tau, \tag{16}$$

where $\tau = t'-t$. Without loss of generality, it is assumed that the wavevector $\boldsymbol{k}$ lies in the $x-z$ plane with (Fig. 3.3.1)

$$\boldsymbol{k} = k_\perp\hat{\boldsymbol{e}}_x + k_z\hat{\boldsymbol{e}}_z. \tag{17}$$

The exponential factor occurring in the orbit integral in (12) can then be expressed as

$$\exp[\mathrm{i}\boldsymbol{k}\cdot(\boldsymbol{x}'-\boldsymbol{x})-\mathrm{i}\omega\tau] = \exp\left(\mathrm{i}k_z v_z\tau-\mathrm{i}\omega\tau+\mathrm{i}\frac{k_\perp v_\perp}{\omega_{cj}}[\sin\phi-\sin(\phi-\omega_{cj}\tau)]\right)$$
$$=\sum_{m=-\infty}^{\infty}\sum_{n=-\infty}^{\infty}J_m\left(\frac{k_\perp v_\perp}{\omega_{cj}}\right)J_n\left(\frac{k_\perp v_\perp}{\omega_{cj}}\right)$$
$$\times\exp[\mathrm{i}(m-n)\phi]\exp[\mathrm{i}(k_z v_z+n\omega_{cj}-\omega)\tau], \tag{18}$$

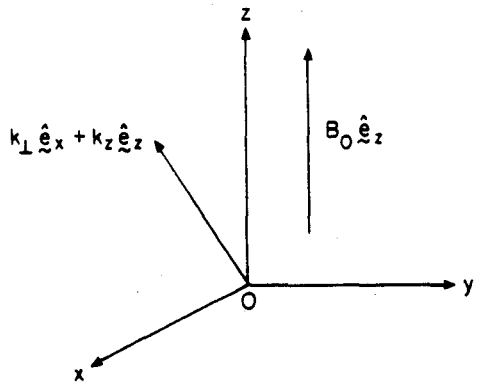

Fig. 3.3.1. Coordinate system and propagation direction.

where $J_n(b)$ is the Bessel function of the first kind of order n, and use has been made of the identity

$$\exp(ib\sin a) = \sum_{m=-\infty}^{\infty} J_m(b)\exp(ima).$$

Substituting (13), (15), (17) and (18) into (12), and carrying out the integration over τ with $\mathrm{Im}\,\omega > 0$, it is straightforward to show that the perturbed distribution function $\widehat{\delta f_j}(\boldsymbol{k}, v, \omega)$ can be expressed as

$$\begin{aligned}\widehat{\delta f_j}(\boldsymbol{k}, v, \omega) = -\frac{i\hat{n}_j e_j}{m_j} \sum_{m=-\infty}^{\infty} \sum_{n=-\infty}^{\infty} \frac{J_m(b_j)\exp[i(m-n)\phi]}{(\omega - n\omega_{cj} - k_z v_z)} \\ \times \left\{ \frac{nJ_n(b_j)}{b_j}\left[\frac{\partial}{\partial v_\perp}F_j - \frac{k_z v_z}{\omega}\left(\frac{\partial}{\partial v_\perp}F_j - \frac{v_\perp}{v_z}\frac{\partial F_j}{\partial v_z}\right)\right]\widehat{\delta E}_x \right. \\ + iJ_n'(b_j)\left[\frac{\partial}{\partial v_\perp}F_j - \frac{k_z v_z}{\omega}\left(\frac{\partial}{\partial v_\perp}F_j - \frac{v_\perp}{v_z}\frac{\partial F_j}{\partial v_z}\right)\right]\widehat{\delta E}_y \\ \left. + J_n(b_j)\left[\frac{\partial}{\partial v_z}F_j + \frac{n\omega_{cj}}{\omega}\left(\frac{v_z}{v_\perp}\frac{\partial F_j}{\partial v_\perp} - \frac{\partial}{\partial v_z}F\right)\right]\widehat{\delta E}_z \right\}. \end{aligned} \tag{19}$$

where $b_j \equiv k_\perp v_\perp / \omega_{cj}$, $J_n'(b_j)$ denotes $(\mathrm{d}/\mathrm{d}b_j)J_n(b_j)$, and use has been made of the identities $J_{n-1}(b_j) - J_{n+1}(b_j) = 2J_n'(b_j)$ and $J_{n-1}(b_j) + J_{n+1}(b_j) = (2n/b_j)J_n(b_j)$.

The form of the perturbed distribution function $\widehat{\delta f_j}(\boldsymbol{k}, v, \omega)$ given in (19) can be substituted into the Maxwell equation (11) to determine the self-consistent development of the field perturbations. In this regard, when evaluating the perturbed current density in (11), the expression

$$\int \mathrm{d}^3 v = \int_0^{2\pi} \mathrm{d}\phi \int_0^{\infty} \mathrm{d}v_\perp\, v_\perp \int_{-\infty}^{\infty} \mathrm{d}v_z$$

and the identity

$$\sum_{m=-\infty}^{\infty} J_m(b_j)\int_0^{2\pi}\frac{d\phi}{2\pi}\exp[i(m-n)\phi](v_\perp\cos\phi, v_\perp\sin\phi, v_z)$$
$$= \left[(nv_\perp/b_j)J_n(b_j), -iv_\perp J_n'(b_j), v_z J_n(b_j)\right]. \tag{20}$$

are used. Substituting (19) into (11) then gives

$$\boldsymbol{D}(\boldsymbol{k},\omega)\cdot\widehat{\delta\boldsymbol{E}} = 0 \tag{21}$$

where the nine matrix elements $D_{ij}(\boldsymbol{k},\omega)$ are evaluated directly from (11), (19) and (20). The condition for a non-trivial solution to (21) is that the determinant of the 3×3 matrix $\{D_{ij}(\boldsymbol{k},\omega)\}$ be equal to zero, which gives the desired dispersion relation

$$\det\{D_{ij}(\boldsymbol{k},\omega)\} = 0, \tag{22}$$

relating the wavenumber $\boldsymbol{k}$ and the complex oscillation frequency ω. Substituting (19) and (20) into (11) readily gives the elements of the dispersion tensor

$$D_{xx}(\boldsymbol{k},\omega) = 1 - \frac{c^2k_z^2}{\omega^2} + \sum_j\frac{\omega_{pj}^2}{\omega}\sum_{n=-\infty}^{\infty}\int d^3v\, v_\perp\frac{(n^2/b_j^2)J_n^2(b_j)}{(\omega - n\omega_{cj} - k_zv_z)}$$
$$\times\left[\frac{\partial}{\partial v_\perp}F_j - \frac{k_zv_z}{\omega}\left(\frac{\partial}{\partial v_\perp}F_j - \frac{v_\perp}{v_z}\frac{\partial}{\partial v_z}F_j\right)\right], \tag{23}$$

$$D_{xy}(\boldsymbol{k},\omega) = i\sum_j\frac{\omega_{pj}^2}{\omega}\sum_{n=-\infty}^{\infty}\int d^3v\, v_\perp\frac{(n/b_j)J_n(b_j)J_n'(b_j)}{(\omega - n\omega_{cj} - k_zv_z)}$$
$$\times\left[\frac{\partial}{\partial v_\perp}F_j - \frac{k_zv_z}{\omega}\left(\frac{\partial}{\partial v_\perp}F_j - \frac{v_\perp}{v_z}\frac{\partial}{\partial v_z}F_j\right)\right]$$
$$= -D_{yx}(\boldsymbol{k},\omega), \tag{24}$$

$$D_{xz}(\boldsymbol{k},\omega) = \frac{c^2k_zk_\perp}{\omega^2} + \sum_j\frac{\omega_{pj}^2}{\omega}\sum_{n=-\infty}^{\infty}\int d^3v\, v_\perp\frac{(n/b_j)J_n^2(b_j)}{(\omega - n\omega_{cj} - k_zv_z)}$$
$$\times\left[\frac{\partial}{\partial v_z}F_j + \frac{n\omega_{cj}}{\omega}\left(\frac{v_z}{v_\perp}\frac{\partial F_j}{\partial v_\perp} - \frac{\partial}{\partial v_z}F_j\right)\right], \tag{25}$$

$$D_{yy}(\boldsymbol{k},\omega) = 1 - \frac{c^2(k_z^2+k_\perp^2)}{\omega^2} + \sum_j\frac{\omega_{pj}^2}{\omega}\sum_{n=-\infty}^{\infty}\int d^3v\, v_\perp\frac{[J_n'(b_j)]^2}{(\omega - n\omega_{cj} - k_zv_z)}$$
$$\times\left[\frac{\partial}{\partial v_\perp}F_j - \frac{k_zv_z}{\omega}\left(\frac{\partial}{\partial v_\perp}F_j - \frac{v_\perp}{v_z}\frac{\partial}{\partial v_z}F_j\right)\right], \tag{26}$$

$$D_{yz}(\boldsymbol{k},\omega) = -i\sum_j\frac{\omega_{pj}^2}{\omega}\sum_{n=-\infty}^{\infty}\int d^3v\, v_\perp\frac{J_n(b_j)J_n'(b_j)}{(\omega - n\omega_{cj} - k_zv_z)}$$
$$\times\left[\frac{\partial}{\partial v_z}F_j + \frac{n\omega_{cj}}{\omega}\left(\frac{v_z}{v_\perp}\frac{\partial F_j}{\partial v_\perp} - \frac{\partial}{\partial v_z}F_j\right)\right], \tag{27}$$

$$D_{zx}(\boldsymbol{k},\omega)=\frac{c^2k_zk_\perp}{\omega^2}+\sum_j\frac{\omega_{pj}^2}{\omega}\sum_{n=-\infty}^{\infty}\int d^3v\,v_z\frac{(n/b_j)J_n^2(b_j)}{(\omega-n\omega_{cj}-k_zv_z)}$$
$$\times\left[\frac{\partial}{\partial v_\perp}F_j-\frac{k_zv_z}{\omega}\left(\frac{\partial}{\partial v_\perp}F_j-\frac{v_\perp}{v_z}\frac{\partial}{\partial v_z}F_j\right)\right], \tag{28}$$

$$D_{zy}(\boldsymbol{k},\omega)=i\sum_j\frac{\omega_{pj}^2}{\omega}\sum_{n=-\infty}^{\infty}\int d^3v\,v_z\frac{J_n(b_j)J_n'(b_j)}{(\omega-n\omega_{cj}-k_zv_z)}$$
$$\times\left[\frac{\partial}{\partial v_\perp}F_j-\frac{k_zv_z}{\omega}\left(\frac{\partial}{\partial v_\perp}F_j-\frac{v_\perp}{v_z}\frac{\partial F_j}{\partial v_z}\right)\right], \tag{29}$$

$$D_{zz}(\boldsymbol{k},\omega)=1-\frac{c^2k_\perp^2}{\omega^2}+\sum_j\frac{\omega_{pj}^2}{\omega}\sum_{n=-\infty}^{\infty}\int d^3v\,v_z\frac{J_n^2(b_j)}{(\omega-n\omega_{cj}-k_zv_z)}$$
$$\times\left[\frac{\partial}{\partial v_z}F_j+\frac{n\omega_{cj}}{\omega}\left(\frac{v_z}{v_\perp}\frac{\partial}{\partial v_\perp}F_j-\frac{\partial}{\partial v_z}F_j\right)\right], \tag{30}$$

where

$$\int d^3v=2\pi\int_0^\infty dv_\perp\,v_\perp\int_{-\infty}^{\infty}dv_z,$$

$b_j=k_\perp v_\perp/\omega_{cj}$, $\omega_{pj}^2=4\pi\hat{n}_je_j^2/m_j$ is the plasma frequency squared, and $\mathrm{Im}\,\omega>0$ is assumed.

In summary, the dispersion relation (22) together with the definitions of $D_{ij}(\boldsymbol{k},\omega)$ in (23)–(30) can be used to investigate detailed stability properties of a spatially uniform plasma immersed in a uniform magnetic field $B_0\hat{\boldsymbol{e}}_z$ for a broad range of equilibrium distribution functions $F_j(v_\perp^2, v_z)$. In this regard, it is clear from (23)–(30) that considerable simplification of the matrix elements $D_{ij}(\boldsymbol{k},\omega)$ occurs in several limiting cases, e.g. (a) wave propagation parallel to $B_0\hat{\boldsymbol{e}}_z(k_\perp=0;\ \boldsymbol{k}=k_z\hat{\boldsymbol{e}}_z)$, (b) wave propagation perpendicular to $B_0\hat{\boldsymbol{e}}_z(k_z=0;\ \boldsymbol{k}=k_\perp\hat{\boldsymbol{e}}_x)$, and (c) an isotropic plasma with $F_j=F_j(v_\perp^2+v_z^2)$ and $\partial F_j/\partial v_\perp-(v_\perp/v_z)\partial F_j/\partial v_z=0$. For detailed applications in subsequent sections, (22)–(30) are now simplified for several cases of practical interest.

Propagation parallel to $B_0\hat{\boldsymbol{e}}_z$

In this section, use is made of (21)–(30) to simplify the dispersion relation for wave propagation parallel to $B_0\hat{\boldsymbol{e}}_z$ with

$$k_\perp=0,\qquad \boldsymbol{k}=k_z\hat{\boldsymbol{e}}_z. \tag{31}$$

Making use of $J_0(0)=1$, $J_n(0)=0$ for $|n|>1$ and $J_1(b_j)\simeq b_j/2$, for $|b_j|\ll 1$, it follows directly from (25), (27), (28) and (29) that

$$D_{xz}=D_{zx}=D_{yz}=D_{zy}=0, \tag{32}$$

for $k_\perp=0$. Moreover, the remaining matrix elements for $k_\perp=0$ can be expressed as

$$D_{xx} = D_{yy} = 1 - \frac{c^2 k_z^2}{\omega^2} + \sum_j \frac{\omega_{pj}^2}{\omega} \int d^3v \frac{v_\perp}{4} \left[\frac{\partial}{\partial v_\perp} F_j - \frac{k_z v_z}{\omega} \left(\frac{\partial}{\partial v_\perp} F_j - \frac{v_\perp}{v_z} \frac{\partial F_j}{\partial v_z} \right) \right]$$
$$\times \left(\frac{1}{\omega - \omega_{cj} - k_z v_z} + \frac{1}{\omega + \omega_{cj} - k_z v_z} \right), \tag{33}$$

$$D_{xy} = -D_{yx} = i \sum_j \frac{\omega_{pj}^2}{\omega} \int d^3v \frac{v_\perp}{4} \left[\frac{\partial}{\partial v_\perp} F_j - \frac{k_z v_z}{\omega} \left(\frac{\partial}{\partial v_\perp} F_j - \frac{v_\perp}{v_z} \frac{\partial F_j}{\partial v_z} \right) \right]$$
$$\times \left(\frac{1}{\omega - \omega_{cj} - k_z v_z} - \frac{1}{\omega + \omega_{cj} - k_z v_z} \right), \tag{34}$$

$$D_{zz} = 1 + \sum_j \frac{\omega_{pj}^2}{\omega} \int d^3v \frac{v_z \partial F_j / \partial v_z}{\omega - k_z v_z}$$
$$= 1 + \sum_j \frac{\omega_{pj}^2}{k_z^2} \int d^3v \frac{k_z \partial F_j / \partial v_z}{\omega - k_z v_z}, \tag{35}$$

where $\mathrm{Im}\,\omega > 0$ is assumed. Substituting (32)–(35) into (22) gives the dispersion relation

$$(D_{xx} D_{yy} - D_{xy} D_{yx}) D_{zz} = 0. \tag{36}$$

There are two classes of solutions to (21) and (36). The first class, with $D_{zz} = 0$, corresponds to *longitudinal electrostatic* perturbations with $\widehat{\delta E}_x = 0 = \widehat{\delta E}_y$ and perturbed electric field $\widehat{\delta \boldsymbol{E}} = \widehat{\delta E}_z \hat{\boldsymbol{e}}_z$ parallel to the propagation direction $\boldsymbol{k} = k_z \hat{\boldsymbol{e}}_z$. The second class, with $D_{xx} D_{yy} - D_{xy} D_{yx} = 0$, corresponds to *transverse electromagnetic* perturbations with $\widehat{\delta E}_z = 0$ and perturbed electric field $\widehat{\delta \boldsymbol{E}} = \widehat{\delta E}_x \hat{\boldsymbol{e}}_x + \widehat{\delta E}_y \hat{\boldsymbol{e}}_y$ perpendicular to the propagation direction $\boldsymbol{k} = k_z \hat{\boldsymbol{e}}_z$.

Electrostatic dispersion relation. To summarize, the wave polarization for electrostatic perturbations propagating parallel to $B_0 \hat{\boldsymbol{e}}_z$ is given by

$$\boldsymbol{k} = (0, 0, k_z), \qquad \widehat{\delta \boldsymbol{E}} = (0, 0, \widehat{\delta E}_z), \tag{37}$$

and the dispersion relation $D_{zz} = 0$ can be expressed as

$$D_{zz}(k_z, \omega) = 1 + \sum_j \frac{\omega_{pj}^2}{k_z^2} \int d^3v \frac{k_z \partial F_j / \partial v_z}{\omega - k_z v_z} = 0, \tag{38}$$

where $\mathrm{Im}\,\omega > 0$. As discussed in Section 3.3.3, depending on the functional form of $F_j(v_\perp^2, v_z)$, and the regions of ω- and k_z-space under investigation, (38) constitutes the electrostatic dispersion relation for longitudinal ion waves, electron plasma oscillations, two-stream instabilities, etc., for wave propagation parallel to $B_0 \hat{\boldsymbol{e}}_z$.

Electromagnetic dispersion relation. The wave polarization for transverse electromagnetic perturbations propagating parallel to $B_0 \hat{\boldsymbol{e}}_z$ is given by

$$\boldsymbol{k} = (0, 0, k_z), \qquad \widehat{\delta \boldsymbol{E}} = (\widehat{\delta E}_x, \widehat{\delta E}_y, 0), \tag{39}$$

and the dispersion relation $D_{xx}D_{yy} - D_{xy}D_{yx} = D_{xx}^2 + D_{xy}^2 = (D_{xx} + iD_{xy})(D_{xx} - iD_{xy}) = 0$ reduces to

$$D^{\pm}(k_z, \omega) = 1 - \frac{c^2 k_z^2}{\omega^2} + \sum_j \frac{\omega_{pj}^2}{\omega} \int d^3v \frac{v_\perp}{2} \left[\frac{\partial}{\partial v_\perp} F_j - \frac{k_z v_z}{\omega} \left(\frac{\partial F_j}{\partial v_\perp} - \frac{v_\perp}{v_z} \frac{\partial F_j}{\partial v_z} \right) \right] \times \frac{1}{(\omega \pm \omega_{cj} - k_z v_z)} = 0, \tag{40}$$

where $\mathrm{Im}\,\omega > 0$, and $D^+ = D_{xx} + iD_{xy} = 0$ and $D^- = D_{xx} - iD_{xy} = 0$ correspond to circularly polarized electromagnetic waves with right-hand ($\widehat{\delta E}_x = -i\widehat{\delta E}_y$) and left-hand ($\widehat{\delta E}_x = +i\widehat{\delta E}_y$) polarizations, respectively. As discussed in Section 3.3.5, depending on the regions of ω- and k_z-space under investigation and on the functional form of $F_j(v_\perp^2, v_z)$, (40) is the dispersion relation for electromagnetic waves propagating parallel to $B_0\hat{e}_z$, including Alfvén waves, the firehose instability, ion cyclotron waves, the Alfvén ion cyclotron instability, electron whistler waves, electron cyclotron waves, and (Weibel-like) transverse electromagnetic instabilities driven by an anisotropy in plasma kinetic energy with $\sum_j \hat{n}_j \int d^3v (m_j v_\perp^2/2) F_j$ exceeding $\sum_j \hat{n}_j \int d^3v (m_j v_z^2/2) F_j$ by a sufficient amount.

Propagation perpendicular to $B_0\hat{e}_z$

As a second limiting case, in this section (21)–(30) are examined for wave propagation perpendicular to $B_0\hat{e}_z$ with

$$k_z = 0, \qquad \boldsymbol{k} = k_\perp \hat{e}_x. \tag{41}$$

In addition, to simplify the analysis, it is assumed that there is zero average flow of species j along the field lines with

$$\int_{-\infty}^{\infty} dv_z\, v_z F_j(v_\perp^2, v_z) = 0. \tag{42}$$

Substituting (41) and (42) into (25), (27), (28) and (29) readily gives

$$D_{xz} = D_{zx} = D_{yz} = D_{zy} = 0 \tag{43}$$

for $k_z = 0$. Moreover, the remaining matrix elements for $k_z = 0$ can be expressed as

$$D_{xx} = 1 + \sum_j \frac{\omega_{pj}^2}{\omega} \sum_{n=-\infty}^{\infty} \int d^3v\, v_\perp \frac{(n^2/b_j^2) J_n^2(b_j)}{\omega - n\omega_{cj}} \frac{\partial}{\partial v_\perp} F_j, \tag{44}$$

$$D_{xy} = -D_{yx} = i \sum_j \frac{\omega_{pj}^2}{\omega} \sum_{n=-\infty}^{\infty} \int d^3v\, v_\perp \frac{(n/b_j) J_n(b_j) J_n'(b_j)}{\omega - n\omega_{cj}} \frac{\partial}{\partial v_\perp} F_j, \tag{45}$$

$$D_{yy} = 1 - \frac{c^2 k_\perp^2}{\omega^2} + \sum_j \frac{\omega_{pj}^2}{\omega} \sum_{n=-\infty}^{\infty} \int d^3v\, v_\perp \frac{[J_n'(b_j)]^2}{\omega - n\omega_{cj}} \frac{\partial}{\partial v_\perp} F_j, \tag{46}$$

$$D_{zz} = 1 - \frac{c^2 k_\perp^2}{\omega^2} - \sum_j \frac{\omega_{pj}^2}{\omega^2} + \sum_j \frac{\omega_{pj}^2}{\omega^2} \sum_{n=-\infty}^{\infty} \int d^3v \frac{n\omega_{cj} J_n^2(b_j)}{\omega - n\omega_{cj}} \frac{v_z^2}{v_\perp} \frac{\partial F_j}{\partial v_\perp}, \tag{47}$$

where use has been made of $\int dv_z v_z \partial F_j / \partial v_z = - \int dv_z F_j$ to simplify the expression for D_{zz}. For $\boldsymbol{k} = k_\perp \hat{\boldsymbol{e}}_x$, note from (44)–(47) that the perpendicular particle dynamics plays a very important role in determining detailed wave propagation properties as manifest by the cyclotron resonances in (44)–(47) for $\omega = n\omega_{cj}$, $n = \pm 1, \pm 2, \ldots$. Substituting (43)–(47) into (22) gives the dispersion relation

$$(D_{xx} D_{yy} - D_{xy} D_{yx}) D_{zz} = 0. \tag{48}$$

As for the case of parallel propagation, there are two classes of solutions to (21) and (48). The first class, with $D_{zz} = 0$, corresponds to *transverse electromagnetic* perturbations with $\widehat{\delta E}_x = 0 = \widehat{\delta E}_y$ and perturbed electric field $\widehat{\delta \boldsymbol{E}} = \widehat{\delta E}_z \hat{\boldsymbol{e}}_x$. This is usually called *ordinary-mode* wave propagation. The second class, with $D_{xx} D_{yy} - D_{xy} D_{yx} = 0$, corresponds to the *extraordinary mode* of wave propagation, which generally has *mixed polarization*. That is, with $\widehat{\delta E}_z = 0$ and $\widehat{\delta \boldsymbol{E}} = \widehat{\delta E}_x \hat{\boldsymbol{e}}_x + \widehat{\delta E}_y \hat{\boldsymbol{e}}_y$, the electric field perturbation generally has components both parallel and perpendicular to $\boldsymbol{k} = k_\perp \hat{\boldsymbol{e}}_x$.

Ordinary-mode dispersion relation. To summarize, the wave polarization for ordinary-mode transverse electromagnetic wave perturbations propagating perpendicular to $B_0 \hat{\boldsymbol{e}}_z$ is given by

$$\boldsymbol{k} = (k_\perp, 0, 0), \qquad \widehat{\delta \boldsymbol{E}} = (0, 0, \widehat{\delta E}_z), \tag{49}$$

and the dispersion relation $D_{zz} = 0$ can be expressed as

$$D_{zz}(k_\perp, \omega) = 1 - \frac{c^2 k_\perp^2}{\omega^2} - \sum_j \frac{\omega_{pj}^2}{\omega^2} + \sum_j \frac{\omega_{pj}^2}{\omega^2} \sum_{n=-\infty}^{\infty} \int d^3v \, \frac{n\omega_{cj} J_n^2(b_j)}{\omega - n\omega_{cj}} \frac{v_z^2}{v_\perp} \frac{\partial F_j}{\partial v_\perp} = 0 \tag{50}$$

As discussed in Section 3.3.6, for a cold plasma, or for a moderately warm, isotropic plasma with $|b_j| < 1$, (50) gives the familiar ordinary-mode dispersion relation (for $\omega \neq n\omega_{cj}$) $\omega^2 = c^2 k_\perp^2 + \sum_j \omega_{pj}^2$ plus small thermal corrections. On the other hand, for parallel plasma kinetic energy density $\sum_j \hat{n}_j \int d^3v (m_j v_z^2/2) F_j$ exceeding $\sum_j \hat{n}_j \int d^3v (m_j v_\perp^2/2) F_j$ by a sufficient amount, (50) can lead to the (Weibel-like) electromagnetic filamentation instability.

Extraordinary-mode dispersion relation. In general, the wave polarization for extraordinary-mode propagation perpendicular to $B_0 \hat{\boldsymbol{e}}_z$ is mixed. That is,

$$\boldsymbol{k} = (k_\perp, 0, 0), \qquad \widehat{\delta \boldsymbol{E}} = (\widehat{\delta E}_x, \widehat{\delta E}_y, 0), \tag{51}$$

and the wave perturbation has both longitudinal ($\widehat{\delta E}_x$) and transverse ($\widehat{\delta E}_y$) components relative to the wavevector $\boldsymbol{k} = k_\perp \hat{\boldsymbol{e}}_x$. Moreover, the dispersion relation is given by

$$D_{xx} D_{yy} - D_{xy} D_{yx} = 0, \tag{52}$$

where the matrix elements D_{ij} are defined in (44)–(46). In the general case, (52) does not simplify further. However, there are two limiting regimes of considerable practical interest which are now considered. The first corresponds to longitudinal

(electrostatic) Bernstein waves, and the second to extraordinary-mode transverse electromagnetic waves.

Bernstein waves. For ω and $k_\perp$ corresponding to large perpendicular index of refraction with

$$|c^2k_\perp^2/\omega^2| \gg 1, \tag{53}$$

it is straightforward to show from (44)–(46) and (53) that $|D_{yy}| \gg |D_{xx}|$ and that D_{xx} and D_{xy} are of comparable magnitude. It therefore follows from (44) and $D_{xx}D_{yy} - D_{xy}D_{yx} = 0$ that

$$\begin{aligned} D_{xx}(k_\perp, \omega) &= 1 + \sum_j \frac{\omega_{pj}^2}{\omega} \sum_{n=-\infty}^{\infty} \int d^3v\, v_\perp \frac{\left(n^2/b_j^2\right) J_n^2(b_j)}{\omega - n\omega_{cj}} \frac{\partial}{\partial v_\perp} F_j \\ &= 1 + \sum_j \frac{\omega_{pj}^2}{k_\perp^2} \sum_{n=-\infty}^{\infty} \int d^3v \frac{J_n^2(b_j)}{\omega - n\omega_{cj}} \frac{n\omega_{cj}}{v_\perp} \frac{\partial F_j}{\partial v_\perp} = 0, \end{aligned} \tag{54}$$

is a good approximation to the dispersion relation (52), where use has been made of $\sum_{n=-\infty}^{\infty} nJ_n^2(b_j) = 0$. In this case, $\widehat{\delta E}_y \simeq 0$ and the wave is primarily longitudinal (electrostatic) with electric field perturbation $\widehat{\delta \boldsymbol{E}} = \widehat{\delta E}_x \hat{\boldsymbol{e}}_x$ along the direction of propagation $\boldsymbol{k} = k_\perp \hat{\boldsymbol{e}}_x$. The Bernstein wave dispersion relation (54) clearly includes a wide range of wave propagation behavior ranging from hybrid oscillations for a cold plasma, where $1 = \omega_{pe}^2/(\omega^2 - \omega_{ce}^2) + \omega_{pi}^2/(\omega^2 - \omega_{ci}^2)$, to cyclotron harmonic waves ($\omega \simeq n\omega_{cj}$) when plasma thermal effects are important. Detailed applications and examples are discussed in Section 3.3.6.

Extraordinary-mode electromagnetic waves. For the case of a tenuous plasma with

$$\omega_{pe}^2/c^2k_\perp^2 \ll 1, \tag{55}$$

and high frequency perturbations with

$$|\omega^2/c^2k_\perp^2| \text{ of order unity}, \tag{56}$$

it is straightforward to show from (44)–(46) that the term $D_{xy}D_{yx}$ represents a small contribution to (52), and the dispersion relation $D_{xx}D_{yy} - D_{xy}D_{yx} = 0$ can be approximated by

$$D_{xx}D_{yy} = 0. \tag{57}$$

For $D_{xx} = 0$, the wave polarization corresponds to $\boldsymbol{k} = (k_\perp, 0, 0)$ and $\widehat{\delta \boldsymbol{E}} = (\widehat{\delta E}_x, 0, 0)$, and the dispersion relation reduces to the Bernstein mode dispersion relation $D_{xx} = 0$ discussed in the previous paragraph [Eq. (54)]. On the other hand, for $D_{yy} = 0$, the wave polarization is given by $\boldsymbol{k} = (k_\perp, 0, 0)$ and $\widehat{\delta \boldsymbol{E}} = (0, \widehat{\delta E}_y, 0)$ which corresponds to transverse electromagnetic wave polarization with ω and $k_\perp$ related by

$$D_{yy}(k_\perp, \omega) = 1 - \frac{c^2k_\perp^2}{\omega^2} + \sum_j \frac{\omega_{pj}^2}{\omega} \sum_{n=-\infty}^{\infty} \int d^3v\, v_\perp \frac{\left[J_n'(b_j)\right]^2}{\omega - n\omega_{cj}} \frac{\partial}{\partial v_\perp} F_j = 0. \tag{58}$$

Equation (58) supports solutions ranging from $\omega^2 = c^2k_\perp^2 + \sum_j \omega_{pj}^2\omega^2/(\omega^2 - \omega_{cj}^2)$ for a cold plasma to significant harmonic structure (for $\omega \simeq n\omega_{cj}$) when plasma thermal effects are important.

Electrostatic dispersion relation for a magnetized plasma

In the last two subsections, it has been noted that under special circumstances (e.g. large index of refraction $|c^2k^2/\omega^2| \gg 1$ or low density/short wavelength perturbations with $\omega_{pe}^2/c^2k^2 \ll 1$), the properties of the dispersion relation (22) are such that electrostatic (longitudinal) mode can decouple from the mode with transverse electromagnetic polarization. In this section, use is made of (7) and (19) to determine directly the dispersion relation for electrostatic wave perturbations with $\boldsymbol{k} \times \widehat{\delta \boldsymbol{E}} = 0$ and $\widehat{\delta \boldsymbol{E}} = -i\boldsymbol{k}\widehat{\delta\phi} = -i(k_\perp, 0, k_z)\widehat{\delta\phi}$, where $\widehat{\delta\phi}$ is the perturbed potential, and $\boldsymbol{k}$ has an arbitrary direction with respect to $\boldsymbol{B}_0\hat{\boldsymbol{e}}_z$. The Poisson equation (7) becomes

$$\widehat{\delta\phi} = \frac{4\pi\widehat{\delta\rho}}{(k_\perp^2 + k_z^2)} = 4\pi\sum_j e_j \int d^3v \frac{\widehat{\delta f_j}}{(k_\perp^2 + k_z^2)},$$

where $\widehat{\delta f_j}$ is given by (19). Substituting $\widehat{\delta \boldsymbol{E}} = -i(k_\perp, 0, k_z)\widehat{\delta\phi}$ into (19) then gives

$$D_L(\boldsymbol{k}, \omega)\widehat{\delta\phi} = 0, \tag{59}$$

where the dispersion relation for electrostatic perturbations is given by

$$D_L(\boldsymbol{k}, \omega) = 1 + \sum_j \frac{\omega_{pj}^2}{k^2} \sum_{n=-\infty}^{\infty} \int d^3v \frac{J_n^2(b_j)}{(\omega - n\omega_{cj} - k_z v_z)} \times \left(k_z \frac{\partial F_j}{\partial v_z} + \frac{n\omega_{cj}}{v_\perp} \frac{\partial F_j}{\partial v_\perp} \right) = 0, \tag{60}$$

where $k^2 = k_\perp^2 + k_z^2$, and $\mathrm{Im}\,\omega > 0$ is assumed. Equation (60) reduces directly to the electrostatic dispersion relation (38) for parallel propagation ($k_\perp = 0$) and to the Bernstein mode dispersion relation (54) for perpendicular propagation ($k_z = 0$). As discussed in Section 3.3.7, depending on the form of $F_j(v_\perp^2, v_z)$ and the region of ω- and $\boldsymbol{k}$-space under investigation, (60) can also support unstable solutions ($\mathrm{Im}\,\omega > 0$) corresponding to the modified two-stream instability and the mirror convective loss-cone instability.

Dispersion relation for an unmagnetized plasma

In circumstances where the perturbation frequency is sufficiently high and the perturbation wavelength sufficiently short that

$$|\omega| \gg |\omega_{cj}|, \qquad |k_\perp v_\perp/\omega_{cj}| \gg 1, \tag{61}$$

the particle dynamics is unaffected by the applied magnetic field $\boldsymbol{B}_0$ on the time and length scales of interest. In this case, the particle dynamics and wave propagation

properties correspond to an unmagnetized plasma with

$$\boldsymbol{B}_0 = 0 \tag{62}$$

and free-streaming particle orbits

$$\boldsymbol{x}' = \boldsymbol{x} + \boldsymbol{v}\tau, \qquad \boldsymbol{v}' = \boldsymbol{v}, \tag{63}$$

where $\tau = t' - t$. Assuming $\boldsymbol{B}_0 = 0$ in the present analysis, without loss of generality a Cartesian coordinate system is chosen with $\hat{\boldsymbol{e}}_z$ aligned along the wavevector $\boldsymbol{k}$, i.e.

$$\boldsymbol{k} = k_z \hat{\boldsymbol{e}}_z. \tag{64}$$

In addition, for $\boldsymbol{B}_0 = 0$, perturbations are considered about the class of equilibria

$$f_j^0(\boldsymbol{x}, \boldsymbol{v}) = \hat{n}_j F_j(\boldsymbol{v}), \tag{65}$$

where $\boldsymbol{v} = (v_x, v_y, v_z)$, and $F_j(\boldsymbol{v})$ is normalized according to $\int \mathrm{d}^3\boldsymbol{v} F_j(\boldsymbol{v}) = 1$. Paralleling the analysis leading to (19) and making use of (62)–(65), it is straightforward to show that the perturbed distribution function can be expressed as

$$\widehat{\delta f_j}(\boldsymbol{k}, \boldsymbol{v}, \omega) = -\mathrm{i}\frac{\hat{n}_j e_j}{m_j}\frac{1}{\omega - k_z v_z}\left\{\frac{\partial F_j}{\partial v_z}\widehat{\delta E_z} + \left[\left(1 - \frac{k_z v_z}{\omega}\right)\frac{\partial F_j}{\partial v_x} + \frac{k_z v_x}{\omega}\frac{\partial F_j}{\partial v_z}\right]\widehat{\delta E_x} + \left[\left(1 - \frac{k_z v_z}{\omega}\right)\frac{\partial F_j}{\partial v_y} + \frac{k_z v_y}{\omega}\frac{\partial F_j}{\partial v_z}\right]\widehat{\delta E_y}\right\}. \tag{66}$$

Moreover, the $\nabla \times \widehat{\delta \boldsymbol{B}}$ Maxwell equation (11) reduces to

$$\left(1 - \frac{c^2 k_z^2}{\omega^2}\right)\left(\widehat{\delta E_x}\hat{\boldsymbol{e}}_x + \widehat{\delta E_y}\hat{\boldsymbol{e}}_y\right) + \widehat{\delta E_z}\hat{\boldsymbol{e}}_z + \frac{4\pi \mathrm{i}}{\omega}\sum_j e_j \int \mathrm{d}^3\boldsymbol{v}\, \boldsymbol{v}\widehat{\delta f_j}(\boldsymbol{k}, \boldsymbol{v}, \omega) = 0, \tag{67}$$

where $\widehat{\delta f_j}(\boldsymbol{k}, \boldsymbol{v}, \omega)$ is given by (66).

One of the most important instabilities in an unmagnetized plasma is the electromagnetic Weibel instability driven by energy anisotropy in which the plasma kinetic energy perpendicular to $\boldsymbol{k} = k_z \hat{\boldsymbol{e}}_z$ exceeds the parallel kinetic energy by a sufficiently large amount. The free energy source for this instability can be provided by an anisotropy in *directed* kinetic energy (associated with the *average* motion of species j) as well as an anisotropy in *thermal* kinetic energy. To simplify the present analysis, average motion of species j in the z-direction is allowed for, but it is assumed that

$$\int_{-\infty}^{\infty} \mathrm{d}v_x\, v_x F_j(\boldsymbol{v}) = 0 = \int_{-\infty}^{\infty} \mathrm{d}v_y\, v_y F_j(\boldsymbol{v}). \tag{68}$$

That is, the *net* average motion of species j perpendicular to $\hat{\boldsymbol{e}}_z$ is assumed to be zero. However, the analysis does allow for directed motion perpendicular to $\hat{\boldsymbol{e}}_z$ provided the motion is symmetric, e.g. equidensity counter-streaming electron beams. Substituting (66) into (67) and making use of (68), it is straightforward to show that

$$D_{xy} = D_{xz} = D_{yx} = D_{yz} = D_{zx} = D_{zy} = 0, \tag{69}$$

and the remaining elements of the dielectric tensor $\langle D_{ij}(k_z,\omega)\rangle$ can be expressed as

$$D_{xx}(k_z,\omega)=1-\frac{c^2k_z^2}{\omega^2}+\sum_j\frac{\omega_{pj}^2}{\omega}\int d^3v\,\frac{v_x}{\omega-k_zv_z}\left[\left(1-\frac{k_zv_z}{\omega}\right)\frac{\partial F_j}{\partial v_x}+\frac{k_zv_x}{\omega}\frac{\partial F_j}{\partial v_z}\right], \tag{70}$$

$$D_{yy}(k_z,\omega)=1-\frac{c^2k_z^2}{\omega^2}+\sum_j\frac{\omega_{pj}^2}{\omega}\int d^3v\,\frac{v_y}{\omega-k_zv_z}\left[\left(1-\frac{k_zv_z}{\omega}\right)\frac{\partial F_j}{\partial v_y}+\frac{k_zv_y}{\omega}\frac{\partial F_j}{\partial v_z}\right], \tag{71}$$

$$\begin{aligned}D_{zz}(k_z,\omega)&=1+\sum_j\frac{\omega_{pj}^2}{\omega}\int d^3v\,\frac{v_z}{\omega-k_zv_z}\frac{\partial F_j}{\partial v_z}\\&=1+\sum_j\frac{\omega_{pj}^2}{k_z^2}\int d^3v\,\frac{k_z\partial F_j/\partial v_z}{\omega-k_zv_z},\end{aligned} \tag{72}$$

where $\omega_{pj}^2=4\pi\hat{n}_je_j^2/m_j$, and $\mathrm{Im}\,\omega>0$ is assumed.

Making use of (69)–(72), the dispersion relation $\det\{D_{ij}(k_z,\omega)\}=0$ for an unmagnetized plasma can be expressed as

$$D_{xx}D_{yy}D_{zz}=0. \tag{73}$$

There are two classes of solutions to (73). The first class, with dispersion relation

$$\begin{aligned}D_{xx}(k_z,\omega)&=1-\frac{c^2k_z^2}{\omega^2}+\sum_j\frac{\omega_{pj}^2}{\omega}\int d^3v\,\frac{v_x}{\omega-k_zv_z}\left[\left(1-\frac{k_zv_z}{\omega}\right)\frac{\partial F_j}{\partial v_x}+\frac{k_zv_x}{\omega}\frac{\partial F_j}{\partial v_z}\right]\\&=0,\end{aligned} \tag{74}$$

or

$$\begin{aligned}D_{yy}(k_z,\omega)&=1-\frac{c^2k_z^2}{\omega^2}+\sum_j\frac{\omega_{pj}^2}{\omega}\int d^3v\,\frac{v_y}{\omega-k_zv_z}\left[\left(1-\frac{k_zv_z}{\omega}\right)\frac{\partial F_j}{\partial v_y}+\frac{k_zv_y}{\omega}\frac{\partial F_j}{\partial v_z}\right]\\&=0,\end{aligned} \tag{75}$$

corresponds to purely *transverse electromagnetic* branches with *plane wave* polarizations $\widehat{\delta\boldsymbol{E}}=(\widehat{\delta E}_x,0,0)$ and $\widehat{\delta\boldsymbol{E}}=(0,\widehat{\delta E}_y,0)$, respectively. The second branch, with dispersion relation

$$D_{zz}(k_z,\omega)=1+\sum_j\frac{\omega_{pj}^2}{k_z^2}\int d^3v\,\frac{k_z\partial F_j/\partial v_z}{\omega-k_zv_z}=0, \tag{76}$$

corresponds to an *electrostatic* branch with *longitudinal* polarization $\boldsymbol{k}=(0,0,k_z)$ and $\widehat{\delta\boldsymbol{E}}=(0,0,\widehat{\delta E}_z)$. Depending on the choice of $F_j(\boldsymbol{v})$, (74)–(76) support a broad range of electromagnetic and electrostatic plasma waves and instabilities characteristic of a spatially uniform, unmagnetized plasma (Sections 3.3.3 and 3.3.4).

To conclude this section, the special case is considered where $F_j(\boldsymbol{v})$ is isotropic in the plane perpendicular to $\hat{\boldsymbol{e}}_z$, i.e.

$$F_j(\boldsymbol{v}) = F_j\left(v_\perp^2, v_z\right), \tag{77}$$

where $v_\perp^2 = v_x^2 + v_y^2$. In this case, D_{xx} and D_{yy} can be expressed as

$$\begin{aligned} D_{xx}(k_z,\omega) &= D_{yy}(k_z,\omega) \\ &= 1 - \frac{c^2k_z^2}{\omega^2} + \sum_j \frac{\omega_{pj}^2}{2\omega}\int \mathrm{d}^3v \frac{v_\perp}{\omega - k_z v_z} \\ &\quad \times\left[\left(1 - \frac{k_z v_z}{\omega}\right)\frac{\partial}{\partial v_\perp}F_j\left(v_\perp^2, v_z\right) + \frac{k_z v_\perp}{\omega}\frac{\partial}{\partial v_z}F_j\left(v_\perp^2, v_z\right)\right]. \end{aligned} \tag{78}$$

The definitions of D_{xx} and D_{yy} in (78) are a special case of (74) and (75), valid for distribution functions $F_j(v_\perp^2, v_z)$ isotropic in the plane perpendicular to $\hat{\boldsymbol{e}}_z$. The difference in wave propagation is evident. For general $F_j(\boldsymbol{v})$ subject to (68), it is clear from (74) and (75) that the two transverse electromagnetic dispersion relations, $D_{xx} = 0$ and $D_{yy} = 0$, correspond to two independent *plane-wave* polarizations (with $\widehat{\delta E}_x \neq 0$ and $\widehat{\delta E}_y \neq 0$, respectively) with different wave propagation properties. For $F_j(\boldsymbol{v}) = F_j(v_\perp^2, v_z)$, however, it follows that $D_{xx} = D_{yy}$ [Eq. (78)], and the dispersion relations $D_{xx} = 0$ and $D_{yy} = 0$ are identical. The wave polarization in this case is *elliptical* with $\boldsymbol{k} = (0, 0, k_z)$ and $\widehat{\delta \boldsymbol{E}} = (\widehat{\delta E}_x, \widehat{\delta E}_y, 0)$, where the ratio $\widehat{\delta E}_y/\widehat{\delta E}_x$ is arbitrary.

Electrostatic dispersion relation for an unmagnetized plasma

In circumstances where $\boldsymbol{B}_0 = 0$ and the wave polarization is assumed to be longitudinal with $\boldsymbol{k} \times \widehat{\delta \boldsymbol{E}} = 0$, the derivation of the electrostatic dispersion relation simplifies at the outset. Expressing $\widehat{\delta \boldsymbol{E}} = -\mathrm{i}\boldsymbol{k}\widehat{\delta\phi}$ where $\widehat{\delta\phi}$ is the perturbed potential, (12) reduces to

$$\widehat{\delta f_j}(\boldsymbol{k}, \boldsymbol{v}, \omega) = -\frac{\hat{n}_j e_j}{m_j}\frac{\boldsymbol{k}\cdot\partial F_j/\partial \boldsymbol{v}}{(\omega - \boldsymbol{k}\cdot\boldsymbol{v})}\widehat{\delta\phi}(\boldsymbol{k}, \omega). \tag{79}$$

Poisson's equation $k^2\widehat{\delta\phi} = 4\pi\Sigma_j e_j \int \mathrm{d}^3v\, \widehat{\delta f_j}$ then becomes

$$D(\boldsymbol{k}, \omega)\widehat{\delta\phi} = 0, \tag{80}$$

and the Landau dispersion relation for longitudinal perturbations is given by

$$D(\boldsymbol{k}, \omega) = 1 + \sum_j \frac{\omega_{pj}^2}{k^2}\int \mathrm{d}^3v \frac{\boldsymbol{k}\cdot\partial F_j/\partial \boldsymbol{v}}{\omega - \boldsymbol{k}\cdot\boldsymbol{v}} = 0, \tag{81}$$

where $\mathrm{Im}\,\omega > 0$ is assumed. Of course, (76) is a special case of (81) with wavevector $\boldsymbol{k}$ prescribed by $\boldsymbol{k} = k_z\hat{\boldsymbol{e}}_z$. Depending on the choice of distribution function $F_j(\boldsymbol{v})$ and on the regions of ω- and $\boldsymbol{k}$-space under investigation, (81) supports a wide variety of electrostatic plasma waves and instabilities, including ion waves, the ion acoustic instability, electron plasma oscillations, electrostatic two-stream instabilities, etc.

Specific examples of waves and instabilities associated with (81) are discussed in Section 3.3.3.

3.3.2. *Sufficient condition for stability of spatially uniform equilibria*

In this section, the general class of isotropic equilibria

$$F_j(v_\perp^2, v_z) = F_j(v_\perp^2 + v_z^2) \tag{82}$$

in a magnetized plasma are considered and use is made of the Vlasov–Maxwell equations to derive a sufficient condition for stability of the equilibrium to small-amplitude electromagnetic perturbations with arbitrary polarization. The starting point in this analysis is the nonlinear Vlasov equation

$$\left[\frac{\partial}{\partial t} + \boldsymbol{v}\cdot\frac{\partial}{\partial \boldsymbol{x}} + \frac{e_j}{m_j}\left(\delta\boldsymbol{E}(\boldsymbol{x},t) + \frac{\boldsymbol{v}\times[B_0\hat{\boldsymbol{e}}_z + \delta\boldsymbol{B}(\boldsymbol{x},t)]}{c}\right)\cdot\frac{\partial}{\partial \boldsymbol{v}}\right] f_j(\boldsymbol{x},\boldsymbol{v},t) = 0, \tag{83}$$

where $\delta\boldsymbol{E}(x,t)$ and $\delta\boldsymbol{B}(x,t)$ are determined self-consistently in terms of $f_j(\boldsymbol{x},\boldsymbol{v},t)$ from Maxwell's equations. Here, the distribution function is expressed as its equilibrium value plus a perturbation, i.e.

$$f_j(\boldsymbol{x},\boldsymbol{v},t) = \hat{n}_j F_j(v_\perp^2 + v_z^2) + \delta f_j(\boldsymbol{x},\boldsymbol{v},t), \tag{84}$$

where $\hat{n}_j$ = constant is the ambient density of species j. An exact consequence of the fully nonlinear Vlasov–Maxwell equations is the conservation of total (field plus particle kinetic) energy integrated over the region of phase space $(\boldsymbol{x},\boldsymbol{v})$ occupied by the plasma. In addition, it is readily shown that $(\mathrm{d}/\mathrm{d}t)\int \mathrm{d}^3\boldsymbol{x}\int \mathrm{d}^3\boldsymbol{v}\,G(f_j) = 0$ is an exact consequence of (83), where $G(f_j)$ is a smooth, differentiable function of f_j. Making use of energy conservation and $\int \mathrm{d}^3\boldsymbol{x}\int \mathrm{d}^3\boldsymbol{v}\,G(f_j)$ = constant, it is straightforward to construct the conserved quantity C defined by

$$C = \int \mathrm{d}^3\boldsymbol{x}\left(\frac{(\delta\boldsymbol{E})^2 + (\delta\boldsymbol{B})^2}{8\pi} + \sum_j \int \mathrm{d}^3\boldsymbol{v}\left[\frac{1}{2}m_j(v_\perp^2 + v_z^2)(f_j - \hat{n}_j F_j) + G(f_j) - G(\hat{n}_j F_j)\right]\right), \tag{85}$$

where $\mathrm{d}C/\mathrm{d}t = 0$. In (85), $f_j = \hat{n}_j F_j + \delta f_j$, and the arguments of $\delta\boldsymbol{E}(\boldsymbol{x},t)$, $\delta\boldsymbol{B}(\boldsymbol{x},t)$, $f_j(\boldsymbol{x},\boldsymbol{v},t)$ and $F_j(v_\perp^2 + v_z^2)$ have been suppressed. Note that the constancy of C is an exact consequence of the fully nonlinear Vlasov–Maxwell equations.

Now consider small-amplitude perturbations. Taylor-expanding $G(f_j) = G(\hat{n}_j F_j + \delta f_j)$ for small δf_j gives

$$G(f_j) = G(\hat{n}_j F_j) + G'(\hat{n}_j F_j)\,\delta f_j + G''(\hat{n}_j F_j)\frac{(\delta f_j)^2}{2} + \cdots \tag{86}$$

Correct to second order in the perturbation amplitude, (85) can be expressed as

$$C^{(2)} = \int d^3x \left[\frac{(\delta \boldsymbol{E})^2 + (\delta \boldsymbol{B})^2}{8\pi} + \sum_j \int d^3v \left(\frac{m_j}{2}(v_\perp^2 + v_z^2) + G'(\hat{n}_j F_j) \right) \delta f_j \right.$$
$$\left. + \sum_j \int d^3v G''(\hat{n}_j F_j) \frac{(\delta f_j)^2}{2} \right]. \tag{87}$$

The function $G(\hat{n}_j F_j)$, which has been arbitrary up to this point, is now chosen to satisfy

$$G'(\hat{n}_j F_j) = -\tfrac{1}{2} m_j (v_\perp^2 + v_z^2). \tag{88}$$

Equation (88) implies that the term linear in δf_j vanishes in (87), and $C^{(2)}$ reduces to

$$C^{(2)} = \int d^3x \left(\frac{(\delta \boldsymbol{E})^2 + (\delta \boldsymbol{B})^2}{8\pi} + \sum_j \int d^3v G''(\hat{n}_j F_j) \frac{(\delta f_j)^2}{2} \right). \tag{89}$$

Differentiating (88) with respect to $\hat{n} F_j$ gives

$$G''(\hat{n}_j F_j) = -\frac{m_j / 2\hat{n}_j}{\partial F_j / \partial v^2}, \tag{90}$$

where $v^2 \equiv v_\perp^2 + v_z^2$. Substituting (90) into (89), $C^{(2)}$ can be expressed in the equivalent form

$$C^{(2)} = \int d^3x \left[\frac{(\delta \boldsymbol{E})^2 + (\delta \boldsymbol{B})^2}{8\pi} + \sum_j \frac{m_j}{4\hat{n}_j} \int d^3v (\delta f_j)^2 \left(\frac{-1}{\partial F_j / \partial v^2} \right) \right]. \tag{91}$$

If

$$\partial F_j / \partial v^2 \leqslant 0, \tag{92}$$

it follows from (91) that $C^{(2)}$ is a sum of non-negative terms. Since C is a constant, the perturbations $\delta \boldsymbol{E}(\boldsymbol{x}, t)$, $\delta \boldsymbol{B}(\boldsymbol{x}, t)$ and $\delta f_j(\boldsymbol{x}, \boldsymbol{v}, t)$ cannot grow without bound when (92) is satisfied. Therefore, a sufficient condition for linear stability can be stated as follows: If $F_j(v_\perp^2 + v_z^2)$ is a monotonic decreasing function of $(v_\perp^2 + v_z^2)$ for all plasma components j, the equilibrium is stable to small-amplitude electromagnetic perturbations with arbitrary polarization. This is a statement of Newcomb's theorem for perturbations about a spatially uniform plasma immersed in a uniform magnetic field $B_0 \hat{\boldsymbol{e}}_z$.

Important generalizations of the preceding analysis can be made. For example, the stability theorem can be extended to show that $\partial F_j / \partial v^2 \leqslant 0$, for each j, is a sufficient condition for *nonlinear* stability of F_j to arbitrary-amplitute perturbations. In addition, for a radially confined, fully nonneutral electron plasma column it can be shown that $\partial f_e^0(H - \omega_r P_\theta) / \partial (H - \omega_r P_\theta) \leqslant 0$ is a sufficient condition for stability, where H is the energy, P_θ is the canonical angular momentum, and ω_r = constant is the angular rotation frequency.

3.3.3. Electrostatic waves and instabilities in an unmagnetized plasma

It is evident from the discussion in Section 3.3.2 that instability ($\mathrm{Im}\,\omega > 0$) is necessarily associated with nonthermal equilibrium features in which the distribution function $F_j(v)$ departs from being a monotonically decreasing function of v^2. That is, the free energy source for wave amplification is provided by the relative directed motion between plasma components and/or an anisotropy in plasma kinetic energy. In this section, a variety of longitudinal plasma waves and instabilities in an unmagnetized plasma are investigated, making use of the electrostatic dispersion relation (81).

It is important to note that the stability analysis presented in Section 3.3.3 is also valid for the case of electrostatic waves propagating *parallel* to a uniform magnetic field $\boldsymbol{B}_0 = B_0\hat{\boldsymbol{e}}_z$ with $B_0 \neq 0$. This follows since the longitudinal dispersion relation $D_{zz}(\boldsymbol{k}, \omega) = 0$ in (38) is identical to (81) for $\boldsymbol{k} = k_z\hat{\boldsymbol{e}}_z$ and $F_j(v) = F_j(v_\perp^2, v_z)$.

Weak electrostatic instability

Defining $\omega = \omega_r + i\gamma$, where $\omega_r = \mathrm{Re}\,\omega$ is the real oscillation frequency and $\gamma = \mathrm{Im}\,\omega$ is the growth rate, with $\gamma > 0$ corresponding to instability, the electrostatic dispersion relation (81) for an unmagnetized plasma can be expressed as

$$D(\boldsymbol{k}, \omega_r + i\gamma) = 0, \tag{93}$$

where the Landau dielectric function is defined by

$$D(\boldsymbol{k}, \omega_r + i\gamma) = 1 + \sum_j \frac{\omega_{pj}^2}{k^2} \int d^3v \frac{\boldsymbol{k} \cdot \partial F_j / \partial \boldsymbol{v}}{\omega_r - \boldsymbol{k} \cdot \boldsymbol{v} + i\gamma} \tag{94}$$

for $\mathrm{Im}\,\omega = \gamma > 0$. Defining $D_r = \mathrm{Re}\,D(\boldsymbol{k}, \omega_r + i\gamma)$ and $D_i = \mathrm{Im}\,D(\boldsymbol{k}, \omega_r + i\gamma)$, and Taylor-expanding $D = D_r + iD_i = 0$ for weak instability (small γ and D_i), it is straightforward to show that the dispersion relation (93) can be expressed as

$$0 = D_r(\boldsymbol{k}, \omega_r) + i\left(\gamma \frac{\partial}{\partial \omega_r} D_r(\boldsymbol{k}, \omega_r) + D_i(\boldsymbol{k}, \omega_r)\right) + \cdots. \tag{95}$$

Making use of

$$\lim_{\gamma \to 0_+} \frac{1}{\omega_r - \boldsymbol{k} \cdot \boldsymbol{v} + i\gamma} = \mathrm{P}\frac{1}{\omega_r - \boldsymbol{k} \cdot \boldsymbol{v}} - i\pi\delta(\omega_r - \boldsymbol{k} \cdot \boldsymbol{v}), \tag{96}$$

where P denotes *Cauchy* principal value, and setting the real and imaginary parts of (95) equal to zero gives

$$D_r(\boldsymbol{k}, \omega_r) = 1 + \sum_j \frac{\omega_{pj}^2}{k^2} \mathrm{P} \int d^3v \frac{\boldsymbol{k} \cdot \partial F_j / \partial \boldsymbol{v}}{\omega_r - \boldsymbol{k} \cdot \boldsymbol{v}} = 0, \tag{97}$$

and

$$\gamma = -\frac{D_i(\boldsymbol{k}, \omega_r)}{\partial D_r(\boldsymbol{k}, \omega_r)/\partial \omega_r}$$

$$= \left(\pi \sum_j \frac{\omega_{pj}^2}{k^2} \int d^3v\, \delta(\omega_r - \boldsymbol{k}\cdot\boldsymbol{v})\, \boldsymbol{k}\cdot\frac{\partial F_j}{\partial \boldsymbol{v}} \right) \left(-\sum_j \frac{\omega_{pj}^2}{k^2} P\int d^3v \frac{\boldsymbol{k}\cdot\partial F_j/\partial \boldsymbol{v}}{(\omega_r - \boldsymbol{k}\cdot\boldsymbol{v})^2} \right)^{-1}. \tag{98}$$

For specified equilibrium distribution $F_j(\boldsymbol{v})$, (97) determines the real oscillation frequency ω_r, and (98) determines the growth rate γ for the case of weak instability or damping (e.g. $|\gamma| \ll |\omega_r|$ or $|kV_j|$, where V_j is the characteristic speed of species j). Two important symmetries follow directly from (97) and (98). In particular,

$$\omega_r(-\boldsymbol{k}) = -\omega_r(\boldsymbol{k}), \qquad \gamma(-\boldsymbol{k}) = \gamma(\boldsymbol{k}), \tag{99}$$

are self-consistent consequences of (97) and (98) and are directly related to the fact that the perturbed electric field $\delta\boldsymbol{E}(\boldsymbol{x}, t)$ is a real-valued function in (3).

Equations (97) and (98) will be used later in Section 3.3.3 to determine the (weak) growth and damping increments for a variety of electrostatic plasma waves and instabilities including electron plasma oscillations, the bump-in-tail instability, ion waves, and the ion acoustic instability. For present purposes, we summarize the implications of (97) and (98) in circumstances where $F_j(\boldsymbol{v})$ is isotropic with

$$F_j(\boldsymbol{v}) = F_j(v^2), \tag{100}$$

where $v^2 = v_x^2 + v_y^2 + v_z^2$. Making use of $\boldsymbol{k}\cdot\partial F_j(v^2)/\partial \boldsymbol{v} = 2\boldsymbol{k}\cdot\boldsymbol{v}(\partial F_j/\partial v^2)$, (97) and (98) can be expressed as

$$D_r(\boldsymbol{k}, \omega_r) = 1 + \sum_j \frac{\omega_{pj}^2}{k^2} P\int d^3v \frac{2\boldsymbol{k}\cdot\boldsymbol{v}\left(\partial F_j/\partial v^2\right)}{\omega_r - \boldsymbol{k}\cdot\boldsymbol{v}} = 0, \tag{101}$$

and

$$\gamma = \frac{2\pi\omega_r^2 \Sigma_j \left(\omega_{pj}^2/k^2\right) \int d^3v\, \delta(\omega_r - \boldsymbol{k}\cdot\boldsymbol{v})\, \partial F_j/\partial v^2}{\omega_r \partial D_r/\partial \omega_r}. \tag{102}$$

For positive energy waves with $\omega_r \partial D_r/\partial \omega_r > 0$, it is clear from (102) that $\partial F_j/\partial v^2 \leqslant 0$ is a sufficient condition for stability ($\gamma \leqslant 0$), which constitutes a *direct* proof of Newcomb's theorem (Section 3.3.2) in the special case where $\boldsymbol{B}_0 = 0$ and the wave polarization is electrostatic.

The plasma dispersion function

In many applications of interest, the distribution function $F_j(\boldsymbol{v})$ can be approximated by a drifting Maxwellian

$$F_j(\boldsymbol{v}) = \left(\frac{m_j}{2\pi T_j}\right)^{3/2} \exp\left(-\frac{m_j}{2T_j}(\boldsymbol{v} - \boldsymbol{V}_j)^2 \right), \tag{103}$$

where $V_j = \int d^3v\, v F_j$ is the mean velocity, and $T_j = \frac{2}{3}\int d^3v[m_j(v-V_j)^2/2]F_j$ is the temperature of species j. In this case, the velocity integral in the electrostatic dielectric function $D(k, \omega_r + i\gamma)$ defined in (94) can be expressed as

$$\frac{\omega_{pj}^2}{k^2}\int d^3v \frac{k\cdot\partial F_j/\partial v}{\omega_r - k\cdot v + i\gamma} = \frac{2\omega_{pj}^2}{k^2 v_{Tj}^2}\left[1 + \xi_j Z(\xi_j)\right], \tag{104}$$

where

$$Z(\xi_j) = \pi^{-1/2}\int_{-\infty}^{\infty} dx \frac{\exp(-x^2)}{x - \xi_j}, \tag{105}$$

and

$$\xi_j = \frac{\omega_r - k\cdot V_j + i\gamma}{k v_{Tj}}, \tag{106}$$

with $\gamma = \mathrm{Im}\,\omega > 0$. In (104)–(106) $k = k\hat{e}_z$ has been chosen without loss of generality. Moreover, $v_{Tj} \equiv (2T_j/m_j)^{1/2}$ is the thermal speed of species j. The function $Z(\xi_j)$ defined in (105) is referred to as the *plasma dispersion function*. Important for subsequent applications are the asymptotic expansions of $Z(\xi_j)$ for large and small values of $|\xi_j|$, i.e.

$$Z(\xi_j) \simeq -\frac{1}{\xi_j} - \frac{1}{2\xi_j^3} - \frac{3}{4\xi_j^5} - \cdots, \qquad \text{for } |\xi_j| \gg 1, \tag{107}$$

and

$$Z(\xi_j) = -2\xi_j + \frac{4}{3}\xi_j^3 - \cdots + i\sqrt{\pi}\frac{k}{|k|}\exp(-\xi_j^2), \qquad \text{for } |\xi_j| \ll 1. \tag{108}$$

Note that (107) is a valid approximation in the cold-plasma limit with $v_{Tj} = (2T_j/m_j)^{1/2} \to 0$, or in the limit of large relative phase velocity with $|\omega_r - k\cdot V_j + i\gamma|/|k v_{Tj}| \gg 1$. Equations (104)–(108) will be used to investigate detailed stability properties for drifting Maxwellian distributions in a variety of regimes of practical interest.

Electron plasma oscillations and the bump-in-tail instability

As a first example, consider the case of a weak electron beam drifting through a background plasma of Maxwellian electrons and ions with distribution functions (Fig. 3.3.2):

$$F_e(v) = (1-\epsilon)\left(\frac{m_e}{2\pi T_e}\right)^{2/3}\exp\left(-\frac{m_e v^2}{2T_e}\right) + \epsilon\left(\frac{m_e}{2\pi T_b}\right)^{3/2}\exp\left(-\frac{m_e}{2T_b}(v - V_b)^2\right), \tag{109}$$

$$F_i(v) = \left(\frac{m_i}{2\pi T_i}\right)^{3/2}\exp\left(-\frac{m_i v^2}{2T_i}\right), \tag{110}$$

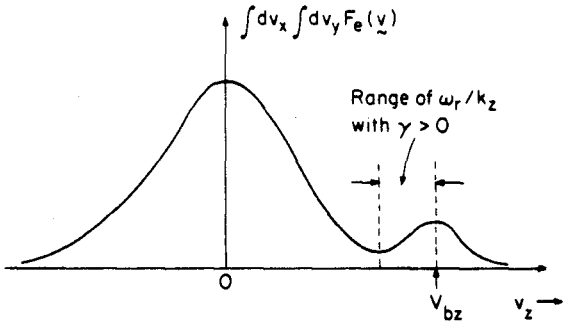

Fig. 3.3.2. Plot of reduced electron distribution functions $\int_{-\infty}^{\infty} dv_x \int_{-\infty}^{\infty} dv_y F_e(v)$ versus v_z for bump-in-tail instability [Eq. (109)].

where $\epsilon = \hat{n}_b/\hat{n}_e \ll 1$ and $|V_b| \gg v_{Te} = (2T_e/m_e)^{1/2}$ are assumed. Without loss of generality, the wavevector $\boldsymbol{k}$ is taken to be in the z-direction with

$$\boldsymbol{k} = k\hat{\boldsymbol{e}}_z, \tag{111}$$

and the component of $\boldsymbol{V}_b$ along $\hat{\boldsymbol{e}}_z$ is denoted by $V_{bz} = \boldsymbol{V}_b \cdot \hat{\boldsymbol{e}}_z$. In this section, high-frequency perturbations are considered and the positive ions are treated as a stationary background with

$$m_i \to \infty, \qquad |\xi_i| \to \infty. \tag{112}$$

It is also assumed that the waves are weakly damped or growing,

$$|\gamma| \ll |\omega_r|, \tag{113}$$

and that the wave phase velocity is large in comparison with the bulk electron thermal speed, i.e. $|\xi_e| \gg 1$ and

$$|\omega_r/k| \gg v_{Te} = (2T_e/m_e)^{1/2}. \tag{114}$$

Weakly damped electron plasma oscillations. In the absence of electron beam,

$$\epsilon = \hat{n}_b/\hat{n}_e = 0, \tag{115}$$

it is straightforward to show from (97), (104), (107) and (109)–(114) that the real oscillation frequency ω_r is determined from

$$D_r(\boldsymbol{k}, \omega_r) = 1 - \frac{\omega_{pe}^2}{\omega_r^2} - 3k^2\lambda_D^2 \frac{\omega_{pe}^4}{\omega_r^4} \cdots = 0, \tag{116}$$

where $\lambda_D^2 = T_e/4\pi\hat{n}_e e^2 = v_{Te}^2/2\omega_{pe}^2$ is the electron Debye length squared, and $k^2\lambda_D^2 \ll 1$ is assumed. Solving iteratively for ω_r^2, (116) gives

$$\omega_r^2 = \omega_{pe}^2(1 + 3k^2\lambda_D^2 + \cdots), \tag{117}$$

which is the familiar Bohm–Gross dispersion relation for electron plasma oscillations with (weak) thermal corrections. Moreover, for $\epsilon = 0$, $m_i \to \infty$ and $k^2\lambda_D^2 \ll 1$, it follows directly from (98), (109) and (116) that the Landau damping increment

($\gamma_L < 0$) is given by

$$\gamma_L = -\left(\frac{\pi}{8}\right)^{1/2}\left(\frac{m_e}{T_e}\right)^{3/2}\frac{\omega_r^4}{k^2|k|}\exp\left(-\frac{m_e}{2T_e}\frac{\omega_r^2}{k^2}\right). \tag{118}$$

For $\omega_r^2 = \omega_{pe}^2(1+3k^2\lambda_D^2+\cdots)$ and $k^2\lambda_D^2 \ll 1$, (118) can be approximated by

$$\frac{\gamma_L}{\omega_{pe}} = -\left(\frac{\pi}{8}\right)^{1/2}\frac{1}{k^2|k|\lambda_D^3}\exp\left(-\frac{1}{2k^2\lambda_D^2}-\frac{3}{2}\right). \tag{119}$$

Note that the damping is weak with $|\gamma_L/\omega_{pe}| \ll 1$. Moreover, $\omega_r^2/k^2v_{Te}^2 \simeq 1/(2k^2\lambda_D^2) \gg 1$, and the wave phase velocity is large in comparison with the bulk electron thermal speed, as assumed in (114).

Bump-in-tail instability. Electrostatic stability properties in the presence of a weak beam are now examined with $\epsilon \neq 0$, where $\epsilon = \hat{n}_b/\hat{n}_e \ll 1$ and $|V_b| \gg v_{Te} = (2T_e/m_e)^{1/2}$ are assumed. Paralleling the analysis in the previous paragraph, it is straightforward to show for $\epsilon \ll 1$ that the real oscillation frequency is determined to good accuracy from (116) and (117). Moreover, for $|\gamma/\omega_r| \ll 1$, substituting (109) and (116) into (98) with $\partial D_r/\partial\omega_r \simeq 2\omega_{pe}^2/\omega_r^3$, it is readily shown that the growth rate γ can be approximated by

$$\begin{aligned}\gamma &= \gamma_L + \gamma_b \\ &= \left(\frac{\pi}{8}\right)^{1/2}\left(\frac{m_e}{T_e}\right)^{3/2}\frac{\omega_r^4}{k^2|k|}\left\{-(1-\epsilon)\exp\left(-\frac{m_e}{2T_e}\frac{\omega_r^2}{k^2}\right)\right. \\ &\qquad \left.+\epsilon\left(\frac{T_e}{T_b}\right)^{3/2}\left(\frac{kV_{bz}-\omega_r}{\omega_r}\right)\exp\left[-\frac{m_e}{2T_b}\left(\frac{\omega_r - kV_{bz}}{k}\right)^2\right]\right\},\end{aligned} \tag{120}$$

where $\omega_r^2 = \omega_{pe}^2(1+3k^2\lambda_D^2+\cdots)$ and $\boldsymbol{k}\cdot\boldsymbol{V}_b = kV_{bz}$. The first term γ_L on the right-hand side of (120) corresponds to Landau damping ($\gamma_L < 0$) of the electron plasma oscillations by the bulk electrons [Eq. (118)]. The second term γ_b on the right-hand side of (120) is associated with the beam electrons and corresponds to wave growth ($\gamma_b > 0$) whenever the phase velocity ω_r/k is smaller than the z-component of the beam velocity V_{bz} (Fig. 3.3.2). Indeed, it follows directly from (120) that

$$\gamma_b \gtrless 0 \quad \text{for} \quad kV_{bz}/\omega_r \gtrless 1. \tag{121}$$

Note also from (120) and (121) that the beam contribution corresponds to damping ($\gamma_b < 0$) when the direction of beam propagation is perpendicular to the wavevector $\boldsymbol{k} = k\hat{\boldsymbol{e}}_z$, i.e. when $V_{bz} = 0$.

Because $\omega_r^2/k^2v_{Te}^2 \simeq \omega_{pe}^2/k^2v_{Te}^2 = 1/(2k^2\lambda_D^2) \gg 1$, it follows that the bulk electron contribution in (120) is exponentially small. Therefore, for wave phase velocity comparable with V_{bz}, for example $|\omega_r/k - V_{bz}| \lesssim 2v_{Tb} = 2(2T_b/m_e)^{1/2}$, it is clear that the beam contribution in (120) dominates for modest values of ϵ, and the growth rate γ can be approximated by

$$\gamma = \sqrt{\pi}\,\frac{\hat{n}_b}{\hat{n}_e}\frac{\omega_r^4}{k^2|k|v_{Tb}^3}\left(\frac{kV_{bz}}{\omega_r}-1\right)\exp\left[-\left(\frac{\omega_r - kV_{bz}}{kv_{Tb}}\right)^2\right], \tag{122}$$

where $v_{Tb} = (2T_b/m_e)^{1/2}$ and $\omega_r^2 = \omega_{pe}^2(1 + 3k^2\lambda_D^2 + \cdots)$. It is clear from (122) that the maximum growth rate occurs for

$$V_{bz} - \omega_r/k = +v_{Tb}/\sqrt{2}, \tag{123}$$

and the characteristic maximum growth rate is given by

$$|\gamma|_{max} = |\omega_r|\left(\frac{\pi}{2}\right)^{1/2}\frac{\hat{n}_b}{\hat{n}_e}\frac{\omega_r^2}{k^2 v_{Tb}^2}\exp(-1/2) \simeq \omega_{pe}\left(\frac{\pi}{2}\right)^{1/2}\frac{\hat{n}_b}{\hat{n}_e}\frac{V_{bz}^2}{v_{Tb}^2}\exp(-1/2), \tag{124}$$

where $\omega_r^2 \simeq \omega_{pe}^2$ and $\omega_r^2 \simeq k^2 V_{bz}^2$ have been approximated in (124). Strictly speaking, the maximum growth estimate in (124) is valid for $V_{bz}^2 \gg v_{Te}^2$. Moreover, $(\hat{n}_b/\hat{n}_e)(V_{bz}^2/v_{Tb}^2) \ll 1$ is required to assure validity of the assumption that the instability is weak with $|\gamma/\omega_r| \ll 1$.

Ion waves and the ion acoustic instability

In this section, electrostatic stability properties are examined in circumstances where there is a (small) relative drift between the plasma electrons and ions. It is assumed that the equilibrium distribution functions can be represented as Maxwellian electrons drifting through a stationary Maxwellian ion background (Fig. 3.3.3),

$$F_e(v) = \left(\frac{m_e}{2\pi T_e}\right)^{3/2}\exp\left(-\frac{m_e}{2T_e}(v - V_e)^2\right), \tag{125}$$

$$F_i(v) = \left(\frac{m_i}{2\pi T_i}\right)^{3/2}\exp\left(-\frac{m_i}{2T_i}v^2\right), \tag{126}$$

where

$$|V_e| \ll v_{Te} = (2T_e/m_e)^{1/2} \tag{127}$$

is assumed in the low-drift-velocity regime. As in the subsection on the plasma dispersion function, it is assumed that the growth rate is small with $|\gamma/\omega_r| \ll 1$, and

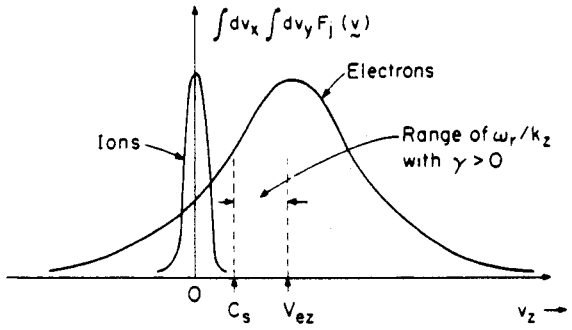

Fig. 3.3.3. Plot of reduced electron and ion distribution functions $\int_{-\infty}^{\infty} dv_x \int_{-\infty}^{\infty} dv_y F_j(v)$ versus v_z for ion acoustic instability [(125) and (126)].

the wavevector $\boldsymbol{k}$ is taken to be in the z-direction with $\boldsymbol{k} = k\hat{\boldsymbol{e}}_z$. Moreover, consistent with the assumption of weak growth (or damping), it is assumed that the electrons are hot in comparison with the ions in the present analysis, i.e.

$$T_e \gg T_i. \tag{128}$$

Substituting (125) and (126) into (94) and making use of (104), it is straightforward to show that the electrostatic dispersion relation (93) can be expressed as

$$D(\boldsymbol{k}, \omega_r + i\gamma) = 1 + \frac{2\omega_{pi}^2}{k^2 v_{Ti}^2}\left[1 + \xi_i Z(\xi_i)\right] + \frac{2\omega_{pe}^2}{k^2 v_{Te}^2}\left[1 + \xi_e Z(\xi_e)\right] = 0, \tag{129}$$

where $Z(\xi_i)$ is the plasma dispersion function defined in (105), and ξ_e and ξ_i are defined by

$$\xi_e = \frac{\omega_r - kV_{ez} + i\gamma}{kv_{Te}}, \qquad \xi_i = \frac{\omega_r + i\gamma}{kv_{Ti}}, \tag{130}$$

where $v_{Tj} = (2T_j/m_j)^{1/2}$ and $\boldsymbol{k} \cdot \boldsymbol{V}_e = kV_{ez}$. Within the context of (127) and (128), the dispersion relation (129) supports weakly growing or damped solutions with $|\gamma/\omega_r| \ll 1$ for phase velocities in the range

$$|\omega_r/k| \gg v_{Ti}, \qquad |\omega_r/k - V_{ez}| \ll v_{Te} \tag{131}$$

Making use of the asymptotic expansions of $Z(\xi_j)$ given in (107) and (108) for $|\xi_i| \gg 1$ and $|\xi_e| \ll 1$, it is straightforward to show that the real oscillation frequency ω_r is determined from the approximation dispersion relation

$$D_r(\boldsymbol{k}, \omega_r) = 1 - \frac{\omega_{pi}^2}{\omega_r^2} + \frac{1}{k^2\lambda_D^2} = 0, \tag{132}$$

where $D_r(\boldsymbol{k}, \omega_r)$ is defined in (97), and $\lambda_D^2 = T_e/4\pi n_e e^2$ is the electron Debye length squared. Solving (132) gives

$$\omega_r^2 = \frac{\omega_{pi}^2}{1 + 1/k^2\lambda_D^2} = \frac{k^2 c_s^2}{1 + k^2\lambda_D^2}, \tag{133}$$

where $c_s = (T_e/m_i)^{1/2}$ is the ion sound speed. It is clear from (133) that the (low) oscillation frequency ranges from $\omega_r^2 = k^2 c_s^2$ for $k^2\lambda_D^2 \ll 1$, to $\omega_r^2 = \omega_{pi}^2$ for $k^2\lambda_D^2 \gg 1$.

To evaluate the growth rate γ for the choice of distribution functions in (125) and (126) use is made of (98) and (132). This readily gives

$$\begin{aligned}\gamma &= -\pi\frac{\omega_r^3}{2\omega_{pi}^2}\sum_j \frac{\omega_{pj}^2}{k^2}\int d^3v\,\delta(\omega_r - kv_z)k\frac{\partial}{\partial v_z}F_j(v) \\ &= \left(\frac{\pi}{8}\right)^{1/2}\frac{\omega_r^4}{\omega_{pi}^2|k|c_s}\frac{1}{k^2\lambda_D^2}\left\{-Z_i\left(\frac{T_e}{T_i}\right)^{3/2}\exp\left(-\frac{\omega_r^2}{k^2 v_{Ti}^2}\right)\right. \\ &\qquad \left. + \left(\frac{m_e}{m_i}\right)^{1/2}\left(\frac{kV_{ez}}{\omega_r} - 1\right)\exp\left[-\left(\frac{\omega_r - kV_{ez}}{kv_{Te}}\right)^2\right]\right\}.\end{aligned} \tag{134}$$

where $\lambda_D^2 = T_e/4\pi\hat{n}_e e^2$, $e_i = Z_i e$ is the ion charge, and use has been made of equilibrium charge neutrality, $\hat{n}_i Z_i e + \hat{n}_e(-e) = 0$. Making use of (131) to approximate the electron exponential factor in (134) by unity, the expression for γ in (134) reduces to

$$\gamma = \left(\frac{\pi}{8}\right)^{1/2} \frac{|\omega_r|}{(1+k^2\lambda_D^2)^{3/2}} \left[-Z_i \left(\frac{T_e}{T_i}\right)^{3/2} \exp\left(-\frac{T_e}{2T_i(1+k^2\lambda_D^2)}\right) + \left(\frac{m_e}{m_i}\right)^{1/2} \left(\frac{kV_{ez}}{\omega_r} - 1\right)\right], \tag{135}$$

where use has been made of $\omega_r^2 = k^2 c_s^2/(1+k^2\lambda_D^2)$.

Note from (135) that the ion contribution to the growth rate γ (denoted by γ_i) always corresponds to damping with $\gamma_i < 0$. Moreover, for $k^2\lambda_D^2 \leq 1$ and $T_e \gg T_i$, the ion Landau damping in (135) is exponentially small. On the other hand, as T_i/T_e is increased to values of order unity, the ion waves are heavily damped with $|\gamma_i/\omega_r| \approx 1$, and the assumptions leading to (135) are no longer valid.

The electron contribution to the growth rate γ in (135) (denoted by γ_e) corresponds to growth or damping depending on the sign of $kV_{ez}/\omega_r - 1$. In particular,

$$\gamma_e \gtrless 0 \text{ for } kV_{ez}/\omega_r \gtrless 1 \tag{136}$$

follows directly from (135).

To conclude this section, we briefly summarize the growth rate properties for stable ion wave oscillations and the ion acoustic instability in circumstances where $T_e \gg T_i$ and the ion Landau damping contribution in (135) is negligibly small.

Weakly damped ion waves. For $T_e \gg T_i$, and zero relative drift between electrons and ions,

$$V_e = 0, \tag{137}$$

the growth rate γ in (135) can be approximated by

$$\gamma = -\left(\frac{\pi m_e}{8m_i}\right)^{1/2} \frac{|\omega_r|}{(1+k^2\lambda_D^2)^{3/2}} = -\left(\frac{\pi m_e}{8m_i}\right)^{1/2} \frac{|k|c_s}{(1+k^2\lambda_D^2)^2}. \tag{138}$$

where $\omega_r^2 = k^2 c_s^2/(1+k^2\lambda_D^2)$. Equation (138) corresponds to a weak damping ($|\gamma/\omega_r| \ll 1$) of the ion waves by the background plasma electrons.

Ion acoustic instability. For $T_e \gg T_i$ and $V_{ez} \neq 0$, (135) predicts instability ($\gamma > 0$) whenever the relative drift between electrons and ions is sufficiently large that $kV_{ez}/\omega_r > 1$. Moreover the growth rate γ can be approximated by (Fig. 3.3.3)

$$\gamma = \left(\frac{\pi m_e}{8m_i}\right)^{1/2} \frac{|\omega_r|}{(1+k^2\lambda_D^2)^{3/2}} \left(\frac{kV_{ez}}{\omega_r} - 1\right). \tag{139}$$

where $\omega_r^2 = k^2 c_s^2/(1+k^2\lambda_D^2)$. Introducing the angle θ between $\boldsymbol{k} = k\hat{\boldsymbol{e}}_z$ and $\boldsymbol{V}_e$, the

quantity V_{ez} can be represented as $V_{ez} = V_e \cos\theta$ where $V_e = |V_e|$. For $k^2\lambda_D^2 \ll 1$, it then follows from (139) that instability exists within the cone $0 \leq \theta < \theta_0$, where

$$\cos^2\theta > \cos^2\theta_0 \equiv c_s^2/V_e^2, \tag{140}$$

which requires $V_e > c_s$ for existence of the instability.

Electron–ion two-stream instability

In this section, the electrostatic stability properties are considered for electrons drifting through background plasma ions in circumstances where the relative streaming velocity is large (Fig. 3.3.4)

$$|V_e| \gg v_{Te}, v_{Ti}, \tag{141}$$

and the corresponding instability is strong. As in the previous subsection, it is assumed that the electron and ion distributions are Maxwellian [(125) and (126)], and the electrostatic dispersion relation is given by (129). It is further assumed that

$$|\xi_i| = \left|\frac{\omega_r + i\gamma}{k v_{Ti}}\right| \gg 1, \qquad |\xi_e| = \left|\frac{\omega_r - kV_{ez} + i\gamma}{k v_{Te}}\right| \gg 1, \tag{142}$$

and resonant wave–particle effects are neglected in the region of ω- and $\boldsymbol{k}$-space under investigation. Making use of (142), and (107) with $Z(\xi_j) \simeq -1/\xi_j - 1/2\xi_j^3$, it is straightforward to show that (129) can be approximated by the cold-plasma dispersion relation

$$D(\boldsymbol{k}, \omega_r + i\gamma) = 1 - \frac{\omega_{pi}^2}{(\omega_r + i\gamma)^2} - \frac{\omega_{pe}^2}{(\omega_r - kV_{ez} + i\gamma)^2} = 0, \tag{143}$$

where $\boldsymbol{k} = k\hat{\boldsymbol{e}}_z$ and $\boldsymbol{k}\cdot\boldsymbol{V}_e = kV_{ez}$.

For $V_{ez} \neq 0$, (143) has four solutions for the complex oscillation frequency $\omega_r + i\gamma$. Two branches correspond to stable oscillations with $\gamma = 0$. The other two solutions for $\omega_r + i\gamma$ form conjugate pairs. After some straightforward algebra, it is found that

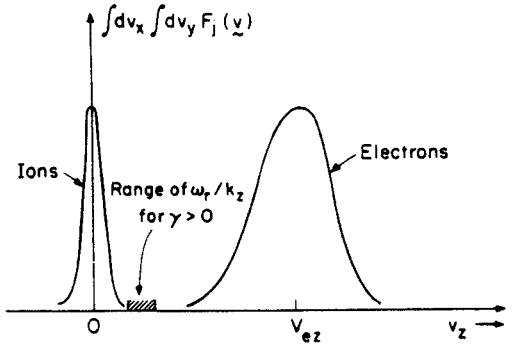

Fig. 3.3.4. Plot of reduced electron and ion distribution functions $\int_{-\infty}^{\infty} dv_x \int_{-\infty}^{\infty} dv_y F_j(v)$ for strong electron–ion two-stream instability.

the unstable branch exhibits growth ($\gamma > 0$) for k in the range

$$0 < |kV_{ez}| < \omega_{pe}\left[1 + \left(\omega_{pi}^2/\omega_{pe}^2\right)^{1/3}\right]^{3/2}. \tag{144}$$

Moreover, maximum growth occurs for $k^2 = k_M^2 \simeq \omega_{pe}^2/V_{ez}^2$, with corresponding real oscillation frequency and growth rate at maximum growth given by the approximate expressions

$$[\omega_r/k]_{max} = \tfrac{1}{2}\left(\omega_{pi}^2/2\omega_{pe}^2\right)^{1/3}|V_{ez}| = \tfrac{1}{2}\left(Z_i m_e/2m_i\right)^{1/3}|V_{ez}|, \tag{145}$$

$$[\gamma]_{max} = \omega_{pe}\tfrac{1}{2}\sqrt{3}\left(\omega_{pi}^2/2\omega_{pe}^2\right)^{1/3} = \omega_{pe}\tfrac{1}{2}\sqrt{3}\left(Z_i m_e/2m_i\right)^{1/3}, \tag{146}$$

where $e_i = Z_i e$ is the ion charge, and use has been made of equilibrium charge neutrality, $\hat{n}_i(Z_i e) + \hat{n}_e(-e) = 0$. Note from (146) that the growth rate for the electron–ion two-stream instability can be substantial, with $[\gamma]_{max} \simeq \omega_{pe}/18$ for hydrogen ions with $Z_i = 1$ and $m_e/m_i = 1/1836$.

Finally, in (143), resonant Landau damping by the plasma ions has been neglected within the context of the assumption $|\xi_i| = |(\omega_r + i\gamma)/kv_{Ti}| \gg 1$. From (145) and (146), this is a valid approximation provided the ions are sufficiently cold that

$$\left(Z_i m_e/2m_i\right)^{2/3} \gg v_{Ti}^2/V_{ez}^2 = 2T_i/m_i V_{ez}^2. \tag{147}$$

Necessary and sufficient condition for instability

In this section are investigated the properties of the dielectric function $D(\boldsymbol{k}, \omega)$ defined in (94) for general $F_j(\boldsymbol{v})$ to determine the necessary and sufficient condition for electrostatic instability. The resulting condition, known as the Penrose criterion, can be used to determine stability behavior, range of unstable $\boldsymbol{k}$-values, etc., for various choices of $F_j(\boldsymbol{v})$. It is useful to introduce the one-dimensional distribution function $\hat{F}(u)$ projected along the wavevector $\boldsymbol{k}$,

$$\hat{F}(u) = \int d^3v\, \delta\left(u - \frac{\boldsymbol{k}\cdot\boldsymbol{v}}{|k|}\right)\left(F_e(\boldsymbol{v}) + \frac{Z_i m_e}{m_i} F_i(\boldsymbol{v})\right), \tag{148}$$

where $|k| = |\boldsymbol{k}|$, $Z_i m_e/m_i = \omega_{pi}^2/\omega_{pe}^2$, and use has been made of equilibrium charge neutrality, $\hat{n}_i(Z_i e) + \hat{n}_e(-e) = 0$. From (148), note that $\hat{F}(u)$ is a weighted composite of $F_e(\boldsymbol{v})$ and $F_i(\boldsymbol{v})$, with the ion distribution function being weighted by $\omega_{pi}^2/\omega_{pe}^2$. Making use of (148), it is straightforward to show that the dielectric function $D(\boldsymbol{k}, \omega)$ defined in (94) can be expressed in the equivalent form

$$D(\boldsymbol{k}, \omega) = 1 + \frac{\omega_{pe}^2}{k^2}\int_{-\infty}^{\infty} du\, \frac{\partial \hat{F}(u)/\partial u}{\omega/|k| - u}, \tag{149}$$

where ω is complex, and $\operatorname{Im}\omega > 0$ is assumed in (149). For future reference, the real and imaginary parts of $D(\boldsymbol{k}, \omega)$, evaluated for *real* ω, can be expressed as

$$D_r(\boldsymbol{k}, \omega_r) = 1 + \frac{\omega_{pe}^2}{k^2}\mathrm{P}\int_{-\infty}^{\infty} du\, \frac{\partial \hat{F}(u)/\partial u}{\omega_r/|k| - u}, \tag{150}$$

$$D_i(\boldsymbol{k}, \omega_r) = -\pi\, \frac{\omega_{pe}^2}{k^2}\, \frac{\partial \hat{F}(u)}{\partial u}\bigg|_{u = \omega_r/|k|}. \tag{151}$$

where $\omega_r = \mathrm{Re}\,\omega$, and use has been made of

$$\lim_{\gamma \to 0_+} \frac{1}{(\omega_r + i\gamma)/|k| - u} = \mathrm{P}\frac{1}{\omega_r/|k| - u} - i\pi\delta\left(u - \frac{\omega_r}{|k|}\right),$$

where P denotes the Cauchy principal value.

An outline of the derivation of the Penrose criterion proceeds as follows. Assuming $D(\boldsymbol{k}, \omega)$ is an analytic function of ω in the upper half ω-plane, the number N of solutions to the dispersion relation $D(\boldsymbol{k}, \omega) = 0$ with $\mathrm{Im}\,\omega > 0$ (i.e. the number of *unstable* modes) is given by

$$N = \frac{1}{2\pi i}\int_C \frac{d\omega}{D(\boldsymbol{k}, \omega)}\frac{\partial}{\partial \omega} D(\boldsymbol{k}, \omega), \tag{152}$$

where $D(\boldsymbol{k}, \omega)$ is defined in (149). In (152), the contour C proceeds along the Re-ω axis from $\omega_r = -\infty$ to $\omega_r = +\infty$, and closes on a large semicircle (with $|\omega| \to \infty$) in the upper half ω-plane. From (149), $D(\boldsymbol{k}, |\omega| \to \infty) = 1$, and the only contribution to (152) occurs along that portion of the contour C along the real-ω axis where

$$D(\boldsymbol{k}, \omega_r) = D_r(\boldsymbol{k}, \omega_r) + i D_i(\boldsymbol{k}, \omega_r). \tag{153}$$

Equation (152) therefore reduces to

$$N = \frac{1}{2\pi i}\ln\left(\frac{D(\boldsymbol{k}, \omega_r = +\infty)}{D(\boldsymbol{k}, \omega_r = -\infty)}\right). \tag{154}$$

Choosing the phase of $D(\boldsymbol{k}, \omega_r)$ such that $D(\boldsymbol{k}, \omega_r = -\infty) = +1$, it is found that $D(\boldsymbol{k}, \omega_r = +\infty) = \exp(2\pi i N)$. That is to say:

> The number N of unstable solutions (with $\mathrm{Im}\,\omega > 0$) to $D(\boldsymbol{k}, \omega) = 0$ is equal to the number of times that the contour $\Gamma = D_r(\boldsymbol{k}, \omega_r) + i D_i(\boldsymbol{k}, \omega_r)$ encircles the origin in the complex $D_r + iD_i$ plane as ω_r ranges from $-\infty$ to $+\infty$.

The preceding statement constitutes a very powerful means to determine the necessary and sufficient condition for instability of $\hat{F}(u)$. For present purposes, the case is considered where $\hat{F}(u)$ is a double-peaked distribution function (Fig. 3.3.5)

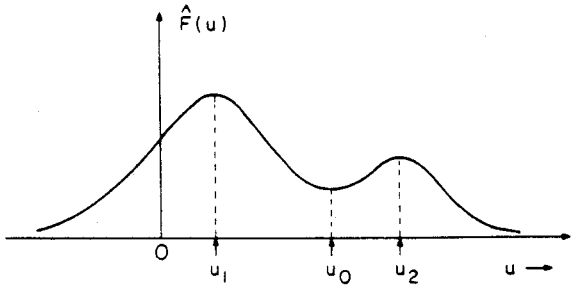

Fig. 3.3.5. Double-peaked distribution function $\hat{F}(u)$ assumed in derivation of Penrose criterion.

with a single minimum (excluding $u = \pm\infty$) at $u = u_0$, a primary (largest) maximum at $u = u_1$, and a secondary (smallest) maximum at $u = u_2$. Tracing out the curve $\Gamma = D_r(\boldsymbol{k}, \omega_r) + i D_i(\boldsymbol{k}, \omega_r)$ in the complex (D_r, D_i) plane for ω_r ranging from $\omega_r = -\infty$ to $\omega_r = +\infty$ gives the general behavior illustrated in Fig 3.3.6. Note from (150) that $D_r(\boldsymbol{k}, \omega_r)$ can be expressed in the equivalent form

$$D_r(\boldsymbol{k}, \omega_r) = 1 - \frac{\omega_{pe}^2}{k^2} \int_{-\infty}^{\infty} du \, \frac{\hat{F}(u) - \hat{F}(\omega_r/|k|)}{(u - \omega_r/|k|)^2}. \tag{155}$$

It is straightforward to show from (155) and Fig. 3.3.6 that

$$D_r(\boldsymbol{k}, \omega_r = |k|u_1) > 1,$$
$$D_r(\boldsymbol{k}, \omega_r = |k|u_2) > D_r(\boldsymbol{k}, \omega_r = |k|u_0). \tag{156}$$

From Fig. 3.3.6, the condition for instability (that $\Gamma = D_r + i D_i$ encircles the origin) therefore becomes $D_r(\boldsymbol{k}, \omega_r = |k|u_0) < 0 < D_r(\boldsymbol{k}, \omega_r = |k|u_2)$, which can be expressed as

$$\omega_{pe}^2 \int_{-\infty}^{\infty} du \, \frac{\hat{F}(u) - \hat{F}(u_2)}{(u - u_2)^2} < k^2 < \omega_{pe}^2 \int_{-\infty}^{\infty} du \, \frac{\hat{F}(u) - \hat{F}(u_0)}{(u - u_0)^2}. \tag{157}$$

It is clear from (157) that a *necessary and sufficient condition for instability* is given by

$$P(\hat{F}) \equiv \omega_{pe}^2 \int_{-\infty}^{\infty} du \, \frac{\hat{F}(u) - \hat{F}(u_0)}{(u - u_0)^2} > 0. \tag{158}$$

Equation (158) is known as the *Penrose criterion for instability*. Note from (158) that the depression in $\hat{F}(u)$ as measured by $\hat{F}(u_0)$ must be sufficiently large for $P(\hat{F}) > 0$ to be satisfied. In addition, it is clear from (157) and Fig. 3.3.6 that if the secondary

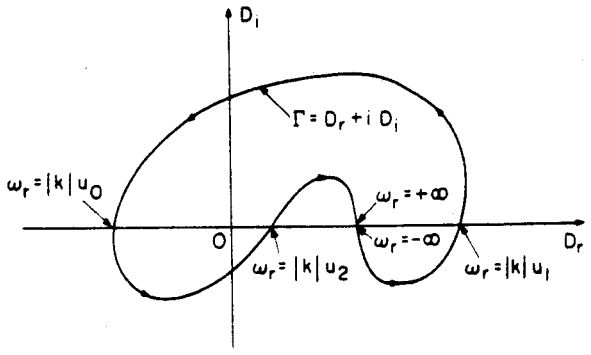

Fig. 3.3.6. Plot of Penrose curve $\Gamma = D_r + i D_i$[(151) and (155)] in complex (D_r, D_i) plane for ω_r ranging from $-\infty$ to $+\infty$. Here, $D_r(\boldsymbol{k}, \omega_r = |k|u_0) < 0 < D_r(\boldsymbol{k}, \omega_r = |k|u_2)$ is required for existence of instability ($\gamma > 0$).

maximum $\hat{F}(u_2)$ is sufficiently large, the inequality $D(\boldsymbol{k}, \omega_r = |k|u_2) > 1$ pertains, and hence

$$\omega_{pe}^2 \int_{-\infty}^{\infty} du \frac{\hat{F}(u) - \hat{F}(u_2)}{(u-u_2)^2} < 0,$$

may be satisfied. We therefore conclude, whenever the Penrose criterion (158) is satisfied, that the range of unstable $\boldsymbol{k}$-values (where $\gamma > 0$) is given by

$$k_{min}^2 < k^2 < k_0^2, \tag{159}$$

where k_0^2 and k_{min}^2 are defined by

$$k_0^2 \equiv \omega_{pe}^2 \int_{-\infty}^{\infty} du \frac{\hat{F}(u) - \hat{F}(u_0)}{(u-u_0)^2}, \tag{160}$$

and k_{min}^2 is the maximum of 0 or $\hat{k}^2$, where

$$\hat{k}^2 \equiv \omega_{pe}^2 \int_{-\infty}^{\infty} du \frac{\hat{F}(u) - \hat{F}(u_2)}{(u-u_2)^2}. \tag{161}$$

To summarize, (158)–(161) can be used to investigate stability behavior for a variety of choices of distribution function $\hat{F}(u)$. Although (158) does not provide detailed information on the size of the growth rate γ, it does determine whether or not a given $\hat{F}(u)$ is unstable, and the corresponding range of unstable $\boldsymbol{k}$-values [Eq. (159)] when instability exists. We reiterate that (158) has been derived for a double-peaked distribution function with maxima at $u = u_1$ and $u = u_2$. Of course, the techniques outlined here can be extended to the case where $\hat{F}(u)$ has multiple maxima.

Penrose criterion for counterstreaming electrons and ions

As an interesting practical application of the Penrose criterion (158) derived in the previous subsection, the case is considered where $\hat{F}(u)$ corresponds to Maxwellian electrons drifting with velocity V_d through a Maxwellian ion background,

$$\hat{F}(u) = \frac{1}{\sqrt{\pi}\, v_{Te}} \left[\exp\left(- \frac{(u-V_d)^2}{v_{Te}^2} \right) + Z_i \frac{m_e}{m_i} \frac{v_{Te}}{v_{Ti}} \exp\left(- \frac{u^2}{v_{Ti}^2} \right) \right], \tag{162}$$

where $v_{Te} = (2T_e/m_e)^{1/2}$ and $v_{Ti} = (2T_i/m_i)^{1/2}$. From (162), the distribution function $\hat{F}(u)$ has a minimum with $\partial \hat{F}(u)/\partial u = 0$ at $u = u_0$, where

$$\left(\frac{V_d - u_0}{v_{Te}} \right) \exp\left(- \frac{(u_0 - V_d)^2}{v_{Te}^2} \right) = Z_i \frac{T_e}{T_i} \frac{u_0}{v_{Ti}} \exp\left(- \frac{u_0^2}{v_{Ti}^2} \right). \tag{163}$$

Equation (163) can be used to determine $u_0 = u_0(V_d/v_{Te}, T_e/T_i, m_e/m_i)$ numerically for a wide range of system parameters. Introducing the dimensionless quantities $\hat{V}_d \equiv V_d/v_{Te}$ and $\hat{u}_0 \equiv u_0/v_{Te}$, and the dimensionless velocity variable $\hat{u} \equiv u/v_{Te}$,

the Penrose function $P(\hat{F})$ defined in (158) can be expressed as

$$\frac{v_{Te}^2}{\omega_{pe}^2} P(\hat{F}) = \pi^{-1/2} \int_{-\infty}^{\infty} \frac{d\hat{u}}{(\hat{u}-\hat{u}_0)^2} \left\{ \exp\left[-(\hat{u}-\hat{V}_d)^2\right] - \exp\left[-(\hat{u}_0-\hat{V}_d)^2\right] + Z_i \left(\frac{m_e}{m_i}\right)^{1/2} \left(\frac{T_e}{T_i}\right)^{1/2} \left[\exp\left(-\frac{T_e}{T_i}\frac{m_i}{m_e}\hat{u}^2 \right) - \exp\left(-\frac{T_e}{T_i}\frac{m_i}{m_e}\hat{u}_0^2 \right) \right] \right\}, \tag{164}$$

for the choice of distribution function in (162). In (164), $\hat{u}_0 = u_0/v_{Te}$ is determined from (163). For specified Z_i and m_e/m_i, (164) can be solved numerically to determine the region of V_d/v_{Te} and T_e/T_i parameter space corresponding to instability with $P(\hat{F}) > 0$, and hence $\gamma > 0$. The results are summarized in Fig. 3.3.7 for hydrogen plasma with $Z_i = 1$ and $m_e/m_i = 1/1836$. The solid curve in Fig. 3.3.7 corresponds to marginal stability with $P(\hat{F}) = 0$ and $\gamma = 0$. The region of $(V_d/v_{Te}, T_e/T_i)$ space above the curve corresponds to instability with $\gamma > 0$, whereas

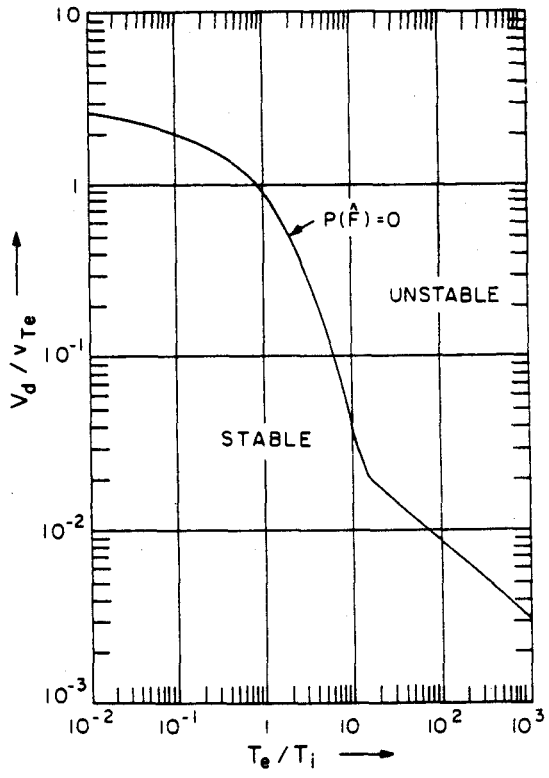

Fig. 3.3.7. Plot of V_d/v_{Te} versus T_e/T_i marginal stability curve ($\gamma = 0$) obtained from $P(\hat{F}) = 0$ for counterstreaming electrons and ions [Eq. (164)] where $Z_i = 1$ and $m_e/m_i = 1/1836$ are assumed. Region *above* the curve is unstable ($\gamma > 0$). (Numerical results due to Dr. Robert D. Estes.)

the region below the curve corresponds to damped oscillations. Note that the ion acoustic instability and the strong electron–ion two-stream instability occur in rather restricted regions of parameter space in Fig. 3.3.7. Equation (164) and Fig. 3.3.7 of course delineate the entire region where instability exists for a continuum range of V_d/v_{Te} and T_e/T_i.

Penrose criterion for counterstreaming plasmas

As a second application of the Penrose criterion (158), the case is considered where the distribution function $\hat{F}(u)$ corresponds to equidensity, Maxwellian plasmas counterstreaming with drift velocities $\pm V_d$,

$$\hat{F}(u) = \frac{1}{2\sqrt{\pi}\, v_{Te}}\left[\exp\left(-\frac{(u-V_d)^2}{v_{Te}^2}\right)+\exp\left(-\frac{(u+V_d)^2}{v_{Te}^2}\right)\right.$$
$$\left.+\, Z_i\frac{m_e}{m_i}\frac{v_{Te}}{v_{Ti}}\exp\left(-\frac{(u-V_d)^2}{v_{Ti}^2}\right)+Z_i\frac{m_e}{m_i}\frac{v_{Te}}{v_{Ti}}\exp\left(-\frac{(u+V_d)^2}{v_{Ti}^2}\right)\right], \tag{165}$$

where $v_{Tj} = (2T_j/m_j)^{1/2}$ for $j = e,i$. It is clear from (165) that $\hat{F}(u)$ has a single minimum at $u = u_0 = 0$. Moreover, substituting (165) into (158), the Penrose function $P(\hat{F})$ can be expressed as

$$\frac{2v_{Te}^2}{\omega_{pe}^2}P(\hat{F}) = \pi^{-1/2}\int_{-\infty}^{\infty}\frac{d\hat{u}}{\hat{u}^2}\left\{\exp\left[-(\hat{u}-\hat{V}_d)^2\right]+\exp\left[-(\hat{u}+\hat{V}_d)^2\right]-2\exp(-\hat{V}_d^2)\right.$$
$$+\, Z_i\left(\frac{m_e}{m_i}\right)^{1/2}\left(\frac{T_e}{T_i}\right)^{1/2}\left[\exp\left(-\frac{T_e}{T_i}\frac{m_i}{m_e}(\hat{u}-\hat{V}_d)^2\right)\right.$$
$$\left.\left.+\exp\left(-\frac{T_e}{T_i}\frac{m_i}{m_e}(\hat{u}+\hat{V}_d)^2\right)-2\exp\left(-\frac{T_e}{T_i}\frac{m_i}{m_e}\hat{V}_d^2\right)\right]\right\} \tag{166}$$

where $\hat{V}_d \equiv V_d/v_{Te}$ and $\hat{u} = u/v_{Te}$. For specified Z_i and m_e/m_i, (166) can be solved numerically to determine the region of $2V_d/V_{Te}$ and T_e/T_i parameter space corresponding to instability with $P(\hat{F}) > 0$ and $\gamma > 0$. The results are summarized in Fig. 3.3.8 for counterstreaming hydrogen plasmas with $Z_i = 1$ and $m_e/m_i = 1/1836$. The solid curve in Fig. 3.3.8 correspond to marginal stability with $P(\hat{F}) = 0$ and $\gamma = 0$.

3.3.4. *Electromagnetic waves and instabilities in an unmagnetized plasma*

Introduction and dispersion relation

In Section 3.3.1, it was indicated that a sufficiently large anisotropy in plasma kinetic energy can provide the free energy source to drive plasma instabilities with

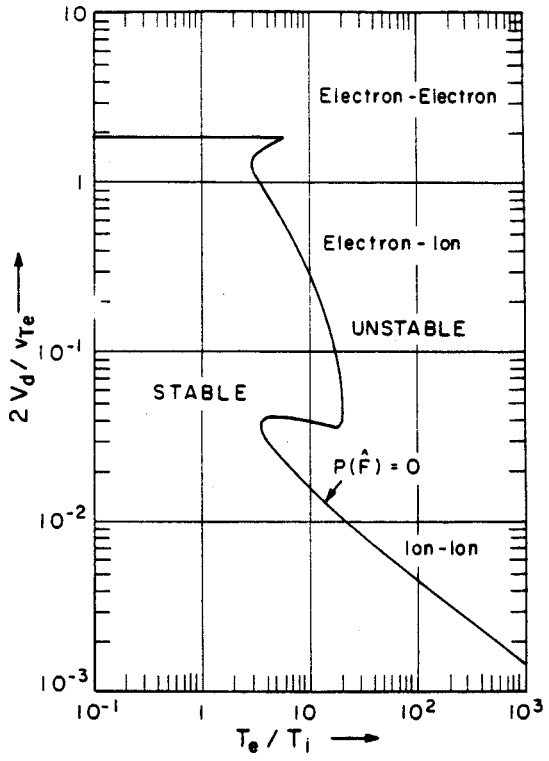

Fig. 3.3.8. Plot of $2V_d/v_{Te}$ versus T_e/T_i marginal stability curve ($\gamma = 0$) obtained from $P(\hat{F}) = 0$ for equidensity counterstreaming plasmas [Eq. (166)] where $Z_i = 1$ and $m_e/m_i = 1/1836$ are assumed. Region *above* the curve is unstable ($\gamma > 0$). (Numerical results due to Dr. Robert D. Estes.)

transverse electromagnetic polarization, i.e. with electric field perturbation $\delta\hat{\boldsymbol{E}}$ perpendicular to the wavevector $\boldsymbol{k}$. In the present analysis, an unmagnetized plasma with $\boldsymbol{B}_0 = 0$ is considered, and use is made of the electromagnetic dispersion relation (74), which corresponds to the plane wave polarization

$$\boldsymbol{k} = (0,0,k), \qquad \widehat{\delta\boldsymbol{E}} = (\widehat{\delta E}_x, 0, 0), \tag{167}$$

with wave propagation in the z-direction $\boldsymbol{k} = k\hat{\boldsymbol{e}}_z$. Denoting $\omega = \omega_r + i\gamma$, the dispersion relation $D_{xx}(\boldsymbol{k}, \omega_r + i\gamma) = 0$ in (74) can be expressed as

$$\begin{aligned} D(\boldsymbol{k}, \omega_r + i\gamma) = 1 &- \frac{c^2k^2}{(\omega_r + i\gamma)^2} - \sum_j \frac{\omega_{pj}^2}{(\omega_r + i\gamma)^2} \\ &+ \sum_j \frac{\omega_{pj}^2}{(\omega_r + i\gamma)^2} \int d^3v\, v_x^2 \frac{k\,\partial F_j/\partial v_z}{\omega_r - kv_z + i\gamma} \\ &= 0, \end{aligned} \tag{168}$$

where $\gamma = \mathrm{Im}\,\omega > 0$ is assumed, and use has been made of $\int d^3v\, v_x \partial F_j/\partial v_x = -1$. Moreover, the short-hand notation $D_{xx} \equiv D$ has been introduced in (168).

It is important to note that the electromagnetic stability analysis presented in Section 3.3.4 is also approximately valid for a magnetized plasma with $\boldsymbol{B}_0 \neq 0$ provided the perturbations have sufficiently short wavelength and sufficiently high frequency that the plasma species are effectively unmagnetized, i.e. provided $|\omega/\omega_{cj}| \gg 1$ and $|k_\perp v_{Tj}/\omega_{cj}| \gg 1$.

As indicated in Section 3.3.1, one of the most fundamental instabilities associated with (168) is the electromagnetic Weibel instability driven by energy anisotropy in which the plasma kinetic energy perpendicular to $\boldsymbol{k} = k\hat{\boldsymbol{e}}_z$ exceeds the parallel kinetic energy by a sufficiently large amount. To illustrate basic stability properties, for the sake of definiteness the case is considered where the jth species distribution function corresponds to equidensity, anisotropic Maxwellians counterstreaming perpendicular to the propagation direction with

$$F_j(v) = \frac{1}{2}\left(\frac{m_j}{2\pi T_{j\parallel}}\right)^{1/2} \exp\left(-\frac{m_j v_z^2}{2T_{j\parallel}}\right)\left(\frac{m_j}{2\pi T_{j\perp}}\right) \times \left[\exp\left(-\frac{m_j}{2T_{j\perp}}\left[(v_x - V_j)^2 + (v_y - U_j)^2\right]\right) + \exp\left(-\frac{m_j}{2T_{j\perp}}\left[(v_x + V_j)^2 + (v_y + U_j)^2\right]\right)\right]. \tag{169}$$

After some straightforward algebra that makes use of (104), the dispersion relation (168) can be expressed as

$$D(\boldsymbol{k}, \omega_r + i\gamma) = 1 - \frac{c^2k^2}{(\omega_r + i\gamma)^2} - \sum_j \frac{\omega_{pj}^2}{(\omega_r + i\gamma)^2} + \sum_j \frac{\omega_{pj}^2}{(\omega_r + i\gamma)^2}\frac{T_{j\perp} + m_j V_j^2}{T_{j\parallel}}\left[1 + \xi_j Z(\xi_j)\right] = 0, \tag{170}$$

where $Z(\xi_j)$ is the plasma dispersion function defined in (105), and ξ_j is defined by

$$\xi_j = (\omega_r + i\gamma)/kv_{Tj}, \tag{171}$$

where $v_{Tj} \equiv (2T_{j\parallel}/m_j)^{1/2}$ is the parallel thermal speed of species j. For the sake of completeness, note that the dispersion relation $D_{yy}(\boldsymbol{k}, \omega_r + i\gamma) = 0$ in (75) is identical to (170) with the replacement $V_j^2 \to U_j^2$, where $\pm U_j$ are the directed streaming velocities in the y-direction.

Equation (170) supports two classes of solutions. The first class corresponds to fast ($\omega_r^2/k^2 > c^2$), stable ($\gamma = 0$) electromagnetic waves propagating with phase velocity exceeding the speed of light. The second class corresponds to purely growing (or purely damped) solutions with $\omega_r = 0$ and $\gamma \neq 0$, whenever the anisotropy condition $(T_{j\perp} + m_j V_j^2)/T_{j\parallel} > 1$ is satisfied.

These two classes of solutions are now considered in more detail.

Fast-wave propagation

For *fast* electromagnetic wave propagation with

$$|\omega_r^2/k^2| > c^2, \tag{172}$$

it follows for a nonrelativistic plasma that $|\xi_j| \gg 1$ for $j = e, i$. Approximating $Z(\xi_j) \simeq -1/\xi_j - 1/2\xi_j^3 - \cdots$ [Eq. (107)], the dispersion relation (170) supports purely oscillatory solutions with $\gamma = 0$ and ω_r determined from

$$0 = 1 - \frac{c^2k^2}{\omega_r^2} - \sum_j \frac{\omega_{pj}^2}{\omega_r^2} - \sum_j \frac{\omega_{pj}^2}{\omega_r^2} \frac{T_{j\perp} + m_j V_j^2}{T_{j\parallel}} \frac{k^2 T_{j\parallel}}{m_j \omega_r^2}. \tag{173}$$

Solving (173) iteratively for ω_r^2 gives

$$\omega_r^2 = c^2k^2 + \sum_j \omega_{pj}^2 + \sum_j \omega_{pj}^2 \frac{\left(T_{j\perp}/m_j c^2 + V_j^2/c^2\right)}{1 + \sum_{j'} \omega_{pj'}^2/c^2k^2}. \tag{174}$$

For the nonrelativistic plasma regime assumed here, note from (174) that the correction term proportional to $(T_{j\perp}/m_j c^2 + V_j^2/c^2)$ is small, and the cold-plasma dispersion relation $\omega_r^2 = c^2k^2 + \sum_j \omega_{pj}^2$ is an excellent approximation to (174). This conclusion is independent of the degree of anisotropy.

Necessary and sufficient condition for instability

It is relatively straightforward to generalize the electrostatic Penrose criterion derived in Section 3.3.3 to the case where the wave polarization is electromagnetic and the dispersion relation is given by (168). To avoid a double pole at $\omega = 0$, define

$$\hat{D}(\boldsymbol{k}, \omega) = \omega^2 D(\boldsymbol{k}, \omega)$$

$$= \omega^2 - c^2k^2 - \sum_j \omega_{pj}^2 + \sum_j \omega_{pj}^2 \int d^3v\, v_x^2 \frac{k\,\partial F_j/\partial v_z}{\omega - kv_z}, \tag{175}$$

where $\mathrm{Im}\,\omega > 0$ in (175). Introducing $\hat{D}_r + i\hat{D}_i = \hat{D}(\boldsymbol{k}, \omega)$, where $\hat{D}_r = \mathrm{Re}\,\hat{D}$ and $\hat{D}_i = \mathrm{Im}\,\hat{D}$, it follows from (175) and

$$\lim_{\gamma \to 0_+} \frac{1}{\omega_r - kv_z + i\gamma} = P\frac{1}{\omega_r - kv_z} - i\pi\delta(\omega_r - kv_z), \tag{176}$$

that

$$\hat{D}_r(\boldsymbol{k}, \omega_r) = \omega_r^2 - c^2k^2 - \sum_j \omega_{pj}^2 + \sum_j \omega_{pj}^2 P \int d^3v\, v_x^2 \frac{k\,\partial F_j/\partial v_z}{\omega_r - kv_z}, \tag{177}$$

$$\hat{D}_i(\boldsymbol{k}, \omega_r) = -\pi \sum_j \omega_{pj}^2 \int d^3v\, v_x^2 \delta(\omega_r - kv_z) k \frac{\partial F_j}{\partial v_z}, \tag{178}$$

where P denotes Cauchy principal value. For the class of symmetric equilibria with a single maximum at $v_z = 0$ [as in (169)], it can be shown that

$$\hat{D}_r(\boldsymbol{k}, \omega_r = 0) > 0 \tag{179}$$

is required for existence of unstable solutions to $D(\boldsymbol{k}, \omega_r + i\gamma) = 0$ with $\gamma > 0$ and $\omega_r = 0$. Equation (179) determines the necessary and sufficient condition for instability,

$$P(F) = -\sum_j \omega_{pj}^2 \left(1 + \mathrm{P} \int d^3v \frac{v_x^2}{v_z} \frac{\partial F_j}{\partial v_z} \right) > 0, \tag{180}$$

as well as the range of unstable k-values corresponding to $\gamma > 0$, i.e.

$$0 < k^2 < k_0^2, \tag{181}$$

where

$$k_0^2 \equiv -\sum_j \frac{\omega_{pj}^2}{c^2} \left(1 + \mathrm{P} \int d^3v \frac{v_x^2}{v_z} \frac{\partial F_j}{\partial v_z} \right). \tag{182}$$

Use is now made of (170) and (178)–(182) to investigate detailed electromagnetic stability properties for the anisotropic counterstreaming Maxwellian plasmas described by (169). Making use of (169) and (180), the necessary and sufficient condition for instability can be expressed as

$$\sum_j \omega_{pj}^2 \left(\frac{T_{j\perp} + m_j V_j^2}{T_{j\parallel}} - 1 \right) > 0, \tag{183}$$

and the range of unstable k-values is given by

$$0 < k^2 < k_0^2 \equiv \sum_j \frac{\omega_{pj}^2}{c^2} \left(\frac{T_{j\perp} + m_j V_j^2}{T_{j\parallel}} - 1 \right) \tag{184}$$

whenever (183) is satisfied. Note from (183) and (184) that both thermal anisotropy ($T_{j\perp}/T_{j\parallel} > 1$) and anisotropy associated with directed kinetic energy ($m_j V_j^2 / T_{j\parallel} > 1$) can provide the free energy source to drive the instability. In the special case of an isotropic plasma with $V_j = 0$ and $T_{j\perp} = T_{j\parallel}$, it follows from (182) that $k_0^2 = 0$ and the system is stable. The necessary and sufficient condition for instability given in (183) can also be expressed as

$$\frac{T_{e\perp} + m_e V_e^2}{T_{e\parallel}} + Z_i \frac{m_e}{m_i} \frac{T_{i\perp} + m_i V_i^2}{T_{i\parallel}} > 1 + Z_i \frac{m_e}{m_i}, \tag{185}$$

where $e_i = Z_i e$ is the ion charge, and use has been made of equilibrium charge neutrality $\hat{n}_i (Z_i e) + \hat{n}_e (-e) = 0$ to express $\omega_{pi}^2 / \omega_{pe}^2 = Z_i m_e / m_i$. Making use of (185), the region of $(T_{e\perp} + m_e V_e^2)/T_{e\parallel}$ versus $(T_{i\perp} + m_i V_i^2)/T_{i\parallel}$ space corresponding to instability is plotted in Fig. 3.3.9. For specified $(T_{e\perp} + m_e V_e^2)/T_{e\parallel}$, we note from Eq. (185) and Fig. 3.3.9 that a relatively large value of ion anisotropy $(T_{i\perp} + m_i V_i^2)/T_{i\parallel}$ is required to drive instability.

Weibel instability for weakly anisotropic plasma

As an example, in this section the case is considered where there is no streaming motion of the plasma ($V_e = V_i = 0$), the positive ions are isotropic ($T_{i\perp} = T_{i\parallel}$), and

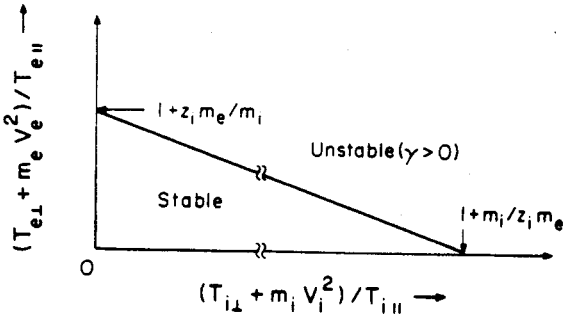

Fig. 3.3.9. Necessary and sufficient condition for Weibel instability in equidensity, counterstreaming plasmas [Eq. (185)]. Region *above* the curve corresponds to instability ($\gamma > 0$).

the electron thermal anistropy is assumed to be weak with

$$|(T_{e\perp} - T_{e\parallel})/T_{e\parallel}| \ll 1. \tag{186}$$

From (184), the range of unstable k-values is given by

$$0 < k^2 < k_0^2 \equiv \frac{\omega_{pe}^2}{c^2}\left(\frac{T_{e\perp}}{T_{e\parallel}} - 1\right) \tag{187}$$

where $k_0^2 c^2/\omega_{pe}^2 \ll 1$. In addition, the ions are treated as infinitely massive with $m_i \to \infty$ and $|\xi_i| \gg 1$. Assuming $\omega_r = 0$, and neglecting the displacement current ($\gamma^2 \ll c^2 k^2$) in (170), the dispersion relation can be approximated by

$$0 = c^2 k^2 + \omega_{pe}^2\left(1 - \frac{T_{e\perp}}{T_{e\parallel}}\right) - \frac{T_{e\perp}}{T_{e\parallel}}\omega_{pe}^2 \xi_e Z(\xi_e), \tag{188}$$

where $\xi_e = i\gamma/k v_{Te}$ and $v_{Te} = (2T_{e\parallel}/m_e)^{1/2}$. For the case of weak anisotropy, (188) supports weakly unstable solutions with $|\xi_e| \ll 1$. Approximating, $Z(\xi_e) \simeq -2\xi_e$ [Eq. (108)], it is found from (188) that

$$\gamma^2 = \frac{1}{2}\frac{v_{Te}^2}{c^2}\omega_{pe}^2 \frac{T_{e\parallel}}{T_{e\perp}}\left(\frac{T_{e\perp}}{T_{e\parallel}} - 1\right)^2 \frac{k^2}{k_0^2}\left(1 - \frac{k^2}{k_0^2}\right) \tag{189}$$

for $0 < k^2 < k_0^2$ (Fig. 3.3.10). In (189), maximum growth occurs for $k^2 = k_0^2/2$, and the corresponding maximum growth rate $[\gamma]_{max}$ is given by

$$[\gamma]_{max} = \frac{v_{Te}}{c}\omega_{pe}\left(\frac{1}{8}\frac{T_{e\parallel}}{T_{e\perp}}\right)^{1/2}\left|\frac{T_{e\perp}}{T_{e\parallel}} - 1\right|$$

$$= k_0 v_{Te}\left(\frac{1}{8}\frac{T_{e\parallel}}{T_{e\perp}}\right)^{1/2}\left|\frac{T_{e\perp}}{T_{e\parallel}} - 1\right|^{1/2}. \tag{190}$$

Equation (188) can be solved numerically for the case of arbitrary anisotropy. When $T_{e\perp}/T_{e\parallel} - 1$ is of order unity or larger, the maximum growth rate of course exceeds

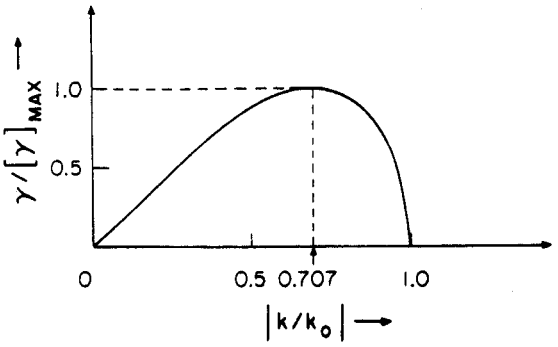

Fig. 3.3.10. Plot of growth rate γ versus $|k/k_0|$ for weak electron Weibel instability [(189) and (190)].

the value in (190). The range of unstable k-values, however, is still given by the expression (187).

Strong filamentation instability for counterstreaming ion beams

As a second example that illustrates several important features of electromagnetic Weibel instabilities, the case is considered where the energy anisotropy is provided by cold, counter-streaming ion beams with directed x-velocities $\pm V_i$, and

$$T_{i\parallel} \to 0, \qquad T_{i\perp} \to 0. \tag{191}$$

It is further assumed that the ion beams propagate through a hot, isotropic electron background with $V_e = 0$ and $T_{e\perp} = T_{e\parallel} \equiv T_e$. Assuming $\omega_r = 0$ and that the electrons are sufficiently hot that $|\xi_e| = |i\gamma/kv_{Te}| \ll 1$, it is straightforward to show that the dispersion relation (170) can be approximated by

$$0 = c^2k^2 + \sum_j \omega_{pj}^2 + \omega_{pe}^2\left(2\frac{\gamma^2}{k^2v_{Te}^2}\right) - \omega_{pi}^2V_i^2\frac{k^2}{\gamma^2}, \tag{192}$$

where use has been made of $Z(\xi_e) \simeq -2\xi_e$ and $Z(\xi_i) \simeq -1/\xi_i - 1/2\xi_i^2$ and the displacement current has been neglected in (192) ($\gamma^2 \ll c^2k^2$). Neglecting $\omega_{pe}^2\gamma^2/k^2v_{Te}^2$ in comparison with ω_{pe}^2, (192) gives the approximate result (Fig. 3.3.11)

$$\gamma^2 = \frac{V_i^2}{c^2}\frac{\omega_{pi}^2}{\left(1+\sum_j\omega_{pj}^2/c^2k^2\right)}. \tag{193}$$

Since $T_{i\parallel} \to 0$ has been assumed, the range of unstable k-values in (193) corresponds to $0 < k^2 < k_0^2 \to \infty$, which is consistent with (184). Moreover, maximum growth occurs for $c^2k^2 \gg \omega_{pe}^2$, with

$$[\gamma]_{max} = (V_i/c)\omega_{pi}. \tag{194}$$

Of course, a modest value of $T_{i\parallel}$ will cause the γ versus k curve in Fig. 3.3.11 to turn

over, and the growth rate γ approaches zero for $k = k_0$ where $c^2k_0^2/\omega_{pi}^2 = (T_{i\perp} + m_iV_i^2)/T_{i\parallel} - 1$ [Eq. (184)].

To conclude Section 3.3.4, it is evident that two rather extreme examples of electromagnetic Weibel instabilities have been examined in the last two subsections. It should be emphasized, however, that the dispersion relations (168) and (170) can be used to investigate anisotropy-driven electromagnetic instabilities for a wide range of circumstances.

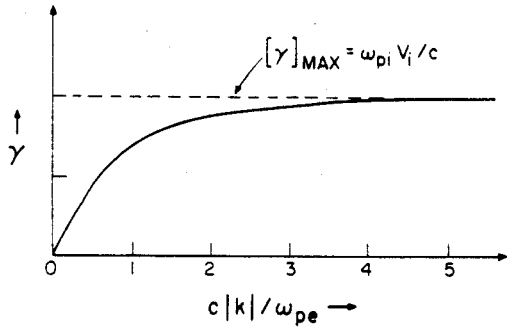

Fig. 3.3.11. Plot of growth rate γ versus $c|k|/\omega_{pe}$ for strong counterstreaming ion Weibel instability [(193) and (194)].

3.3.5. *Waves and instabilities for propagation parallel to B_0*

Introduction and dispersion relation

In Section 3.3.1 were derived the electrostatic dispersion relation $D_{zz}(k_z, \omega) = 0$ [Eq. (38)] and the transverse electromagnetic dispersion relation $D^{\pm}(k_z, \omega) = 0$ [Eq. (40)] for wave propagation parallel to a uniform magnetic field $\boldsymbol{B}_0 = B_0\hat{\boldsymbol{e}}_z$. The analysis in Section 3.3.1 was carried out for general equilibrium distribution function $F_j(v_\perp^2, v_z)$, and wavevector

$$\boldsymbol{k} = k_z\hat{\boldsymbol{e}}_z. \tag{195}$$

From (38), it is clear that the electrostatic dispersion relation for waves propagating parallel to the magnetic field is identical to the familiar electrostatic dispersion relation for an unmagnetized plasma given in (81) and studied extensively in Section 3.3.3. That is, as expected, for wavevector $\boldsymbol{k}$ parallel to $B_0\hat{\boldsymbol{e}}_z$, the electrostatic stability properties are unaffected by the presence of the magnetic field. Therefore, throughout the remainder of Section 3.3.5, stability properties associated with the transverse electromagnetic dispersion relation $D^{\pm}(k_z, \omega) = 0$ in (40) are investigated.

Integrating by parts with respect to $v_\perp$ in (40), the dispersion relation can be expressed as

$$D^{\pm}(k_z, \omega_r + i\gamma) = 1 - \frac{c^2 k_z^2}{(\omega_r + i\gamma)^2} - \sum_j \frac{\omega_{pj}^2}{(\omega_r + i\gamma)^2} \int d^3v \frac{\left[(\omega_r - k_z v_z + i\gamma) F_j - (k_z v_\perp^2/2)\partial F_j/\partial v_z\right]}{(\omega_r \pm \omega_{cj} - k_z v_z + i\gamma)} = 0, \tag{196}$$

where

$$\int d^3v = 2\pi \int_{-\infty}^{\infty} dv_z \int_0^{\infty} dv_\perp v_\perp,$$

$\omega = \omega_r + i\gamma$ is the complex oscillation frequency, $\omega_{cj} = e_j B_0/m_j c$ is the cyclotron frequency, and $\mathrm{Im}\,\omega = \gamma > 0$ is assumed in (196). The wave polarization associated with (196) is given by

$$\boldsymbol{k} = (0, 0, k_z), \qquad \widehat{\delta \boldsymbol{E}} = \left(\mp i\widehat{\delta E_y}, \widehat{\delta E_y}, 0\right), \tag{197}$$

where $D^+ = 0$ and $D^- = 0$ correspond to circularly polarized electromagnetic waves with right-hand ($\widehat{\delta E_x} = -i\widehat{\delta E_y}$) and left-hand ($\widehat{\delta E_x} = +i\widehat{\delta E_y}$) polarizations, respectively. It is evident from (196) that the detailed dependence of $F_j(v_\perp^2, v_z)$ on $v_\perp^2$ does not have to be specified in analyzing the dispersion relation. Therefore, for present purposes, it is assumed that $F_j(v_\perp^2, v_z)$ is of the form

$$F_j(v_\perp^2, v_z) = \left(\frac{m_j}{2\pi T_{j\parallel}}\right)^{1/2} \exp\left(-\frac{m_j v_z^2}{2T_{j\parallel}}\right) G_j(v_\perp^2), \tag{198}$$

where

$$2\pi \int_0^{\infty} dv_\perp v_\perp G_j(v_\perp^2) = 1.$$

Because the $v_\perp^2$ moment of F_j occurs in (196), the *effective perpendicular temperature* $T_{j\perp}$ is defined by

$$T_{j\perp} = 2\pi \int_0^{\infty} dv_\perp v_\perp \left(\frac{m_j}{2} v_\perp^2\right) G_j(v_\perp^2). \tag{199}$$

Substituting (198) and (199) into (196) then gives the dispersion relation

$$D^{\pm}(k_z, \omega_r + i\gamma) = 1 - \frac{c^2 k_z^2}{(\omega_r + i\gamma)^2} + \sum_j \frac{\omega_{pj}^2}{(\omega_r + i\gamma)^2} \times \left[\frac{(\omega_r + i\gamma)}{k_z v_{Tj}} Z(\xi_j^{\pm}) - \left(1 - \frac{T_{j\perp}}{T_{j\parallel}}\right)\left(1 + \xi_j^{\pm} Z(\xi_j^{\pm})\right)\right] = 0, \tag{200}$$

where $v_{Tj} = (2T_{j\|}/m_j)^{1/2}$ is the parallel thermal speed, $Z(\xi_j^{\pm})$ is the plasma dispersion function defined in (105), and $\xi_j^{\pm}$ is defined by

$$\xi_j^{\pm} = (\omega_r \pm \omega_{cj} + i\gamma)/k_z v_{Tj}. \tag{201}$$

Depending on the region of ω- and k_z-space under investigation, and the degree and nature ($T_{j\|} \gtrless T_{j\perp}$) of the temperature anisotropy, the electromagnetic dispersion relation (200) supports a wide variety of waves and instabilities including the firehose instability, the electromagnetic ion cyclotron instability, and the electron Whistler instability. These instabilities are examined in detail in the last three subsections of Section 3.3.5. To orient the reader and establish the basic normal modes of the system, in the next subsection (200) is considered in the limit of a cold, isotropic plasma.

Waves in a cold plasma

For a cold, isotropic plasma with $T_{j\perp} = T_{j\|} \equiv T_j \to 0$, consider (200) with $|\xi_j^{\pm}| = |(\omega_r \pm \omega_{cj} + i\gamma)/k_z v_{Tj}| \gg 1$. Approximating $Z(\xi_j^{\pm}) \simeq -1/\xi_j$ [Eq. (107)], the dispersion relation supports only solutions with real oscillation frequency ($\gamma = 0$), and (200) reduces to

$$D^{\pm}(k_z, \omega_r) = 1 - \frac{c^2 k_z^2}{\omega_r^2} - \frac{\omega_{pe}^2}{\omega_r(\omega_r \pm \omega_{ce})} - \frac{\omega_{pi}^2}{\omega_r(\omega_r \pm \omega_{ci})} = 0 \tag{202}$$

for a two-species plasma. For each sign (+ or −), (202) supports six real solutions for ω_r. For present purposes, it is useful to briefly consider (202) in several limiting frequency regimes.

Alfvén waves. Assuming low-frequency perturbations with

$$|\omega_r| \ll |\omega_{ci}|, |\omega_{ce}|, \tag{203}$$

and making use of equilibrium charge neutrality, $\omega_{pe}^2/(\pm\omega_{ce}) + \omega_{pi}^2/(\pm\omega_{ci}) = 0$, (202) can be expanded to $O(1/\omega_{cj}^2)$ for strong magnetic field to give the approximate dispersion relation

$$\omega_r^2 = \frac{k_z^2 c^2}{1 + \sum_j \omega_{pj}^2/\omega_{cj}^2} = \frac{k_z^2 V_A^2}{1 + V_A^2/c^2}, \tag{204}$$

where the Alfvén velocity V_A is defined by $c^2/V_A^2 = \sum_j \omega_{pj}^2/\omega_{cj}^2 = \sum_j 4\pi \hat{n}_j m_j c^2/B_0^2$. Note that $c^2/V_A^2 = \omega_{pi}^2/\omega_{ci}^2 \gg 1$ for typical plasmas, so that $\omega_r^2 = k_z^2 V_A^2$ is a good approximation to (204).

Later in Section 3.3.5, assuming a warm, anisotropic plasma with $T_{j\|}$ exceeding $T_{j\perp}$ by a sufficiently large amount, it will be seen that the low-frequency Alfvén branch exhibits strong instability (called the firehose instability).

Ion cyclotron waves. Assuming strongly magnetized electrons with

$$|\omega_r| \ll |\omega_{ce}|, \tag{205}$$

but allowing for ω_r to extend to the ion cyclotron range of frequencies, (202) can be expanded to $O(1/\omega_{ce}^2)$ to give

$$D(k_z, \omega_r) = 1 - \frac{c^2 k_z^2}{\omega_r^2} + \frac{\omega_{pe}^2}{\omega_{ce}^2} - \frac{\omega_{pe}^2}{\omega_r(\pm\omega_{ce})} - \frac{\omega_{pi}^2}{\omega_r(\omega_r \pm \omega_{ci})} = 0. \tag{206}$$

Making use of equilibrium charge neutrality, $\omega_{pe}^2/(\pm\omega_{ce}) + \omega_{pi}^2/(\pm\omega_{ci}) = 0$, Eq. (206) can be expressed in the equivalent form

$$0 = 1 - \frac{c^2 k_z^2}{\omega_r^2} + \frac{\omega_{pe}^2}{\omega_{ce}^2} + \frac{\omega_{pi}^2}{(\pm\omega_{ci})(\omega_r \pm \omega_{ci})}. \tag{207}$$

For $|\omega_r| \ll |\omega_{ci}|$, (207) reduces directly in the Alfvén wave dispersion relation given in (204). For $|\omega_r| \lesssim |\omega_{ci}|$, use is made of the fact that the final term in (207) is large in comparison with $1 + \omega_{pe}^2/\omega_{ce}^2$ (assuming $\omega_{pi}^2/\omega_{ci}^2 \gg 1$), and (207) can be approximated by

$$\omega_r = \mp\,\omega_{ci}\left(1 - \omega_r^2/k_z^2 V_A^2\right), \tag{208}$$

where $V_A^2/c^2 \simeq \omega_{ci}^2/\omega_{pi}^2$. For $|\omega_r| \ll |\omega_{ci}|$, (208) gives $\omega_r^2 \simeq k_z^2 V_A^2$, as expected. For increasing values of $|\omega_r|$, the ion cyclotron branch in (208) asymptotes with $\omega_r \to \mp\,\omega_{ci}$ when $k_z^2 V_A^2/\omega_{ci}^2 \gg 1$.

Later in Section 3.3.5, for a warm anisotropic plasma with $T_{i\perp}$ exceeding $T_{i\parallel}$ by a sufficiently large amount, it will be seen that the ion cyclotron branch exhibits a strong (Weibel-like) electromagnetic instability with characteristic growth rate of order ω_{ci} when the anisotropy is large.

Electron cyclotron (Whistler) waves. For high-frequency perturbations with

$$|\omega_r| \gg |\omega_{ci}|, \tag{209}$$

and $c^2 k_z^2 \gg \omega_{pi}^2$, the ion term is negligibly small in (202), and the dispersion relation can be approximated by

$$0 = 1 - c^2 k_z^2/\omega_r^2 - \omega_{pe}^2/\left[\omega_r(\omega_r \pm \omega_{ce})\right]. \tag{210}$$

Equation (210) is the dispersion relation for electron cyclotron (or so-called *electron Whistler*) waves. For a moderately dense plasma with $\omega_{pe}^2/\omega_{ce}^2 \gg 1$ and perturbation frequency $|\omega_r|$ comparable in size with $|\omega_{ce}|$, the contribution by the displacement current in (210) is negligibly small, and the dispersion relation can be approximated by

$$\omega_r = \mp\,\omega_{ce} c^2 k_z^2/\left(\omega_{pe}^2 + c^2 k_z^2\right). \tag{211}$$

It is clear from (211) that the real frequency ω_r can span a large range, with ω_r asymptoting at $\mp\,\omega_{ce}$ for $c^2 k_z^2 \gg \omega_{pe}^2$.

As for the ion cyclotron branch, it will be seen later in Section 3.3.5 that the electron cyclotron branch exhibits a Weibel-like instability for $T_{e\perp} > T_{e\parallel}$.

Fast electromagnetic waves. For completeness, at very high frequencies with

$$|\omega_r| \gg |\omega_{ce}|, |\omega_{ci}|, \tag{212}$$

the dispersion relation (202) can be approximated by

$$\omega_r^2 = c^2 k_z^2 + \sum_j \omega_{pj}^2. \tag{213}$$

As expected, (213) is identical to the cold-plasma dispersion relation for electromagnetic wave propagation in an unmagnetized plasma (Section 3.3.4).

Firehose instability

The full dispersion relation (200) is now considered, allowing for energy anisotropy with $T_{j\parallel} \neq T_{j\perp}$. Expanding (200) for long axial wavelengths with

$$|\xi_j^{\pm}| = |(\omega_r \pm \omega_{cj} + i\gamma)/k_z v_{Tj}| \gg 1, \tag{214}$$

and retaining terms to $O[k_z^2 v_{Tj}^2/(\omega_r \pm \omega_{cj} + i\gamma)^2]$, the dispersion relation (200) can be approximated by

$$D^{\pm}(k_z, \omega_r + i\gamma) = 1 - \frac{c^2 k_z^2}{(\omega_r + i\gamma)^2} - \sum_j \frac{\omega_{pj}^2}{(\omega_r + i\gamma)(\omega_r \pm \omega_{cj} + i\gamma)}$$

$$+ \sum_j \frac{\omega_{pj}^2}{(\omega_r + i\gamma)^2}\left(1 - \frac{T_{j\perp}}{T_{j\parallel}}\right)\frac{(k_z^2 T_{j\parallel}/m_j)}{(\omega_r \pm \omega_{cj} + i\gamma)^2} = 0, \tag{215}$$

where use has been made of $Z(\xi_j^{\pm}) = -1/\xi_j - 1/2\xi_j^3$ [Eq. (107)]. Paralleling the analysis in the previous subsection that led to the Alfvén wave dispersion relation (204), it is assumed that the perturbation frequency is low with $|\omega_r + i\gamma| \ll |\omega_{ci}|, |\omega_{ce}|$. Expanding (215) correct to $O(1/\omega_{cj}^2)$, and making use of equilibrium charge neutrality, $\omega_{pi}^2/(\pm\omega_{ci}) + \omega_{pe}^2/(\pm\omega_{ce}) = 0$, gives

$$0 = 1 - \frac{c^2 k_z^2}{(\omega_r + i\gamma)^2} + \sum_j \frac{\omega_{pj}^2}{\omega_{cj}^2} + \sum_j \frac{\omega_{pj}^2}{\omega_{cj}^2}\frac{k_z^2(T_{j\parallel} - T_{j\perp})/m_j}{(\omega_r + i\gamma)^2}. \tag{216}$$

where

$$\sum_j \omega_{pj}^2/\omega_{cj}^2 \equiv c^2/V_A^2 = \sum_j 4\pi \hat{n}_j m_j c^2/B_0^2,$$

$$\sum_j \omega_{pj}^2(T_{j\parallel} - T_{j\perp})/m_j\omega_{cj}^2 = \sum_j 4\pi\hat{n}_j(T_{j\parallel} - T_{j\perp})c^2/B_0^2 \equiv (4\pi c^2/B_0^2)(P_\parallel - P_\perp).$$

Here, $P_\parallel = \sum_j \hat{n}_j T_{j\parallel}$ is the parallel pressure, and $P_\perp = \sum_j \hat{n}_j T_{j\perp}$ is the perpendicular pressure. Solving (216) gives

$$(\omega_r + i\gamma)^2 = -\frac{k_z^2 V_A^2}{1 + V_A^2/c^2}\left(\frac{P_\parallel - P_\perp - B_0^2/4\pi}{B_0^2/4\pi}\right). \tag{217}$$

For an isotropic plasma with $P_\parallel = P_\perp$, (217) reduces to the Alfvén wave dispersion relation with $\gamma = 0$ and $\omega_r^2 = k_z^2 V_A^2/(1 + V_A^2/c^2)$. On the other hand, for

$$\beta_\parallel > \beta_\perp + 2, \tag{218}$$

where $\beta_\parallel = 8\pi P_\parallel / B_0^2$ and $\beta_\perp = 8\pi P_\perp / B_0^2$ are the parallel and perpendicular plasma betas, respectively, the dispersion relation predicts purely growing (and purely damped) solutions with $\omega_r = 0$ and

$$\gamma^2 = \frac{1}{2} \frac{k_z^2 V_A^2}{1 + V_A^2/c^2} \left[\beta_\parallel - \beta_\perp - 2 \right]. \tag{219}$$

Note from (219) that the lowest-order growth rate diverges for large k_z. If higher-order contributions in $k_z v_{Tj} / (\pm \omega_{cj})$ are retained in expanding the dispersion relation (200), finite-Larmor-radius corrections to (216) are obtained that are quartic in k_z. These corrections are of such a nature that the growth rate γ passes through a maximum (as a function of k_z) and goes to zero at some sufficiently large wavenumber k_0. In addition, the oscillation frequency ω_r is nonzero to this accuracy. After some straightforward algebra, it can be shown that γ and ω_r are given by the approximate expressions

$$\gamma^2 = \gamma_0^2 \left(1 - k_z^2 / k_0^2 \right), \qquad \omega_r^2 = \gamma_0^2 k_z^2 / k_0^2, \tag{220}$$

for $0 < k_z^2 < k_0^2$. In (220), γ_0 is the lowest-order growth rate calculated in (219), and the cutoff wavenumber k_0 is defined by

$$k_0^2 = 4 (\gamma_0 / k_z)^2 \left(1 + \sum_j \frac{\omega_{pj}^2}{\omega_{cj}^2} \right)^2 \times \left(\sum_j \frac{\omega_{pj}^2}{\omega_{cj}^3} \left[(\gamma_0 / k_z)^2 + (2T_{j\perp} - 3T_{j\parallel}) / m_j \right] + O\left(1/\omega_{cj}^4 \right) \right)^{-2}. \tag{221}$$

In obtaining (220) and (221), it has been assumed that the plasma beta, $\beta = 8\pi \sum_j \hat{n}_j (T_{j\parallel} + T_{j\perp}) / B_0^2$ is large ($\beta \gg 1$). Of course, $\beta_\parallel > \beta_\perp + 2$ is already required from (218) for instability to exist. From (220), the growth rate satisfies $\gamma \simeq \gamma_0$ for $|k_z| \ll |k_0|$, passes through a maximum at $|k_z| = |k_0| / \sqrt{2}$, and goes to zero at $|k_z| = |k_0|$ (Fig. 3.3.12).

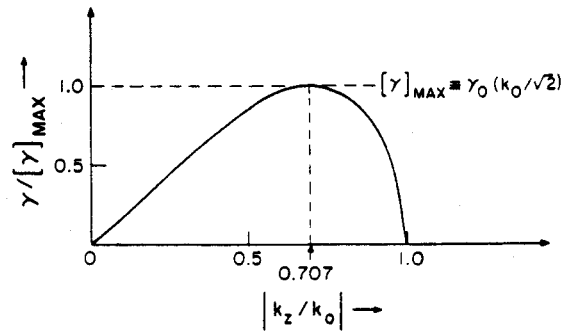

Fig. 3.3.12. Plot of growth rate γ versus $|k_z/k_0|$ for firehose instability [Eq. (220)]. Here $[\gamma]_{max} = \gamma_0 (k_z = k_0/\sqrt{2})$, where γ_0 is defined in (219).

Electromagnetic ion cyclotron instability

The dispersion relation (200) is now considered in the ion cyclotron range of frequencies. For present purposes, it is assumed that the electrons are isotropic with $T_{e\perp} = T_{e\parallel} \equiv T_e$, and strongly magnetized with $|\omega_r + i\gamma| \ll |\omega_{ce}|$ and $|k_z v_{Te}| \ll |\omega_r \pm \omega_{ce} + i\gamma|$. An ion energy anisotropy, however, is allowed with

$$T_{i\perp} > T_{i\parallel}. \tag{222}$$

The electromagnetic (Weibel-like) instability, which is driven by excess perpendicular ion kinetic energy, can play a very important role in magnetic mirror configurations with perpendicular neutral beam injection. Mirror systems also have a natural tendency to lose ions with sizeable kinetic energy along the field lines, so that $T_{i\perp}$ can often exceed the effective parallel temperature. Making use of the approximations enumerated above, the dispersion relation (200) can be expressed as

$$D^{\pm}(k_z, \omega_r + i\gamma) = 1 - \frac{c^2 k_z^2}{(\omega_r + i\gamma)^2} + \frac{\omega_{pe}^2}{\omega_{ce}^2} - \frac{\omega_{pe}^2}{(\omega_r + i\gamma)(\pm\omega_{ce})}$$
$$+ \frac{\omega_{pi}^2}{(\omega_r + i\gamma)^2}\left[\frac{(\omega_r + i\gamma)}{k_z v_{Ti}} Z(\xi_i^{\pm}) - \left(1 - \frac{T_{i\perp}}{T_{i\parallel}}\right)\left[1 + \xi_i^{\pm} Z(\xi_i^{\pm})\right]\right] = 0, \tag{223}$$

where $v_{Ti} = (2T_{i\parallel}/m_i)^{1/2}$ and $\xi_i^{\pm} = (\omega_r \pm \omega_{ci} + i\gamma)/k_z v_{Ti}$. In (223), $\omega_{pe}^2/(\pm\omega_{ce}) = -\omega_{pi}^2/(\pm\omega_{ci})$ follows from equilibrium charge neutrality. For isotropic ions with $T_{i\perp} = T_{i\parallel}$, (223) permits only stable solutions with $\mathrm{Im}\,\omega = \gamma \leqslant 0$. For $T_{i\perp} > T_{i\parallel}$, and $\beta_{i\perp} = 8\pi \hat{n}_i T_{i\perp}/B_0^2$ of order unity, however, (223) has an unstable branch with characteristic frequency $|\omega_r + i\gamma| \approx |\omega_{ci}|$ and characteristic wavenumber $|k_z| \approx \omega_{pi}/c$.

Before discussing detailed solutions to (223), it is instructive to simplify (223) in the limiting case $T_{i\parallel} \to 0$. Expanding with $|\xi_i^{\pm}| \gg 1$, the dispersion relation (223) for $T_{i\parallel} \to 0$ becomes

$$0 = 1 - \frac{c^2 k_z^2}{(\omega_r + i\gamma)^2} + \frac{\omega_{pe}^2}{\omega_{ce}^2} - \frac{\omega_{pe}^2}{(\omega_r + i\gamma)(\pm\omega_{ce})}$$
$$- \frac{\omega_{pi}^2}{(\omega_r + i\gamma)^2}\left(\frac{(\omega_r + i\gamma)}{(\omega_r \pm \omega_{ci} + i\gamma)} + \frac{(k_z^2 T_{i\perp}/m_i c^2)}{(\omega_r \pm \omega_{ci} + i\gamma)^2}\right). \tag{224}$$

Because $|c^2 k_z^2/(\omega_r + i\gamma)^2| \gg 1 + \omega_{pe}^2/\omega_{ce}^2$ in the region of ω- and k_z-space under investigation, the dispersion relation (224) can be approximated by

$$0 = -c^2 k_z^2 + \frac{\omega_{pi}^2}{(\pm\omega_{ci})}\frac{(\omega_r + i\gamma)^2}{(\omega_r \pm \omega_{ci} + i\gamma)} - \frac{1}{2}\beta_{i\perp} c^2 k_z^2 \frac{\omega_{ci}^2}{(\omega_r \pm \omega_{ci} + i\gamma)^2}, \tag{225}$$

where $\beta_{i\perp} = 8\pi \hat{n}_i T_{i\perp}/B_0^2 = (\omega_{pi}^2/\omega_{ci}^2)(2T_{i\perp}/m_i c^2)$, and use has been made of $\omega_{pe}^2/(\pm\omega_{ce}) = -\omega_{pi}^2/(\pm\omega_{ci})$. The cubic equation (225) can be solved exactly for the complex eigenfrequency $\omega_r + i\gamma$. Moreover, it is straightforward to show that maxi-

mum growth occurs for $c^2k_z^2 \gg \omega_{pi}^2$ where $\omega_r \simeq \mp \omega_{ci}$ and

$$[\gamma]_{max} \simeq (\beta_{i\perp}/2)^{1/2}\omega_{ci}. \tag{226}$$

This gives a good estimate of the characteristic frequency and instability growth rate in the limit of extreme energy anisotropy.

Although maximum growth when $T_{i\parallel} = 0$ occurs for very short wavelengths ($c^2k_z^2 \gg \omega_{pi}^2$), it should be emphasized that when the full dispersion relation (223) is solved for the case $T_{i\parallel} \neq 0$ the instability bandwidth is finite with characteristic wavelength $k_z^{-1} \approx c/\omega_{pi}$ (Fig. 3.3.13). Assuming $|c^2k_z^2/(\omega_r + i\gamma)^2| \gg 1 + \omega_{pe}^2/\omega_{ce}^2$, the dispersion relation (223) with $T_{i\parallel} \neq 0$ can be expressed as

$$D^{\pm}(k_z, \omega_r + i\gamma)(\omega_r + i\gamma)^2 = -c^2k_z^2 + \omega_{pi}^2\frac{(\omega_r + i\gamma)}{(\pm\omega_{ci})}$$

$$+ \omega_{pi}^2\left(\frac{(\omega_r + i\gamma)}{k_z v_{Ti}}Z(\xi_i^{\pm}) - \left(1 - \frac{T_{i\perp}}{T_{i\parallel}}\right)\left[1 + \xi_i^{\pm}Z(\xi_i^{\pm})\right]\right) = 0, \tag{227}$$

where use has been made of $\omega_{pe}^2/(\pm\omega_{ce}) = -\omega_{pi}^2/(\pm\omega_{ci})$. Numerical solutions to (227) are presented in Figs. 3.3.13 and 3.3.14, where normalized growth rate γ/ω_{ci} and normalized real frequency $|\omega_r|/\omega_{ci}$ are plotted versus $c|k_z|/\omega_{pi}$ for hydrogen plasma with $Z_i = 1$ and $m_e/m_i = 1/1836$, and perpendicular ion beta $\beta_{i\perp} = 1$. For increasing values of $T_{i\perp}/T_{i\parallel}$, it is evident from Fig. 3.3.13 that both the growth rate and bandwidth of the instability increase substantially. Moreover, for sufficiently large anisotropy $T_{i\perp}/T_{i\parallel}$, it is found that the characteristic maximum growth rate $[\gamma]_{max}$ obtained from (227) scales as $(\beta_{i\perp}/2)^{1/2}\omega_{ci}$ [see also (226)]. Finally, although cold, isotropic electrons with $T_{e\perp} = T_{e\parallel} = T_e \to 0$ have been assumed in (227), it can be shown that the instability results are insensitive to the choice of T_e as long as the electron beta satisfies $\beta_e \ll (m_i/m_e)^{1/2}$.

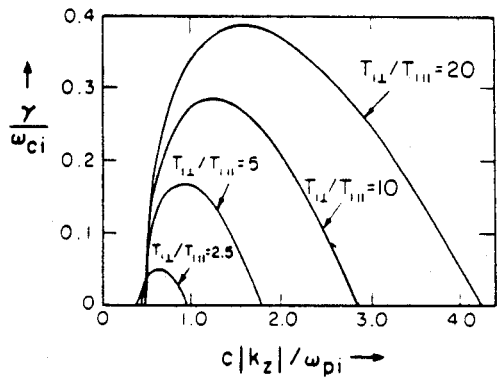

Fig. 3.3.13. Plot of normalized growth rate γ/ω_{ci} versus $c|k_z|/\omega_{pi}$ for electromagnetic ion cyclotron instability assuming $\beta_{i\perp} = 8\pi n_i T_{i\perp}/B_0^2 = 1$ and hydrogen plasma with $Z_i = 1$ and $m_e/m_i = 1/1836$ [Eq. (227)]. (Fig. 2 from Davidson, R.C., and J. Ogden, 1975, Phys. Fluids 18, 1047.)

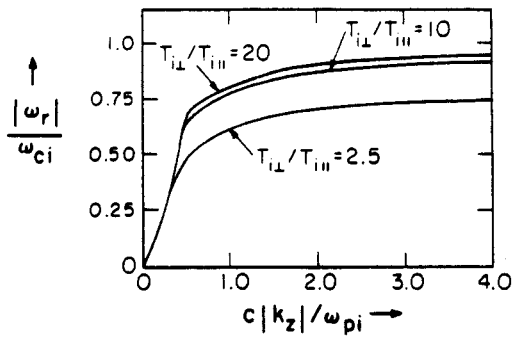

Fig. 3.3.14. Plot of normalized real frequency $|\omega_r|/\omega_{ci}$ versus $c|k_z|/\omega_{pi}$ for electromagnetic ion cyclotron instability assuming hydrogen plasma and $\beta_{i\perp}=1$ [Eq. (227)]. (Fig. 3 from Davidson, R.C. and J. Ogden, 1975, Phys. Fluids 18, 1047.)

Within the context of the approximations in (227), it is straightforward to deduce the values of ω and k_z at marginal stability. The conditions

$$\lim_{\gamma\to 0_+} \mathrm{Re}\, D^{\pm}(k_z, \omega_r+i\gamma)=0=\lim_{\gamma\to 0_+} \mathrm{Im}\, D^{\pm}(k_z, \omega_r+i\gamma) \tag{228}$$

readily yield $(\omega_r, k_z)=(0,0)$ and $(\omega_r, k_z)=(\omega_0, k_0)$, where

$$\omega_0^2=\omega_{ci}^2(1-T_{i\parallel}/T_{i\perp})^2, \tag{229}$$

and

$$k_0^2=\frac{\omega_{pi}^2}{c^2}\frac{(T_{i\perp}-T_{i\parallel})^2}{T_{i\parallel}T_{i\perp}}. \tag{230}$$

The values of k_0 and ω_0 obtained from (229) and (230) are in excellent agreement with those obtained from Figs. 3.3.13 and 3.3.14, where k_0 refers to the right-most $\gamma=0$ intercepts in Fig. 3.3.13. In this regard, it is important to note that the growth rate for $0<c|k_z|/\omega_{pi}\lesssim 0.5$, although exceptionally small in units of ω_{ci} (Fig. 3.3.13), is nonzero except in the limiting case $T_{i\parallel}=0$.

Electron cyclotron (Whistler) instability

In this section, the dispersion relation (200) is considered in the electron cyclotron range of frequencies. For $T_{e\perp}>T_{e\parallel}$, (200) supports a Weibel-like instability driven by the electron energy anisotropy. The mechanism for this instability is similar to the mechanism for the ion cyclotron instability discussed in the last subsection. Treating the ions as infinitely massive with $m_i\to\infty$ and $|\xi_i^{\pm}|\gg 1$, the dispersion relation (200) becomes

$$D^{\pm}(k_z, \omega_r+i\gamma)=1-\frac{c^2k_z^2}{(\omega_r+i\gamma)^2}+\frac{\omega_{pe}^2}{(\omega_r+i\gamma)^2}\left[\frac{(\omega_r+i\gamma)}{k_z v_{Te}}Z(\xi_e^{\pm})-\left(1-\frac{T_{e\perp}}{T_{e\parallel}}\right)\left[1+\xi_e^{\pm}Z(\xi_e^{\pm})\right]\right]=0, \tag{231}$$

where $v_{Te} = (2T_{e\parallel}/m_e)^{1/2}$, $\xi_e^{\pm} = (\omega_r \pm \omega_{ce} + i\gamma)/k_z v_{Te}$, and $Z(\xi_e^{\pm})$ is the plasma dispersion function defined in (105). For present purposes, the case of weak energy anisotropy with

$$|(T_{e\perp} - T_{e\parallel})/T_{e\parallel}| \ll 1 \tag{232}$$

is considered, assuming that the instability growth rate is small with

$$|\gamma| \ll |k_z v_{Te}| \ll |\omega_r \pm \omega_{ce}|. \tag{233}$$

Defining $D_r^{\pm}(k_z, \omega_r) = \lim_{\gamma \to 0_+} \mathrm{Re}\, D(k_z, \omega_r + i\gamma)$, and $D_i^{\pm}(k_z, \omega_r) = \lim_{\gamma \to 0_+} \mathrm{Im}\, D(k_z, \omega_r + i\gamma)$, it is straightforward to show that

$$\begin{aligned} D_r^{\pm}(k_z, \omega_r) &= 1 - \frac{c^2 k_z^2}{\omega_r^2} - \frac{\omega_{pe}^2}{\omega_r(\omega_r \pm \omega_{ce})} + \left(1 - \frac{T_{e\perp}}{T_{e\parallel}}\right) \frac{\omega_{pe}^2}{\omega_r^2} \frac{k_z^2 T_{e\parallel}/m_e}{(\omega_r \pm \omega_{ce})^2} \\ &\simeq 1 - \frac{c^2 k_z^2}{\omega_r^2} - \frac{\omega_{pe}^2}{\omega_r(\omega_r \pm \omega_{ce})}, \end{aligned} \tag{234}$$

and

$$D_i^{\pm}(k_z, \omega_r) = \sqrt{\pi}\, \frac{\omega_r}{|k_z| v_{Te}} \frac{\omega_{pe}^2}{\omega_r^2} \left[1 - \left(1 - \frac{T_{e\perp}}{T_{e\parallel}}\right) \frac{(\omega_r \pm \omega_{ce})}{\omega_r}\right] \exp\left(-\frac{(\omega_r \pm \omega_{ce})^2}{k_z^2 v_{Te}^2}\right). \tag{235}$$

The final term in the first line of (234) has been neglected by virtue of the inequalities (232) and (233).

Paralleling the analysis in the first subsection of Section 3.3.3, the real oscillation frequency ω_r is determined from

$$D_r^{\pm}(k_z, \omega_r) = 1 - \frac{c^2 k_z^2}{\omega_r^2} - \frac{\omega_{pe}^2}{\omega_r(\omega_r \pm \omega_{ce})} = 0, \tag{236}$$

and the growth rate γ is given by

$$\begin{aligned} \gamma &= -\frac{D_i(k_z, \omega_r)}{\partial D_r(k_z, \omega_r)/\partial \omega_r} \\ &= \sqrt{\pi}\, \frac{\omega_r^2}{|k_z| v_{Te}} \frac{\omega_{pe}^2}{\omega_r^2} \left[-1 + \left(1 - \frac{T_{e\perp}}{T_{e\parallel}}\right) \frac{(\omega_r \pm \omega_{ce})}{\omega_r}\right] \exp\left(-\frac{(\omega_r \pm \omega_{ce})^2}{k_z^2 v_{Te}^2}\right) \\ &\quad \times \left(1 + \frac{c^2 k_z^2}{\omega_r^2} + \frac{\omega_{pe}^2}{(\omega_r \pm \omega_{ce})^2}\right)^{-1}, \end{aligned} \tag{237}$$

where use has been made of (236) in determining $\partial D_r/\partial \omega_r$ in (237).

For an isotropic plasma with $T_{e\perp} = T_{e\parallel}$, it is clear from (237) that $\gamma < 0$ and the waves are weakly *damped* by resonant electrons with $k_z v_z = \omega_r \pm \omega_{ce}$. On the other

hand, for $T_{e\perp} > T_{e\parallel}$, the energy anisotropy can cause wave *growth* ($\gamma > 0$) in (237). To illustrate this effect, consider the moderate density regime where $\omega_{pe}^2/\omega_{ce}^2 \gg 1$, and the displacement current is negligibly small in (236). In this case, (236) gives

$$\omega_r \pm \omega_{ce} = \pm\, \omega_{ce} \frac{\omega_{pe}^2}{\omega_{pe}^2 + c^2 k_z^2}, \tag{238}$$

and $(\omega_r \pm \omega_{ce})/\omega_r = -(\omega_{pe}^2/c^2 k_z^2)$. It follows from (237) that instability exists ($\gamma > 0$) whenever the inequality

$$k_z^2 < \frac{\omega_{pe}^2}{c^2}\left(\frac{T_{e\perp}}{T_{e\parallel}} - 1\right) \tag{239}$$

is satisfied.

3.3.6. *Waves and instabilities for propagation perpendicular to B_0*

In Section 3.3.1 the ordinary-mode and extraordinary-mode dispersion relations [(50) and (52), respectively] were derived for wave propagation perpendicular to a uniform, applied magnetic field $\boldsymbol{B}_0 = B_0\hat{\boldsymbol{e}}_z$. The analysis in Section 3.3.1 was carried out for wavevector

$$\boldsymbol{k} = k_\perp \hat{\boldsymbol{e}}_x, \tag{240}$$

and general equilibrium distribution function $F_j(v_\perp^2, v_z)$ subject to zero average flow in the axial direction, i.e., $\int_{-\infty}^{\infty} dv_z\, v_z F_j(v_\perp^2, v_z) = 0$ in (42). In this section, plasma stability properties are considered for wave propagation perpendicular to $B_0\hat{\boldsymbol{e}}_z$ with particular emphasis on ordinary-mode electromagnetic instabilities driven by energy anisotropy and on electrostatic instabilities associated with the Bernstein-mode dispersion relation (54) when there are nonthermal loss-cone features associated with the equilibrium distribution function $F_j(v_\perp^2, v_z)$.

Ordinary-mode dispersion relation

Assuming wave polarization

$$\boldsymbol{k} = (k_\perp, 0, 0), \qquad \widehat{\delta \boldsymbol{E}} = (0, 0, \widehat{\delta E_z}), \tag{241}$$

and expressing $\omega = \omega_r + i\gamma$, the ordinary-mode dispersion relation (50) can be expressed as

$$D_{zz}(k_\perp, \omega_r + i\gamma) = 1 - \frac{c^2 k_\perp^2}{(\omega_r + i\gamma)^2} - \sum_j \frac{\omega_{pj}^2}{(\omega_r + i\gamma)^2}$$
$$+ \sum_j \sum_{n=-\infty}^{\infty} \frac{\omega_{pj}^2}{(\omega_r + i\gamma)^2} \frac{n\omega_{cj}}{\omega_r + i\gamma - n\omega_{cj}} \int d^3v J_n^2(b_j) \frac{v_z^2}{v_\perp} \frac{\partial F_j}{\partial v_\perp} = 0, \tag{242}$$

where $\omega_{cj} = e_j B_0/m_j c$ is the cyclotron frequency, and $b_j = k_\perp v_\perp/\omega_{cj}$. As indicated

in Section 3.3.1, the dispersion relation (242) predicts an electromagnetic Weibel-like instability when the plasma kinetic energy along the magnetic field, $\hat{n}_j \int d^3v\, (m_j v_z^2/2) F_j$, exceeds the perpendicular kinetic energy, $\hat{n}_j \int d^3v\, (m_j v_\perp^2/2) F_j$, by a sufficiently large amount. To illustrate the essential features of this *ordinary-mode electromagnetic instability*, consider the case where the equilibrium distribution functions are bi-Maxwellian,

$$F_j(v_\perp^2, v_z) = \left(\frac{m_j}{2\pi T_{j\parallel}}\right)^{1/2}\left(\frac{m_j}{2\pi T_{j\perp}}\right)\exp\left(-\frac{m_j v_\perp^2}{2T_{j\perp}} - \frac{m_j v_z^2}{2T_{j\parallel}}\right). \tag{243}$$

Substituting (243) into (242) gives the dispersion relation

$$(\omega_r + i\gamma)^2 = c^2 k_\perp^2 + \sum_j \omega_{pj}^2 + \sum_j \sum_{n=-\infty}^{\infty} \omega_{pj}^2 \frac{T_{j\parallel}}{T_{j\perp}} \frac{n\omega_{cj}}{\omega_r + i\gamma - n\omega_{cj}} \exp(-\lambda_j) I_n(\lambda_j), \tag{244}$$

where $\lambda_j = k_\perp^2 T_{j\perp}/m_j\omega_{cj}^2$, and $I_n(\lambda_j)$ is the modified Bessel function of the first kind of order n. If $F_j(v_\perp^2, v_z)$ in (243) is replaced by equidensity bi-Maxwellian plasmas counterstreaming with velocities $\pm V_j$ in the z-direction, the resulting dispersion relation is identical to (244) with the replacement $T_{j\parallel} \to T_{j\parallel} + m_j V_j^2$.

As for the case of an unmagnetized plasma (Section 3.3.4), the dispersion relation (244) supports stable ($\gamma = 0$) fast-wave solutions with $\omega_r^2/k_\perp^2 > c^2$. Moreover, except very close to cyclotron resonance ($\omega_r \simeq n\omega_{cj}$), the thermal corrections in (244) are small for a nonrelativistic plasma, and the fast-wave ordinary-mode dispersion relation is given by $\omega_r^2 = c^2 k_\perp^2 + \sum_j \omega_{pj}^2$ to good accuracy.

Depending on the degree of energy anisotropy, the ordinary-mode dispersion relation (244) also supports purely growing (or damped) slow-wave solutions with $\omega_r = 0$ and $\gamma \neq 0$. This case is now considered in more detail.

Ordinary-mode electromagnetic instability

Assuming

$$\omega_r = 0, \tag{245}$$

and making use of $I_{-n}(\lambda_j) = I_n(\lambda_j)$, the terms in (244) can be rearranged and the dispersion relation expressed in the equivalent form

$$\gamma^2 L(k_\perp, \gamma^2) = R(k_\perp), \tag{246}$$

where

$$L(k_\perp, \gamma^2) = 1 + \sum_j \frac{T_{j\parallel}}{T_{j\perp}} \sum_{n=0} \frac{\omega_{pj}^2}{n^2\omega_{cj}^2 + \gamma^2} \exp(-\lambda_j) I_n(\lambda_j), \tag{247}$$

and

$$R(k_\perp) = \sum_j \omega_{pj}^2 \left[\left(\frac{T_{j\parallel}}{T_{j\perp}} - 1\right) - \frac{T_{j\parallel}}{T_{j\perp}} \exp(-\lambda_j) I_0(\lambda_j)\right] - c^2 k_\perp^2. \tag{248}$$

Since the dispersion relation (246) depends on γ^2, the solutions $\pm\gamma$ occur in conjugate pairs. Moreover, since $L(k_\perp, \gamma^2)$ is manifestly positive, the necessary and sufficient condition for instability is given by

$$R(k_\perp) > 0. \tag{249}$$

Equation (248) determines the condition on system parameters $T_{j\|}/T_{j\perp}$, ω_{pj}^2, etc. for instability to exist. Moreover, the range of unstable $k_\perp$-values is given by

$$k_{\min}^2 < k_\perp^2 < k_0^2, \tag{250}$$

where k_0 and $k_{\min}$ solve $R(k_0) = 0 = R(k_{\min})$ with $\gamma(k_0) = 0 = \gamma(k_{\min})$. For an isotropic plasma with $T_{j\|} = T_{j\perp}$, note from (248) that $R(k_\perp) < 0$ for all values of $k_\perp$, and the plasma is stable. Indeed, it is clear from (248) and (249) that instability exists only if $T_{j\|}$ exceeds $T_{j\perp}$ by a sufficiently large amount for some plasma species j. Because $L(k_\perp, \gamma^2) \leqslant L(k_\perp, \gamma^2 = 0)$ follows from (247), a lower bound on the growth rate in the region $R(k_\perp) \geqslant 0$ is readily obtained, namely

$$\gamma^2 \geqslant R(k_\perp)/L(k_\perp, 0), \tag{251}$$

for $k_{\min}^2 < k_\perp^2 < k_0^2$.

As a simple example for direct computation, consider the case where the ions are isotropic with $T_{i\|} = T_{i\perp}$ and $O(m_e/m_i)$ terms are neglected. Extension of the analysis to include ion anisotropy and finite ion mass is straightforward. Retaining only electron terms, (248) can be expressed as

$$R(k_\perp) = \omega_{pe}^2 \frac{T_{e\|}}{T_{e\perp}} \left[\left(1 - \frac{T_{e\perp}}{T_{e\|}} \right) - G(\lambda_e) \right], \tag{252}$$

where

$$G(\lambda_e) = (2/\beta_{e\|})\lambda_e + \exp(-\lambda_e) I_0(\lambda_e). \tag{253}$$

In (253), $\lambda_e = k_\perp^2 T_{e\perp}/m_e\omega_{ce}^2$, and $\beta_{e\|} = 8\pi \hat{n}_e T_{e\|}/B_0^2$ is the parallel electron beta. The quantity $G(\lambda_e)$ is plotted as a function of λ_e for various values of the parameter $\beta_{e\|}$ in Fig. 3.3.15. For an appropriate choice of $T_{e\perp}/T_{e\|} < 1$, it is clear that the constant function $(1 - T_{e\perp}/T_{e\|})$ will intersect the curve $G(\lambda_e)$ at two values of λ_e when $\beta_{e\|} > 2$. These intersection points determine the marginal stability point, $k_{\min}$ and k_0, where $\gamma = 0$. The unstable region of $(T_{e\perp}/T_{e\|}, \beta_{e\|})$ space is illustrated in Fig. 3.3.16. In the limiting case where $\beta_{e\|} \gg 1$ (weak magnetic field), it is straightforward to show that $\lambda_0 = k_0^2 T_{e\perp}/m_e\omega_{ce}^2$ is determined (approximately) from $\lambda_0 = (\beta_{e\|}/2)(1 - T_{e\perp}/T_{e\|})$, or equivalently $k_0^2 = (\omega_{pe}^2/c^2)(T_{e\|}/T_{e\perp} - 1)$, which should be compared with the unmagnetized result in (187).

Electrostatic dispersion relation for propagation perpendicular to B_0

Circumstances are now considered where the extraordinary-mode dispersion relation (52) factors approximately into longitudinal ($D_{xx} = 0$) and transverse ($D_{yy} = 0$)

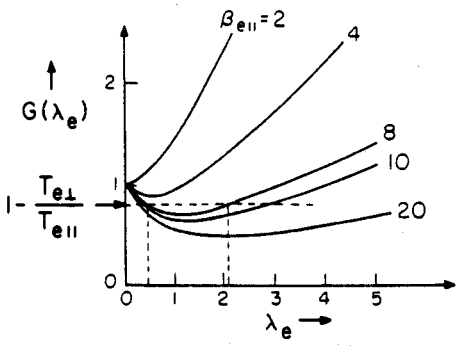

Fig. 3.3.15. Plot of $G(\lambda_e)$ versus λ_e for various values of $\beta_{e\|}=8\pi\hat{n}_e T_{e\|}/B_0^2$ for ordinary-mode electromagnetic instability [Eq. (253)].

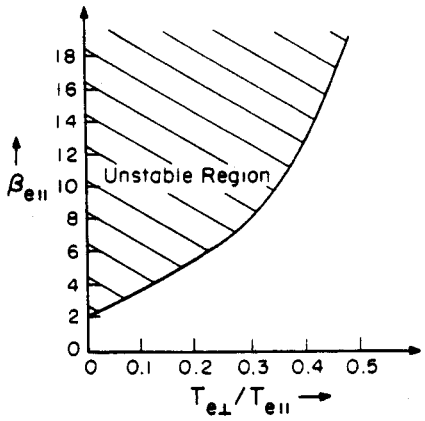

Fig. 3.3.16. Region of $(T_{e\perp}/T_{e\|}, \beta_{e\|})$ parameter space for ordinary-mode electromagnetic instability.

branches. In particular, the longitudinal branch with electrostatic wave polarization

$$\boldsymbol{k}=(k_\perp,0,0), \qquad \widehat{\delta \boldsymbol{E}}=(\widehat{\delta E}_x,0,0) \tag{254}$$

is considered. The dispersion relation $D_{xx}(k_\perp,\omega)=0$ in (54) can be expressed as

$$D_{xx}(k_\perp,\omega_r+i\gamma)=1+\sum_j \frac{\omega_{pj}^2}{k_\perp^2}\sum_{n=-\infty}^{\infty}\int d^3v \frac{n^2\omega_{cj}^2}{(\omega_r+i\gamma)^2-n^2\omega_{cj}^2}\frac{J_n^2(b_j)}{v_\perp}\frac{\partial F_j}{\partial v_\perp}=0, \tag{255}$$

where $\omega=\omega_r+i\gamma$ is the complex oscillation frequency, and $b_j=k_\perp v_\perp/\omega_{cj}$. Setting real and imaginary parts of (255) separately equal to zero gives, after some

straightforward algebra,

$$0 = 1 + \sum_j \frac{2\omega_{pj}^2}{k_\perp^2} \sum_{n=1}^{\infty} \frac{\left(\omega_r^2 - n^2\omega_{cj}^2 - \gamma^2\right) n^2\omega_{cj}^2}{\left[(\omega_r - n\omega_{cj})^2 + \gamma^2\right]\left[(\omega_r + n\omega_{cj})^2 + \gamma^2\right]} \times \int d^3v J_n^2(b_j) \frac{1}{v_\perp} \frac{\partial F_j}{\partial v_\perp}, \tag{256}$$

and

$$0 = \gamma\omega_r \sum_j \frac{\omega_{pj}^2}{k_\perp^2} \sum_{n=1}^{\infty} \frac{n^2\omega_{cj}^2}{\left[(\omega_r - n\omega_{cj})^2 + \gamma^2\right]\left[(\omega_r + n\omega_{cj})^2 + \gamma^2\right]} \times \int d^3v J_n^2(b_j) \frac{1}{v_\perp} \frac{\partial F_j}{\partial v_\perp}. \tag{257}$$

Assuming $\omega_r \neq 0$, it follows from (257) that $\partial F_j/\partial v_\perp^2 \leqslant 0$ is a sufficient condition for stability. That is, if $F_j(v_\perp^2, v_z)$ is a monotonic decreasing function of $v_\perp^2$ with $\partial F_j/\partial v_\perp^2 \leqslant 0$, every term in the summation over n in (257) has the same sign, and the only allowed solution to (257) is $\gamma = 0$, which corresponds to stable oscillations. In circumstances where $\gamma = 0$, (256) reduces to

$$0 = 1 + \sum_j \frac{2\omega_{pj}^2}{k_\perp^2} \sum_{n=1}^{\infty} \frac{n^2\omega_{cj}^2}{\omega_r^2 - n^2\omega_{cj}^2} \int d^3v J_n^2(b_j) \frac{1}{v_\perp} \frac{\partial F_j}{\partial v_\perp}, \tag{258}$$

which determines the real oscillation frequency ω_r as a function of $k_\perp$ and equilibrium plasma properties.

It is evident from the discussion in the preceding paragraph that $\partial F_j/\partial v_\perp^2 > 0$ over a sufficiently large region of $v_\perp$-space is a necessary condition for instability to exist. In this regard, when $\partial F_j/\partial v_\perp^2 > 0$ over a large enough region and the plasma density is sufficiently high, it will be shown later in Section 3.3.6 that (256) and (257) support purely growing (or purely damped) solutions with $\gamma \neq 0$ and $\omega_r = 0$. In this case, the dispersion relation (256) reduces to

$$0 = 1 - \sum_j \frac{2\omega_{pj}^2}{k_\perp^2} \sum_{n=1}^{\infty} \frac{n^2\omega_{cj}^2}{n^2\omega_{cj}^2 + \gamma^2} \int d^3v J_n^2(b_j) \frac{1}{v_\perp} \frac{\partial F_j}{\partial v_\perp}, \tag{259}$$

which can be used to calculate the growth rate γ.

Stable cyclotron harmonic oscillations

As a simple application of the electrostatic dispersion relation (255) corresponding to stable oscillations with $\gamma = 0$, consider the case where $F_j(v_\perp^2, v_z)$ has a Maxwellian dependence on $v_\perp$, i.e.

$$F_j(v_\perp^2, v_z) = \left(\frac{m_j}{2\pi T_{j\perp}}\right) \exp\left(-\frac{m_j v_\perp^2}{2T_{j\perp}}\right) G(v_z), \tag{260}$$

where $\int_{-\infty}^{\infty} dv_z G(v_z) = 1$. Substituting (260) into (255) or (258) gives

$$0 = 1 - \sum_j \frac{2\omega_{pj}^2}{\omega_{cj}^2} \sum_{n=1}^{\infty} \frac{n^2\omega_{cj}^2}{\omega_r^2 - n^2\omega_{cj}^2} \frac{I_n(\lambda_j)}{\lambda_j} \exp(-\lambda_j), \tag{261}$$

where $\lambda_j = k_\perp^2 T_{j\perp}/m_j\omega_{cj}^2$, and $I_n(\lambda_j)$ is the modified Bessel function of the first kind of order n. Since $\partial F_j/\partial v_\perp^2 \leqslant 0$, the growth rate $\gamma = 0$ follows from the discussion in the last subsection, and (261) can be used to determine the real oscillation frequency ω_r.

Equation (261) simplifies in several limiting cases. For purposes of illustration, two examples of stable oscillations are considered here.

Hybrid oscillations in a cold plasma. For $T_{j\perp} \to 0$ and/or sufficiently long perturbation wavelength that

$$\lambda_j = \frac{1}{2}k_\perp^2 \frac{v_{Tj}^2}{\omega_{cj}^2} = \frac{1}{2}k_\perp^2 r_{Lj}^2 \ll 1, \tag{262}$$

only the $n = 1$ term in (261) survives. Making use of $\exp(-\lambda_j)I_1(\lambda_j) \simeq \lambda_j/2$ for $\lambda_j \ll 1$, (261) reduces to

$$0 = 1 - \frac{\omega_{pi}^2}{\omega_r^2 - \omega_{ci}^2} - \frac{\omega_{pe}^2}{\omega_r^2 - \omega_{ce}^2}. \tag{263}$$

Equation (263) supports high-frequency ($\omega_r^2 > \omega_{ce}^2$) and intermediate-frequency ($\omega_{ci}^2 \ll \omega_r^2 \ll \omega_{ce}^2$) solutions given by

$$\omega_r^2 = \omega_{ce}^2 + \omega_{pe}^2 \equiv \omega_{UH}^2, \tag{264}$$

and

$$\omega_r^2 = \frac{\omega_{pi}^2}{1 + \omega_{pe}^2/\omega_{ce}^2} \equiv \omega_{LH}^2, \tag{265}$$

where ω_{UH} and ω_{LH} are upper hybrid and lower hybrid frequencies, respectively, and $\omega_{pi}^2 \gg \omega_{ci}^2$ has been assumed.

Cyclotron harmonic oscillations in a warm plasma. Note from (261) that the inclusion of thermal effects leads to a rich cyclotron harmonic structure in the dispersion relation. For present purposes, high-frequency perturbations with $\omega_r^2 > \omega_{ce}^2$ are considered, and the positive ions in (261) are treated as an infinitely massive background with $m_i \to \infty$. In addition, the plasma density is assumed to be sufficiently low that

$$\omega_{pe}^2/\omega_{ce}^2 < 1. \tag{266}$$

Within the context of (266), the individual harmonic terms in (261) are isolated from neighboring harmonics, and the solutions to the dispersion relation (261) can be

approximated by

$$\omega_r^2 = n^2\omega_{ce}^2\left(1+\frac{2\omega_{pe}^2}{\omega_{ce}^2}\frac{I_n(\lambda_e)}{\lambda_e}\exp(-\lambda_e)\right), \qquad n=1,2,3\cdots. \tag{267}$$

For $\lambda_e \ll 1$, the first harmonic ($n=1$) solution in (267) reduces to the upper hybrid oscillation in (264) with $\omega_r^2 = \omega_{ce}^2 + \omega_{pe}^2$. Unlike a cold plasma, the striking feature of (267) is that the warm plasma dispersion relation permits wave propagation near all harmonics of ω_{ce}. For a tenuous plasma with $\omega_{pe}^2/\omega_{ce}^2 \ll 1$, the propagation bandwidth is narrow, but increases with increasing $\omega_{pe}^2/\omega_{ce}^2$.

For $\omega_{pe}^2/\omega_{ce}^2 > 1$, the approximations used in deriving (267) are no longer valid, and it is necessary to retain several adjacent harmonic terms when analyzing the dispersion relation (261) for a given range of ω_r. Since $\partial F_j/\partial v_\perp^2 \leqslant 0$ for the choice of distribution function in (260), we reiterate that all solutions to the dispersion relation (261) have zero growth rate $\gamma = 0$ independent of the size of $\omega_{pe}^2/\omega_{ce}^2$.

Cyclotron harmonic instability for loss-cone equilibria

In this section, use is made of the electrostatic dispersion relation (255) for propagation perpendicular to $B_0\hat{e}_z$ to investigate cyclotron harmonic instabilities in circumstances where $F_j(v_\perp^2, v_z)$ corresponds to a loss-cone equilibrium with $\partial F_j/\partial v_\perp^2 > 0$ over a significant region of $v_\perp$-space. For purposes of illustration, the ions are treated as an infinitely massive background with $m_i \to \infty$, and the nonthermal equilibrium features are associated with the electron distribution function $F_e(v_\perp^2, v_z)$. The electrostatic dispersion relation (255) can be expressed as

$$D_{xx}(k_\perp, \omega_r + i\gamma) = 1 - \frac{\omega_{pe}^2}{\omega_{ce}^2}\sum_{n=1}^{\infty}\frac{n^2\omega_{ce}^2}{(\omega_r+i\gamma)^2 - n^2\omega_{ce}^2}\chi_n(k_\perp) = 0, \tag{268}$$

where $\chi_n(k_\perp)$ is defined by

$$\chi_n(k_\perp) = -\frac{2\omega_{ce}^2}{k_\perp^2}\int d^3v J_n^2(b_e)\frac{1}{v_\perp}\frac{\partial F_e}{\partial v_\perp}, \tag{269}$$

with $b_e = k_\perp v_\perp/\omega_{ce}$. As an extreme example of a loss-cone equilibrium, consider the electron distribution function

$$F_e(v_\perp^2, v_z) = \frac{1}{(2\pi v_\perp)}\delta(v_\perp - v_0)G(v_z), \tag{270}$$

where $\int_{-\infty}^{\infty} dv_z G(v_z) = 1$. Note that the equilibrium specified by (270) is empty ($F_e = 0$) for small perpendicular velocities $v_\perp < v_0$. Substituting (270) into (269) gives

$$\chi_n(k_\perp) = \frac{2}{b_0}\frac{d}{db_0}\left[J_n^2(b_0)\right], \tag{271}$$

where $b_0^2 = k_\perp^2 v_0^2/\omega_{ce}^2$, and the dispersion relation (268) can be expressed as

$$0 = 1 - \sum_{n=1}^{\infty} \frac{n^2\omega_{ce}^2}{(\omega_r + i\gamma)^2 - n^2\omega_{ce}^2}\left(\frac{\omega_{pe}^2}{\omega_{ce}^2}\frac{2}{b_0}\frac{d}{db_0}J_n^2(b_0)\right). \tag{272}$$

For a tenuous plasma with $\omega_{pe}^2/\omega_{ce}^2 \ll 1$, it is clear from (268) and (269) that the dispersion relation supports stable cyclotron harmonic waves with $\gamma = 0$ and

$$\omega_r^2 = n^2\omega_{ce}^2\left(1 + \frac{\omega_{pe}^2}{\omega_{ce}^2}\chi_n(k_\perp)\right), \qquad n = 1,2,3,.... \tag{273}$$

Equation (273) is an extension of (267) for general distribution function $F_e(v_\perp^2, v_z)$. As indicated in the last subsection, for $\omega_{pe}^2/\omega_{ce}^2 \ll 1$, the bandwidth for each cyclotron harmonic is narrow. However, depending on the sign of χ_n, propagation may be above ($\chi_n > 0$) or below ($\chi_n < 0$) the nth harmonic $\omega_r^2 = n^2\omega_{ce}^2$.

As $\omega_{pe}^2/\omega_{ce}^2$ is increased, the mode structure becomes increasingly broad-band, with significant departures from (273) and sharply defined oscillations at harmonics of ω_{ce}. A careful examination of (268) and (271)–(273) shows that

$$\chi_n > 0 \quad \text{and} \quad \chi_{n+1} < 0 \tag{274}$$

are necessary for instability ($\gamma > 0$) for waves propagating in the frequency range

$$n^2\omega_{ce}^2 < \omega_r^2 < (n+1)^2\omega_{ce}^2, \qquad n \geq 1. \tag{275}$$

Making use of (271) and (274) gives the range of unstable $k_\perp$-values,

$$\alpha_{n,m} < |k_\perp v_0/\omega_{ce}| < \alpha_{n+1,m}, \tag{276}$$

where $\alpha_{n,m}$ is the mth zero of $J_n(x) = 0$. A detailed numerical analysis of (272) shows that

$$\omega_{pe}^2/\omega_{ce}^2 > 6.62, \tag{277}$$

is required for onset of unstable solutions to (272).

As $\omega_{pe}^2/\omega_{ce}^2$ is increased above the value in (277), the growth rate γ becomes larger, and the real frequency mode structure becomes increasingly broad-band. Eventually, for sufficiently large $\omega_{pe}^2/\omega_{ce}^2 = 17.02$, the $n = 1$ mode is depressed to zero frequency ($\omega_r = 0$) for $|k_\perp v_0/\omega_{ce}| \simeq 3$, and there is the onset of purely growing (and purely damped) solutions with $\gamma \neq 0$ and $\omega_r = 0$. For $\omega_r = 0$, the dispersion relation (272) can be expressed as [see also (259)]

$$0 = 1 - \frac{\omega_{pe}^2}{\omega_{ce}^2}\frac{1}{b_0}\frac{d}{db_0}J_0^2(b_0) - \sum_{n=1}^{\infty}\frac{\gamma^2}{\gamma^2 + n^2\omega_{ce}^2}\left(\frac{\omega_{pe}^2}{\omega_{ce}^2}\frac{2}{b_0}\frac{d}{db_0}J_n^2(b_0)\right). \tag{278}$$

A careful examination of (278) shows that $\chi_0 > 0$ and $\chi_1 < 0$ are necessary for instability, and the corresponding range of unstable $k_\perp$-values is given by $\alpha_{0,m} < |k_\perp v_0/\omega_{ce}| < \alpha_{1,m}$. Making use of (278), the density threshold for instability with $\omega_r = 0$ is determined from

$$\frac{\omega_{pe}^2}{\omega_{ce}^2}\left(\frac{1}{b_0}\frac{d}{db_0}J_0^2(b_0)\right) > 1, \tag{279}$$

which gives

$$\omega_{pe}^2/\omega_{ce}^2 > 17.02, \tag{280}$$

for onset of instability.

To conclude this section, note that a similar stability analysis can be carried out for unstable ion loss-cone equilibria $F_i(v_\perp^2, v_z)$.

3.3.7. Electrostatic waves and instabilities in a magnetized plasma

Introduction and dispersion relation

In this section, use is made of the electrostatic dispersion relation (60) derived for a magnetized plasma in Section 3.3.1 to investigate several important instabilities driven by strong nonthermal equilibrium features of the distribution function $F_j(v_\perp^2, v_z)$. The starting point is (60), which can be expressed as

$$\begin{aligned} 0 = D(\boldsymbol{k}, \omega_r + i\gamma) &= 1 + \chi_e(\boldsymbol{k}, \omega_r + i\gamma) + \chi_i(\boldsymbol{k}, \omega_r + i\gamma) \\ &= 1 + \sum_j \frac{\omega_{pj}^2}{k^2} \sum_{n=-\infty}^{\infty} \int d^3v \frac{J_n^2(b_j)}{(\omega_r - n\omega_{cj} - k_z v_z + i\gamma)} \left(k_z \frac{\partial F_j}{\partial v_z} + \frac{n\omega_{cj}}{v_\perp} \frac{\partial F_j}{\partial v_\perp} \right), \end{aligned} \tag{281}$$

where $k^2 = k_\perp^2 + k_z^2$, $b_j = k_\perp v_\perp / \omega_{cj}$, $\omega = \omega_r + i\gamma$ is the complex oscillation frequency, χ_e and χ_i are the electron and ion dielectric responses, respectively, and $\mathrm{Im}\,\omega = \gamma > 0$ is assumed in (281). The wave polarization corresponding to (281) is given by

$$\boldsymbol{k} = (k_\perp, 0, k_z), \qquad \widehat{\delta \boldsymbol{E}} = -i(k_\perp, 0, k_z)\widehat{\delta\phi}, \tag{282}$$

where $\widehat{\delta\phi}$ is the perturbed potential. The dispersion relation (281) is valid for arbitrary angle of propagation with respect to the applied magnetic field $\boldsymbol{B}_0 = B_0 \hat{\boldsymbol{e}}_z$.

Equation (281) supports a broad range of electrostatic waves and instabilities associated with nonthermal features of $F_j(v_\perp^2, v_z)$. In the special case of propagation parallel to $B_0\hat{\boldsymbol{e}}_z$ with $k_\perp = 0$ and $\boldsymbol{k} = k_z\hat{\boldsymbol{e}}_z$, (281) reduces to the familiar electrostatic dispersion relation for an unmagnetized plasma given in (81) which was studied extensively in Section 3.3.3. That is, as expected, for wavevector $\boldsymbol{k}$ parallel to $B_0\hat{\boldsymbol{e}}_z$, the electrostatic stability properties are unaffected by the presence of the magnetic field. In contrast, for $k_\perp \neq 0$, the presence of the magnetic field as well as the choice of distribution function $F_j(v_\perp^2, v_z)$ have an important influence on determining detailed stability properties.

For purposes of illustration, in the remainder of Section 3.3.7, (281) is considered in circumstances where the propagation is nearly perpendicular to $B_0\hat{\boldsymbol{e}}_z$ with

$$k_z^2/k_\perp^2 \ll 1. \tag{283}$$

In addition, it is assumed that the electrons are strongly magnetized and the ions are unmagnetized in the region of ω- and $\boldsymbol{k}$-space under investigation. Within the

context of these approximations, the specific instabilities investigated later in Section 3.3.7 include the convective-loss-cone instability, the ion-ion cross-field instability, and the modified-two-stream instability, all of which are driven by nonthermal equilibrium features of the ion distribution function.

Strongly magnetized electron response

For present purposes, it is assumed that the electron distribution function is an isotropic Maxwellian,

$$F_e(v_\perp^2, v_z) = \left(\frac{m_e}{2\pi T_e}\right)^{3/2} \exp\left(-\frac{m_e}{2T_e}(v_\perp^2 + v_z^2)\right). \tag{284}$$

Substituting (284) into (281) gives, after some straightforward algebra and rearrangement of terms, the electron dielectric response

$$\chi_e(\boldsymbol{k}, \omega_r + i\gamma) = \frac{k_\perp^2}{k^2}\frac{\omega_{pe}^2}{\omega_{ce}^2}\frac{1}{\lambda_e}\left[1 + \exp(-\lambda_e) I_0(\lambda_e)\left(\frac{\omega_r + i\gamma}{k_z v_{Te}}\right) Z\left(\frac{\omega_r + i\gamma}{k_z v_{Te}}\right)\right.$$
$$\left. + \left(\frac{\omega_r + i\gamma}{k_z v_{Te}}\right) \sum_{n=0} \exp(-\lambda_e) I_n(\lambda_e) Z\left(\frac{\omega_r - n\omega_{ce} + i\gamma}{k_z v_{Te}}\right)\right], \tag{285}$$

where $v_{Te} = (2T_e/m_e)^{1/2}$, $\lambda_e = k_\perp^2 T_e/m_e\omega_{ce}^2$, $k^2 = k_\perp^2 + k_z^2$, $Z(\xi)$ is the plasma dispersion function defined in (105), $I_n(\lambda_e)$ is the modified Bessel function of the first kind of order n, and $\sum_{n=0}$ implies deletion of the $n = 0$ term from the summation. In (285), no approximation has been made that k_z is small or that the electrons are strongly magnetized.

It is now assumed that the electrons are strongly magnetized with

$$|\omega_r + i\gamma| \ll |\omega_{ce}|, \tag{286}$$

and that the axial wavelength is sufficiently long and/or the electron temperature is sufficiently low that

$$|k_z v_{Te}| \ll |\omega_r + i\gamma|. \tag{287}$$

Expanding $Z(\xi_e) \simeq -1/\xi_e - 1/2\xi_e^2$ in (285) for $|\xi_e| \gg 1$ then gives to lowest order

$$\chi_e(\boldsymbol{k}, \omega_r + i\gamma) = \frac{\omega_{pe}^2}{\omega_{ce}^2}\frac{k_\perp^2}{k^2}\frac{[1 - \exp(-\lambda_e) I_0(\lambda_e)]}{\lambda_e}$$
$$- \frac{k_z^2}{k^2}\exp(-\lambda_e) I_0(\lambda_e)\frac{\omega_{pe}^2}{(\omega_r + i\gamma)^2}. \tag{288}$$

If, in addition, it is assumed that the perpendicular wavelength is long in comparison with the thermal electron Larmor radius $r_{Le} = v_{Te}/|\omega_{ce}|$, then

$$\lambda_e = \tfrac{1}{2} k_\perp^2 r_{Le}^2 \ll 1, \tag{289}$$

and (288) can be approximated by

$$\chi_e(\boldsymbol{k}, \omega_r + i\gamma) = \frac{\omega_{pe}^2}{\omega_{ce}^2} - \frac{k_z^2}{k^2} \frac{\omega_{pe}^2}{(\omega_r + i\gamma)^2}. \tag{290}$$

In obtaining (290), use has been made of $\exp(-\lambda_e) I_0(\lambda_e) \simeq 1 - \lambda_e$ for $\lambda_e \ll 1$, and $k_\perp^2/(k_\perp^2 + k_z^2) \simeq 1$ for $k_z^2 \ll k_\perp^2$. The frequency-dependent dielectric response in (288) and (290) is proportional to $(k_z^2/k^2)\omega_{pe}^2/(\omega_r + i\gamma)^2$ and is associated with the parallel electron motion. The frequency-independent dielectric response in (288) and (290) is proportional to $\omega_{pe}^2/\omega_{ce}^2$ and is associated with the perpendicular polarization drift of an electron fluid element.

Although $\lambda_e \ll 1$ will be assumed in the applications considered later in Section 3.3.7, it should be emphasized that the expression for χ_e given in (288) is also valid when λ_e is of order unity or larger, provided the inequalities (286) and (287) are satisfied.

Unmagnetized ion response

For present purposes, perturbations are considered with perpendicular wavelength short in comparison with the characteristic ion Larmor radius, and frequency large in comparison with the ion cyclotron frequency, i.e.

$$|k_\perp v_\perp / \omega_{ci}| \gg 1, \qquad |(\omega_r + i\gamma)/\omega_{ci}| \gg 1. \tag{291}$$

Rather than consider the weak magnetic field limit of the ion dielectric response in (281), it is expeditious to make use of the fact that the ions have straight line orbits $\boldsymbol{x}' = \boldsymbol{x} + \boldsymbol{v}\tau$ and $\boldsymbol{v}' = \boldsymbol{v}$ on the time and length scales of interest. A direct calculation of the perturbed ion distribution function $\widehat{\delta f_i}$ then gives (see last subsection of Section 3.3.1),

$$\widehat{\delta f_i} = -\frac{\hat{n}_i e_i}{m_i} \frac{\boldsymbol{k} \cdot \partial F_i / \partial \boldsymbol{v}}{\omega_r - \boldsymbol{k} \cdot \boldsymbol{v} + i\gamma} \widehat{\delta\phi}, \tag{292}$$

and the ion dielectric response can be approximated by

$$\chi_i(\boldsymbol{k}, \omega_r + i\gamma) = \frac{\omega_{pi}^2}{k^2} \int d^3v \frac{\boldsymbol{k} \cdot \partial F_i / \partial \boldsymbol{v}}{\omega_r - \boldsymbol{k} \cdot \boldsymbol{v} + i\gamma}, \tag{293}$$

where $k^2 = k_\perp^2 + k_z^2$ and $\boldsymbol{k} = k_\perp \hat{\boldsymbol{e}}_x + k_z \hat{\boldsymbol{e}}_z$.

Equation (293) is a valid approximation to χ_i within the context of the inequalities (291). Strictly speaking, it is not necessary to assume in (293) that the ion distribution function is isotropic in the plane perpendicular to $B_0\hat{\boldsymbol{e}}_z$ with $F_i(\boldsymbol{v}) = F_i(v_\perp^2, v_z)$. That is, (293) can also be applied for general $F_i(\boldsymbol{v})$ on a timescale shorter than $|\omega_{ci}|^{-1}$ after formation of the plasma.

To summarize, for strongly magnetized electrons ($|\omega_r + i\gamma| \ll |\omega_{ce}|$; $|k_\perp v_{Te}/\omega_{ce}| \ll 1$), and unmagnetized ions ($|\omega_r + i\gamma| \gg |\omega_{ci}|$; $|k_\perp v_{Ti}/\omega_{ci}| \gg 1$), the electrostatic dis-

persion relation (281) can be approximated by

$$D(\boldsymbol{k}, \omega_r + i\gamma) = 1 + \frac{\omega_{pi}^2}{k^2} \int d^3v \frac{\boldsymbol{k} \cdot \partial F_i / \partial \boldsymbol{v}}{\omega_r - \boldsymbol{k} \cdot \boldsymbol{v} + i\gamma} + \frac{\omega_{pe}^2}{\omega_{ce}^2} - \frac{k_z^2}{k^2} \frac{\omega_{pe}^2}{(\omega_r + i\gamma)^2} = 0, \quad (294)$$

where $|k_z v_{Te}| \ll |\omega_r + i\gamma|$ and $k_z^2 \ll k_\perp^2$ are assumed in (294). Specific applications of (294) are now considered.

Convective loss-cone instability

Consider the ion loss-cone equilibrium illustrated in Fig. 3.3.17. Note that

$$G(v_\perp^2) = \pi v_{Ti}^2 \int_{-\infty}^{\infty} dv_z F_i(v_\perp^2, v_z) \quad (295)$$

shows a depletion of particles with small perpendicular speed $v_\perp$. In (295), the scale factor v_{Ti} is the characteristic ion thermal speed. The distribution function shown in Fig. 3.3.17 can arise in a magnetic mirror where particles with small $v_\perp^2$ and large v_z^2 are lost out the ends of the device. Since $k_z^2 \ll k_\perp^2$ is assumed, the approximation $\boldsymbol{k} = k_\perp \hat{\boldsymbol{e}}_x$ is made in the ion dielectric response in (294). Paralleling the analysis in Section 3.3.3, it is also assumed that the growth (or damping) is weak with

$$|\gamma/\omega_r| \ll 1. \quad (296)$$

Making use of (96) and (294), the quantities $D_r = \mathrm{Re}\, D(\boldsymbol{k}, \omega_r + i\gamma)$ and $D_i = \mathrm{Im}\, D(\boldsymbol{k}, \omega_r + i\gamma)$ are evaluated in the limit $\gamma \to 0_+$. This gives

$$D_r(\boldsymbol{k}, \omega_r) = 1 + \frac{2\omega_{pi}^2}{k^2 v_{Ti}^2} P \int \frac{d^2v}{(2\pi)} \frac{2\boldsymbol{k}_\perp \cdot \boldsymbol{v}_\perp \, \partial G / \partial v_\perp^2}{\omega_r - \boldsymbol{k}_\perp \cdot \boldsymbol{v}_\perp} + \frac{\omega_{pe}^2}{\omega_{ce}^2} - \frac{k_z^2}{k^2} \frac{\omega_{pe}^2}{\omega_r^2}, \quad (297)$$

$$D_i(\boldsymbol{k}, \omega_r) = -\pi \frac{2\omega_{pi}^2}{k^2 v_{Ti}^2} \int \frac{d^2v}{(2\pi)} \delta(\omega_r - \boldsymbol{k}_\perp \cdot \boldsymbol{v}_\perp) 2\boldsymbol{k}_\perp \cdot \boldsymbol{v}_\perp \frac{\partial G}{\partial v_\perp^2}$$

$$= -2\pi\omega_r \frac{2\omega_{pi}^2}{k^2 v_{Ti}^2} \int \frac{d^2v}{(2\pi)} \delta(\omega_r - k_\perp v_\perp \cos\phi) \frac{\partial G}{\partial v_\perp^2}. \quad (298)$$

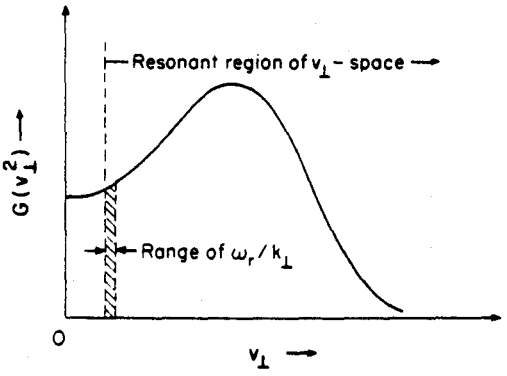

Fig. 3.3.17. Plot of reduced ion equilibrium $G(v_\perp^2) = \pi v_{Ti}^2 \int_{-\infty}^{\infty} dv_z F_i(v_\perp^2, v_z)$ for convective loss-cone instability.

where $\int d^2v = \int_0^{2\pi} d\phi \int_0^\infty dv_\perp\, v_\perp$, P denotes Cauchy principal value, and $\boldsymbol{k}_\perp \cdot \boldsymbol{v}_\perp = k_\perp v_\perp \cos\phi$ with $v_\perp \cos\phi = v_x$. After some straightforward algebra, the integrations over ϕ in (297) and (298) can be carried out to give

$$D_r(\boldsymbol{k}, \omega_r) = 1 + \frac{1}{k^2\lambda_{Di}^2}\left[G(0) + I_r\left(\frac{\omega_r}{k_\perp}\right)\right] + \frac{\omega_{pe}^2}{\omega_{ce}^2} - \frac{k_z^2}{k^2}\frac{\omega_{pe}^2}{\omega_r^2}, \tag{299}$$

and

$$D_i(\boldsymbol{k}, \omega_r) = -\frac{[\operatorname{sgn}\omega_r]}{k^2\lambda_{Di}^2}\int_{\omega_r^2/k_\perp^2}^\infty dv_\perp^2 \frac{\partial G(v_\perp^2)/\partial v_\perp^2}{\left(k_\perp^2 v_\perp^2/\omega_r^2 - 1\right)^{1/2}}, \tag{300}$$

where $\lambda_{Di}^2 \equiv v_{Ti}^2/2\omega_{pi}^2$, and the real ion response I_r is defined by

$$I_r\left(\frac{\omega_r}{k_\perp}\right) \equiv \int_0^{\omega_r^2/k_\perp^2} dv_\perp^2 \frac{\partial G(v_\perp^2)/\partial v_\perp^2}{\left(1 - k_\perp^2 v_\perp^2/\omega_r^2\right)^{1/2}}. \tag{301}$$

From (300), note that the *resonant* region of $v_\perp$-space satisfying $\omega_r = k_\perp v_\perp \cos\phi$ covers the entire region $v_\perp^2 > \omega_r^2/k_\perp^2$, whereas the *nonresonant* (principal-value) contribution with $\omega_r \neq k_\perp v_\perp \cos\phi$ corresponds to $v_\perp^2 < \omega_r^2/k_\perp^2$ in (301). Solving $D_r(\boldsymbol{k}, \omega_r) = 0$ for the real frequency ω_r gives

$$\omega_r^2 = \omega_{pe}^2 \frac{k_z^2\lambda_{Di}^2}{\left[k^2\lambda_{Di}^2\left(1 + \omega_{pe}^2/\omega_{ce}^2\right) + G(0) + I_r\right]}. \tag{302}$$

Moreover, the growth rate $\gamma = -D_i/(\partial D_r/\partial\omega_r)$ is given by

$$\gamma = \tfrac{1}{2}|\omega_r| \int_{\omega_r^2/k_\perp^2}^\infty dv_\perp^2 \frac{\partial G(v_\perp^2)/\partial v_\perp^2}{\left(k_\perp^2 v_\perp^2/\omega_r^2 - 1\right)^{1/2}}\left[k^2\lambda_{Di}^2\left(1 + \omega_{pe}^2/\omega_{ce}^2\right) + G(0) + I_r\right]^{-1}. \tag{303}$$

In obtaining (303) the $\partial I_r/\partial\omega_r$ contribution to $\partial D_r/\partial\omega_r$ has been neglected in comparison with $(\partial/\partial\omega_r)(k_z^2\omega_{pe}^2/k^2\omega_r^2)$. Note from (303) that instability exists ($\gamma > 0$) provided $\partial G/\partial v_\perp^2 > 0$ over a sufficiently large region of $v_\perp$-space, i.e. provided the loss-cone depression in $G(v_\perp^2)$ is sufficiently deep and wide.

Ion–ion cross-field instability

As an example of a strong electrostatic instability, consider the case where $F_i(v)$ corresponds to counterstreaming ion beams propagating perpendicular to the magnetic field $B_0\hat{\boldsymbol{e}}_z$. Assuming

$$k_z = 0, \tag{304}$$

the electrostatic dispersion relation (294) for strongly magnetized electrons and unmagnetized ions can be expressed as

$$D(\boldsymbol{k}_\perp, \omega_r + i\gamma) = 1 + \frac{\omega_{pe}^2}{\omega_{ce}^2} + \frac{\omega_{pi}^2}{k_\perp^2}\int d^3v \frac{\boldsymbol{k}_\perp \cdot \partial F_i(v)/\partial v}{\omega_r - \boldsymbol{k}_\perp \cdot \boldsymbol{v}_\perp + i\gamma} = 0, \tag{305}$$

where $\boldsymbol{k}_\perp = k_\perp \hat{\boldsymbol{e}}_x$. As a simple example that is amenable to direct calculation, it is assumed that the ion distribution function $F_i(\boldsymbol{v})$ corresponds to equidensity, symmetric ion beams counterstreaming with mean velocities $\pm V_d$ in the x-direction,

$$F_i(\boldsymbol{v}) = \frac{\Delta_i}{2\pi}\left(\frac{1}{(v_x - V_d)^2 + \Delta_i^2} + \frac{1}{(v_x + V_d)^2 + \Delta_i^2}\right) G_2(v_y) G_3(v_z), \tag{306}$$

where $\int_{-\infty}^{\infty} dv_y G_2(v_y) = 1 = \int_{-\infty}^{\infty} dv_z G_3(v_z)$, and $\int d^3\boldsymbol{v} F_i(\boldsymbol{v}) = 1$. In (306), Δ_i models the effect of finite ion temperature.

Substituting (306) into Eq. (305) and carrying out the required velocity integration gives

$$D(\boldsymbol{k}_\perp, \omega_r + i\gamma) = 1 + \frac{\omega_{pe}^2}{\omega_{ce}^2} - \frac{(\omega_{pi}^2/2)}{(\omega_r - k_\perp V_d + i\gamma + i|k_\perp \Delta_i|)^2} - \frac{(\omega_{pi}^2/2)}{(\omega_r + k_\perp V_d + i\gamma + i|k_\perp \Delta_i|)^2} = 0. \tag{307}$$

Because of the symmetry in (307), it is straightforward to show that the unstable two-stream solutions to (307) necessarily have $\omega_r = 0$. Introducing the lower hybrid frequency defined by

$$\omega_{LH}^2 = \frac{\omega_{pi}^2}{1 + \omega_{pe}^2/\omega_{ce}^2}, \tag{308}$$

(307) can be expressed as

$$1 = \omega_{LH}^2 \frac{k_\perp^2 V_d^2 - (\gamma + |k_\perp \Delta_i|)^2}{\left[k_\perp^2 V_d^2 + (\gamma + |k_\perp \Delta_i|)^2\right]^2}, \tag{309}$$

for $\omega_r = 0$. From (309), the threshold for instability is given by

$$V_d^2 > \Delta_i^2. \tag{310}$$

That is, the drift velocity must exceed the characteristic ion thermal speed. Solving (309) for the growth rate γ of the unstable branch gives

$$\gamma = \frac{\omega_{LH}}{\sqrt{2}}\left[\left(1 + 8\frac{k_\perp^2 V_d^2}{\omega_{LH}^2}\right)^{1/2} - \left(1 + 2\frac{k_\perp^2 V_d^2}{\omega_{LH}^2}\right)\right]^{1/2} - |k_\perp \Delta_i|, \tag{311}$$

where $V_d^2 > \Delta_i^2$ is required for instability ($\gamma > 0$) at small $k_\perp$.

In the limit of negligible ion thermal effects ($\Delta_i \to 0$), the growth rate γ in (311) assumes its maximum value

$$[\gamma]_{max} = \omega_{LH}/2\sqrt{2}, \tag{312}$$

for $k^2 = k_{max}^2 \equiv \frac{3}{8}k_0^2$, where

$$k_0 = \omega_{LH}/V_d. \tag{313}$$

Here, k_0 corresponds to marginal stability with $\gamma(\pm k_0) = 0$ in (311) when $\Delta_i = 0$.

From (312), it is evident that the ion–ion cross-field instability can have very large growth rate in a parameter regime where the electrons are strongly magnetized ($\omega_{LH} \ll |\omega_{ce}|; |k_0 v_{Te}/\omega_{ce}| \ll 1$), and the ions are effectively unmagnetized ($\omega_{LH} \gg |\omega_{ci}|; |k_0 v_{Ti}/\omega_{ci}| \gg 1$). In this regard, note that $\omega_{LH} \simeq |\omega_{ce}\omega_{ci}|^{1/2}$ follows from (308) for $\omega_{pe}^2/\omega_{ce}^2 \gg 1$.

Modified two-stream instability

For the modified two-stream instability, allowance is made for $k_z \neq 0$ in (294), and it is assumed that there is a single component of ions drifting with velocity V_d in the x-direction,

$$F_i(\boldsymbol{v}) = \left(\frac{m_i}{2\pi T_i}\right)^{1/2} \exp\left(-\frac{m_i}{2T_i}(v_x - V_d)^2\right) G_2(v_y) G_3(v_z), \tag{314}$$

where $\int_{-\infty}^{\infty} dv_y G_2(v_y) = 1 = \int_{-\infty}^{\infty} dv_z G_3(v_z)$. Assuming $k_z^2 \ll k_\perp^2$, the approximation $\boldsymbol{k} = k_\perp \hat{\boldsymbol{e}}_x$ is made, in the ion dielectric response (294). This gives the dispersion relation

$$D(\boldsymbol{k}, \omega_r + i\gamma) = 1 + \frac{2\omega_{pi}^2}{k_\perp^2 v_{Ti}^2}\left[1 + \xi_i Z(\xi_i)\right] + \frac{\omega_{pe}^2}{\omega_{ce}^2} - \frac{k_z^2}{k^2}\frac{\omega_{pe}^2}{(\omega_r + i\gamma)^2} = 0, \tag{315}$$

where $v_{Ti} = (2T_i/m_i)^{1/2}$, $\xi_i = (\omega_r - k_\perp V_d + i\gamma)/k_\perp v_{Ti}$, and $Z(\xi_i)$ is the plasma dispersion function defined in (105). In the limit where

$$|\xi_i| = |(\omega_r - k_\perp V_d + i\gamma)/k_\perp v_{Ti}| \gg 1, \tag{316}$$

the approximation $Z(\xi_i) = -1/\xi_i - 1/2\xi_i^3$ is made and (315) reduces to

$$0 = 1 - \frac{\omega_{LH}^2}{(\omega_r - k_\perp V_d + i\gamma)^2} - \left(\frac{k_z^2}{k^2}\frac{m_i}{Z_i m_e}\right)\frac{\omega_{LH}^2}{(\omega_r + i\gamma)^2}. \tag{317}$$

where $\omega_{LH}^2 = \omega_{pi}^2/(1 + \omega_{pe}^2/\omega_{ce}^2)$, $\omega_{pi}^2/\omega_{pe}^2 = Z_i m_e/m_i$, $e_i = Z_i e$ is the ion charge, and use has been made of equilibrium charge neutrality, $\hat{n}_i(Z_i e) + \hat{n}_e(-e) = 0$.

The dispersion relation (316) is identical in form to the electron–ion two-stream dispersion relation (143) with the replacements in (143)

$$\omega_{pe}^2 \to \omega_{LH}^2, \qquad \omega_{pi}^2 \to \frac{k_z^2}{k^2}\frac{m_i}{Z_i m_e}\omega_{LH}^2. \tag{318}$$

One of the important features of the two-stream instability is that maximum growth rate occurs for equidensity streams. Therefore, from (318), maximum growth occurs for k_z determined from

$$\left[k_z^2/k_\perp^2\right]_{max} = Z_i(m_e/m_i) \ll 1. \tag{319}$$

Moreover, when (319) is satisfied, making use of (317), maximum growth occurs for

$$\left[\omega_r/k_\perp\right]_{max} = V_d/2. \tag{320}$$

Consistent with (319) and (320), the maximum growth rate $[\gamma]_{max}$ is given by

$$[\gamma]_{max} = \omega_{LH}/2 \tag{321}$$

for $[k_\perp^2]_{max} = \frac{3}{8}k_0^2$, where $\gamma(\pm k_0) = 0$, with $k_0 = \sqrt{2}\,\omega_{LH}/V_d$.

Like the ion–ion cross-field instability, the modified-two-stream instability exhibits strong growth with $[\gamma]_{max} \gg |\omega_{ci}|$ and $[\gamma]_{max} \ll |\omega_{ce}|$, which is consistent with the assumptions of strongly magnetized electrons and unmagnetized ions.

Acknowledgement

I wish to thank Professor Ravi Sudan for his encouragement during the preparation of this manuscript. I am also grateful to Dr. Wayne A. McMullin and Dr. Han S. Uhm for assistance in proofreading the manuscript.

References

The following reference list, while forming an incomplete bibliography, identifies several classical papers and early treatises on the kinetic waves and instabilities discussed in this chapter.

Pedagogical treatises on kinetic waves and instabilities in uniform plasma

Bekefi, G., 1966, Radiation Processes in Plasmas (Wiley, New York).
Davidson, R.C., 1972, Methods in Nonlinear Plasma Theory (Academic Press, New York).
Ichimaru, S., 1973, Basic Principles of Plasma Physics—A Statistical Approach (Benjamin, Reading, MA).
Kadomtsev, B.B., 1968, Plasma Turbulence (Academic Press, New York).
Klimontovich, Y.L., 1967, Statistic Theory of Nonequilibrium Processes in Plasmas (MIT Press, Cambridge, MA).
Krall, N.A., and A.W. Trivelpiece, 1973, Principles of Plasma Physics (McGraw Hill, New York).
Mikhailovsky, A.B., 1975, Theory of Plasma Instabilities (Atomizdat, Moscow).
Montgomery, D., and D. Tidman, 1964, Plasma Kinetic Theory (McGraw Hill, New York).
Rosenbluth, M.N., 1956, Los Alamos Lab. Rep. LA-2030.
Rudakov, L.I., and R.Z. Sagdeev, 1975, Problems in Plasma Physics Controlled Fusion, Vol. 3, Ed. M.A. Leontovich (Atomizdat, Moscow) p. 270.
Sagdeev, R.Z., and A.A. Galeev, 1969, Nonlinear Plasma Theory, (revised and edited by T.M. O'Neil and D.L. Book) (Benjamin, New York).
Tsytovich, V.N., 1970, Nonlinear Effects in Plasmas (Plenum, New York).
Stix, T.H., 1962, The Theory of Plasma Waves (McGraw Hill, New York).

Stability theorem for monotonic decreasing $F_j(v^2)$

Bernstein, I.B., 1958, Phys. Rev. 109, 10 (this gives an early published proof of Newcomb's theorem).
Davidson, R.C., 1974, Theory of Nonneutral Plasmas (Benjamin, Reading, MA).
Davidson, R.C., and S.T. Tsai, 1973 J. Plasma Phys. 9, 101.
Fowler, T.K., 1963, J. Math. Phys. 1, 359.
Fowler, T.K., 1968, in: Advances in Plasma Physics, Vol. 1, Eds. A. Simon and W.B. Thompson (Wiley–Interscience, New York) p. 201.

Gardner, C.S., 1963, Phys. Fluids 6, 839.
Sudan, R.N., and M. Rosenbluth, 1976, Phys. Rev. Lett. 36, 972.

Waves and instabilities in an unmagnetized plasma

Bernstein, I.B., and S.K. Trehan, 1960, Nucl. Fusion 1, 3.
Buneman, O. 1959, Phys. Rev. 115, 503.
Davidson, R.C., D.A. Hammer, I. Haber, and C.E. Wagner, 1972, Phys. Fluids 15, 317.
Dawson, J.M., 1961, Phys. Fluids 4, 869.
Drummond, W.E., and D. Pines, 1962, Nucl. Fusion Suppl. 3, 1049.
Fried, B.D., and S.D. Conte, 1961, The Plasma Dispersion Function (Academic Press, New York).
Fried, B.D., and R.W. Gould, 1961, Phys. Fluids 4, 139.
Landau, L.D., 1946, J. Phys. USSR 10, 25.
Penrose, R., 1960, Phys. Fluids 3, 258.
Stringer, T.E., 1964, Plasma Phys. 6, 267.
Vedenov, A.A., E.P. Velikhov, and R.Z. Sagdeev, 1962, Nucl. Fusion Suppl. 2, 465.
Weibel, E.S., 1959, Phys. Rev. Lett. 2, 83.

Electromagnetic waves and instabilities for propagation parallel to $\boldsymbol{B}_0$

Bers, A., and S. Gruber, 1965, Appl. Phys. Lett. 6, 27.
Chandrasekhar, S., A.N. Kaufman, and K.M. Watson, 1958, Proc. R. Soc. A245, 435.
Davidson, R.C., and J.M. Ogden, 1975, Phys. Fluids 18, 1045.
Davidson, R.C., and H.J. Volk, 1968, Phys. Fluids 11, 2259.
Furth, H.P., 1963, Phys. Fluids 6, 48.
Kennel, C.F., and F. Engelmann, 1966, Phys. Fluids 9, 2377.
Kennel, C.F., and H.E. Petschek, 1966, J. Geophys. Res. 71, 1.
Ossakow, S., I. Haber and E. Ott, 1972, Phys. Fluids 15, 1538.
Shapiro, V.D. and V.I. Shevchenkov, 1964, Sov. Phys. JETP 18, 1109.
Sudan, R.N., 1963, Phys. Fluids 6, 57.

Waves and instabilities for propagation perpendicular (and nearly perpendicular) to $\boldsymbol{B}_0$

Aamodt, R., 1967, Plasma Phys. 9, 1573.
Baldwin, D.E., 1977, Rev. Mod. Phys. 49, 317.
Baldwin, D.E., I.B. Bernstein, and M.P.H. Weenink, 1969, in: Advances in Plasma Physics, Vol. 3, Eds. A. Simon and W. Thompson (Wiley–Interscience, New York) p. 1.
Bernstein, I.B., 1958, Phys. Rev. 109, 10.
Bers, A., and S. Gruber, 1965, Appl. Phys. Lett. 6, 27.
Crawford, F.W., and J.A. Tataronis, 1965, J. Appl. Phys. 36, 2930.
Davidson, R.C., and C.S. Wu, 1970, Phys. Fluids 13, 1407.
Dory, R.A., G.E. Guest and E.G. Harris, 1965, Phys. Rev. Lett. 14, 131.
Freidberg, J.P., 1969, Phys. Fluids 12, 1112.
Furth, H.P., 1967, Phys. Fluids 6, 48.
Galeev, A.A., 1967, J. Plasma Phys. 1, 105.
Kesner, J., 1973, Plasma Phys. 15, 577.
Papadopoulos, K., R.C. Davidson, J.M. Dawson, I. Haber, D.A. Hammer, N.A. Krall, and R. Shanny, 1971, Phys. Fluids 14, 849.
Rosenbluth, M.N., and R.F. Post, 1965, Phys. Fluids 8, 547.